Ecological Monographs, 83(3), 2013, pp. 339–382

Transient dominance in a central African rain forest

D. M. Newbery,[1,4] X. M. van der Burgt,[1,5] M. Worbes,[2] and G. B. Chuyong[3]

[1]*Section for Vegetation Ecology, Institute of Plant Sciences, University of Bern, Altenbergrain 21, CH-3013 Bern, Switzerland*
[2]*Crop Production Systems in the Tropics, Georg-August-University, Grisebachstraße 6, D-37077 Göttingen, Germany*
[3]*Department of Botany and Plant Physiology, University of Buea, P.O. Box 63, Buea, S. W. Division, Cameroon*

Abstract. The large-crowned emergent tree *Microberlinia bisulcata* dominates rain forest groves at Korup National Park, Cameroon, along with two codominants, *Tetraberlinia bifoliolata* and *T. korupensis*. *M. bisulcata* has a pronounced modal size frequency distribution around ~110 cm stem diameter: its recruitment potential is very poor. It is a long-lived light-demanding species, one of many found in African forests. *Tetraberlinia* species lack modality, are more shade tolerant, and recruit better. All three species are ectomycorrhizal. *M. bisulcata* dominates grove basal area, even though it has similar numbers of trees (≥50 cm stem diameter) as each of the other two species. This situation presented a conundrum that prompted a long-term study of grove dynamics. Enumerations of two plots (82.5 and 56.25 ha) between 1990 and 2010 showed mortality and recruitment of *M. bisulcata* to be very low (both rates ~0.2% per year) compared with *Tetraberlinia* (2.4% and 0.8% per year), and *M. bisulcata* grows twice as fast as the *Tetraberlinia*. Ordinations indicated that these three species determined community structure by their strong negative associations while other species showed almost none. Ranked species abundance curves fitted the Zipf-Mandelbrot model well and allowed "overdominance" of *M. bisulcata* to be estimated. Spatial analysis indicated strong repulsion by clusters of large (50 to <100 cm) and very large (≥100 cm) *M. bisulcata* of their own medium-sized (10 to <50 cm) trees and all sizes of *Tetraberlinia*. This was interpreted as competition by *M. bisulcata* increasing its dominance, but also inhibition of its own replacement potential. Stem coring showed a modal age of ~200 years for *M. bisulcata*, but with large size variation (50–150 cm). Fifty-year model projections suggested little change in medium, decreases in large, and increases in very large trees of *M. bisulcata*, accompanied by overall decreases in medium and large trees of *Tetraberlinia* species. Realistically increasing very-large-tree mortality led to grove collapse without short-term replacement. *M. bisulcata* most likely depends on climatic events to rebuild its stands: the ratio of disturbance interval to median species' longevity is important. A new theory of transient dominance explains how *M. bisulcata* may be cycling in abundance over time and displaying nonequilibrium dynamics.

Key words: African rain forest; Caesalpiniaceae; cyclic dynamics; grove formation; Korup National Park; mosaic theory; replacement potential; spatial pattern; transient dominance.

Introduction

Areas of rain forest in which one or a few species of main canopy tree are much more abundant and of higher densities locally than co-occurring species not only provide the possibility of feasibly studying how these dominants are adapted to their site conditions, but also how they may alter the site in ways that influence both their own and the other species' long-term dynamics. Dominance by such species need not necessarily be a persistent feature, however. It could also be transient, in the sense that high abundance fluctuates over time. The processes underlying transient dominance might be either deterministic with, for instance, regeneration occurring predictably on a regular cycle, or stochastic, where regeneration increases and decreases unpredictably with no apparent cycle. Forest dynamics in general are most likely to be somewhere in between idealized regularity and irregularity, showing quasi-cycles of varying amplitude as a result of the complex interactions operating between demographic and environmental factors that control their populations. In contrast to species-rich forests, in which the many main canopy species are often of similar low abundance, studies in forests poorer in canopy species might allow more complete explanations of their dynamics, and thereby lead to a deeper understanding of general ecological principles applicable to all rain forests.

Mosaic theory and forest dynamics

The cyclic or mosaic theory of forest regeneration was advanced several decades ago for trees in West and western Central African forests by Aubréville (1938). Its application elsewhere in the tropics has been rather limited, however, and remains, for reasons not yet fully

Manuscript received 2 October 2012; revised 29 January 2013; accepted 4 February 2013; final version received 2 March 2013. Corresponding Editor: R. T. Corlett.
[4] E-mail: david.newbery@ips.unibe.ch
[5] Present address: Herbarium, Royal Botanic Gardens, Kew, Richmond Surrey TW9 3AB United Kingdom.

understood, somewhat special to these forests of Africa (Richards 1996). The model behind the mosaic theory is that patches of one or more co-dominating tree species grow up and then decline at changing locations within any relatively larger area or "block" of forest. They thereby create many shifting patterns on the landscape over time. The theory exemplifies the more general notion of "pattern and process" operating behind all forest dynamics first put forward by Watt (1947). Cyclical mosaics may even be happening at varying rates and on different overlapping spatial scales for different species in any forest area. Nevertheless, to form a model for the theory, common features to the regeneration processes and a defining set of ecological traits are sought.

Changes in tree abundance of a species, temporarily and spatially toward a locally high and aggregated abundance, lead to the notion that transient dominance may be more common than is often admitted. Transient dominance may be a better explanation of overall forest dynamics, structure, and species abundance distributions under the Aubréville (1938) model. Our postulate is that a temporarily dominant species moves over time through a site. It may or may not have occurred previously there. Its life-history characteristics mean that it does not usually stay for long but, under certain conditions, could persist for more extended periods. We therefore evaluate the mosaic theory in a wider and continuous spatial-temporal context. Furthermore, we argue that transient dominance means that trees alter the new (or old) habitat in ways that are increasingly to the species' own advantage at the start of (re-)occupancy, but later those enforced conditions become selective against its continuation. The course of change is not exactly one of facilitation, moving through tolerance, and ending in self-inhibition (Connell and Slatyer 1977) since succession, sensu stricto, is not involved. That would mean pioneer, secondary, and tertiary states (or seres), which is not the case here. End successional states in tropical forests are probably quite rare in any case, because of the very important role of external disturbances operating on a wide range of scales of intensity and with different frequencies (Jones 1945).

In the course of habitat modification, niche partitioning among the other species is expected to be substantially reduced because the environment is made more homogeneous by the dominant species (Whittaker 1975). Moreover, while the dominant competitively suppresses the other species, these latter have fewer opportunities to spatially interact with one another, and the result would be that they become more randomly distributed in the forest with respect to the dominant (although some very few small niches might exist), and their abundances will be determined by the effectiveness they each have in competing with the dominant. Temporarily these other species find places where they can survive by chance: later, when the transient dominance and the implied competition relax, other forces may come into effect that re-determine the relative abundances. The original idea of Aubréville (1938) was that regeneration and replacement of a species occurred largely *away* from where adults formed a current patch, in other words population continuation was ex situ. The work of Letouzey (1968, 1985), however, suggested a more complex and subtle form of dynamics where some species, in some situations, were more or less regenerating and replacing instead in situ. He noted this particularly for several co-occurring abundant caesalps in the Atlantic Coastal forests of Cameroon. The two "situations" form an important contrast within an extended mosaic model. A major aim should be to distinguish those processes that lead to one rather than the other.

Cycles have a strong heuristic appeal in vegetation ecology, whether their return time is regular or irregular (Watt 1947). That a stand can reach a certain abundance (possibly maximal), decline, and then regrow later (in the same location or elsewhere nearby) as a continuous process, could be the outcome of local dynamics at the small-patch scale (hectares, decades) leading to an apparently constant forest composition at the larger forest-block one (square kilometers, centuries), if the various stages or ages of patches are in roughly constant proportions over time. Thus, at the local scale, dynamics will be largely in a state of disequilibrium, but at the forest scale it will tend toward an apparent equilibrium. The interplay between these two scales is most likely determined by forces that directly drive the cycles affecting tree population dynamics (Whitmore 1982). Key considerations, therefore, are how and from where did the current structure originate, why is the spatial form it is in now found, and how will spatial structure change in the future? One scenario is that mosaic dominance arises from scattered individual trees, spreads locally by short-distance dispersal to form aggregations, and these coalesce to form patches (determined also by edaphic conditions being suitable). The patches later decline through a lack of in situ replacement, disintegrate, fragment back into a scattered population, only to re-aggregate later elsewhere. In the other scenario, long-distance dispersal leads to patches establishing and maturing to dominance elsewhere on the landscape (again depending on edaphic conditions), which, when they decline, are once again reliant on long-distance dispersal to reestablish the species at new locations. A mixture of both processes is conceivable, varying in intensity in the past and into the present.

The mosaic idea was criticized by Swaine and Hall (1988), by pointing out that Richards (1952) had misinterpreted a table in Aubréville (1938) in which sapling records had not been distinguished between those not present and those not searched for. Nevertheless, a more certain aspect was the lack of small (juvenile) stems of some canopy species, such as *Piptadeniastrum africanum*, compared with more nu-

merous large (adult) trees within patches. Such an interesting idea had an important stimulating influence on the next two generations of African tropical workers, from Jones (1956), Richards (1963), and Letouzey (1968), through to Alexandre (1989), Poorter et al. (1996), and Gartlan and Newbery (1996).

Microberlinia *groves at Korup*

On the sandy nutrient-poor soils of the southern part of Korup National Park, in southwest Cameroon, one species in particular, *Microberlinia bisulcata* (Caesalpinioideae, Fabaceae), dominates well-defined patches or "groves" (Gartlan et al. 1986, Newbery and Gartlan 1996; see Plate 1). The species forms tall emergent trees with large domed and spreading crowns and extensive buttressing (Newbery et al. 2009). It is found together with two other caesalpiniaceous species that co-dominate the groves, *Tetraberlinia bifoliolata* and *T. korupensis* (Newbery et al. 1998), and all three species, as well as several others less abundant, are ectomycorrhizal (Newbery et al. 1988, 2000). Strong mycorrhizal activity plays a very important role in nutrient cycling of the grove stands at Korup (Newbery et al. 1997). Further, the tree size frequency distribution of *M. bisulcata* is distinctly modal, at ~105 cm stem diameter (Newbery et al. 1998, 2004). The likely quasi-cyclic nature of the population dynamics of *M. bisulcata*, and possibly that of its associates too, became apparent as data sets were assembled on size distributions and growth rates. This led to the current hypothesis of transient dominance.

At Korup, recent recruitment of *M. bisulcata* has been extremely poor. Dominance is apparently "non-persistent" using the terminology of Connell and Lowman (1989). Mast fruiting leads to very high densities of seedlings (Green and Newbery 2002, Newbery et al. 2006*a*), nearly all of which die away within 7–10 years to leave a very low density of saplings and small juvenile trees (Newbery et al. 2006*b*). While we continue to research the dynamics of the seed-to-1-cm-sapling dynamics quite extensively in the field (Newbery et al. 2010, Norghauer and Newbery 2010, 2011; J. M. Norghauer and D. M. Newbery, *unpublished manuscript*), our next set of questions relate to whether these few saplings can replace the juveniles, and whether these relatively sparse juveniles are in turn sufficient in number to replace the eventually dying adults. Could the stand continue as it is by means of steady replacement, or must there be a collapse of the large-tree population followed by grove renewal? Alternatively, will the groves just disappear in the near future as the adults die out without replacement? We have identified, in fact, four groves of *M. bisulcata* in southern Korup (Newbery et al. 2004). Two that are neighbors and form a "grove complex" will be described in detail in this paper. The other two are more isolated, one being smaller and likely older (Newbery et al. 2002) and the other larger and seemingly—from tree sizes—younger (X. van der Burgt and D. M. Newbery, *unpublished data*), will be referred to briefly. *M. bisulcata* also exists in small scattered remnants in Southern Bakundu Forest Reserve, south of Korup (Richards 1963; D. M. Newbery, *personal observation*), at Mokoko, west of Mt. Cameroon (G. B. Chuyong, *personal observation*), and in the neighboring Oban National Park in southeast Nigeria (Hall 1981). Until now, we have been unable to find any patches of young saplings or juveniles of *M. bisulcata* of any size separate from these four groves in Korup (Newbery et al. 2004). We suppose that recent long-distance dispersal has been extremely rare or nonexistent, although that is not to say that it was not more frequent in the past, and the animal dispersers have become extinct. Transport by water, on the fast and high streams in late wet season, is another possibility. There is no evidence of past human settlement in the southern part of KNP (Newbery et al. 1997, 1998, 2004), despite an unfounded implication made by van Gemerden et al. (2003) to the contrary.

Dominance mechanisms

Any regeneration of *M. bisulcata* is currently restricted to within groves, by a short-distance (<60 m) ballistic means of dispersal. Just beyond the groves' perimeters there is, with a single exception, no recruitment of *M. bisulcata*, which makes the groves spatially very well defined (Newbery et al. 1998, 2004). Seedlings of *M. bisulcata* are highly shade-intolerant but at the same time highly light responsive (Green and Newbery 2001*a*, *b*). This suggests that they need repeated periods of release to reach the juvenile tree status that secures their onward growth (Newbery et al. 2010). This type of recruitment is rarely afforded by individual tree falls of either *M. bisulcata* or any other species because single gaps quickly close in and the understorey vegetation smothers small seedlings before they can make sufficient height growth. *M. bisulcata* does, however, survive and grow well from small seedlings under fully lighted conditions, e.g., at our nursery plantation site near to Korup (D. M. Newbery and G. B. Chuyong, *unpublished data*). We have earlier hypothesized that strong external disturbances are needed to establish groves (Newbery et al. 1998, 2004), and here in this paper we further the notion that they may be necessary to maintain the species as a transient dominant. Multiple disturbances, likely in the form of clusters of dry years, are thought to temporarily defoliate the canopy and even enhance mortality of some non-*M. bisulcata* trees, and this allows a cohort to establish and large seedlings and saplings to "ratchet" their growth upward over a period of ~20–30 years. The mosaic idea appears to apply then only in part for this species at Korup: in the presumably almost complete absence of long-distance dispersal, recruitment is restricted to being in situ. With precise structural and dynamic information about the groves though, we may be able to estimate replacement probabilities and use these as a basis for a mathematical model of mosaic dynamics.

For increasing dominance to come about, the most abundant species must have the largest internal effects on the site conditions. Continuation will lead to complete dominance, even monodominance. But this need not necessarily be the case if, at some point in time, dominance feeds back negatively within the ecosystem so that its advance is slowed or even reversed. This could happen relatively early on during the rise in abundance, or later depending on the interacting set of internal and external factors. The two processes have been respectively termed "autogenic" and "allogenic" in succession theory (Tansley 1935, Finegan 1984), and we propose that they might be analogously applied to forest dynamics cycles, as autogenic and allogenic dominance. Rather than a gradual decline happening as mortality slowly increases, with perhaps attendant replacement, the species' stand may become overdominant to such a degree that it tips rapidly away from its temporarily highly unstable state, i.e., the dominance suddenly collapses without attendant replacement because recruitment was limited for too long. A more catastrophic change could be promoted by a disturbance removing the large trees faster than at the intrinsic old-age mortality rate. We show in this paper that the two main groves at Korup have now reached a point close to their inevitable fast decline. We attempt to predict the rate of change and replacement in this context.

Edaphic conditions inside and outside the grove, combined with events that cause a disturbance and release of recruitment, need to be considered together. A forest that loses many large trees of its dominant species is likely to change substantially in many other ways. The dominant is unlikely to completely disappear locally, but become reduced to temporarily low abundance (by definition, if it is transient). Surviving juvenile trees need then to grow fast to replace the adults, and this may involve a lag period for them if the old losses were sudden. External conditions may reoccur, however, to promote that recruitment into the medium and large tree size classes, coming either at the time of collapse or very soon afterward. There is no reason to suppose, though, that these external stochastic conditions would coincide with a particular phase of advanced aging and then dying adults. In forest stands at the point of imminent collapse, it is a question of timing as to whether a required external event happens to occur serendipitously to help recruitment, the basis to allogenic dominance. Coming some time ahead, the potential full effect would be lost: many new recruits would likely stagnate and die out. Alternatively, a decline in the adults per se may create conditions within the stand that encourage the recruitment of their own species, and this is the basis to autogenic dominance directly driven by cohort aging as trees of similar sizes (or ages) reach a period of high mortality simultaneously. In the extended mosaic model, we envisage an interplay between autogenic and allogenic dominance dependent on the frequency of disturbance relative to the life span of adult trees. If adults of a dominant species do, however, alter site conditions internally to make later in situ recruitment always unfavorable, then in the absence of an external disturbance (which in part or fully improves those site conditions), the species can only continue ex situ.

A new framework

Transient dominance in the extended mosaic model can be represented as a two-way table of in situ/ex situ reestablishment vs. presence/absence of disturbance. Aubréville's original (1938) idea concerned ex situ reestablishment not requiring external disturbance (species well dispersed and seedlings shade tolerant), the current proposal for *M. bisulcata* concerns in situ reestablishment, which does require external disturbance (species not well dispersed and seedlings shade intolerant). This is close to what Letouzey (1968) was describing for many Cameroonian caesalps. Ex situ establishment under external disturbance relying on long-distance dispersal of a shade-intolerant species would be the conventional non-persistent secondary succession idea (Finegan 1984); and in situ establishment of a highly shade-tolerant species without disturbance would be the typical case leading to persistent monodominance (Hart 1990, 1995). To achieve transient dominance for a shade-intolerant species, not dispersed over long distances, appears to require a form of disturbance coupled (even synchronized) with the decline of the adults themselves, in order to cause quasi-cycling in their abundance. Unrepeated conditions of release would most likely mean the local extinction and loss of *M. bisculata* from Korup.

Transient dominance can be contrasted with another well known type of dominance. Under monodominance, with persistent recruitment, conditions are created by site and dominant species together that favor this species' own juveniles better than those of other species, e.g., through high shade tolerance, low predator or pathogen attack, ectomycorrhizal networks (Connell and Lowman [1989], but see Torti and Coley [1999] on the mycorrhizal aspect). Without disturbance, probably the most essential feature, the dominants steadily replace other species (Huston 1979, Torti et al. 2001). Longer term, the species becomes highly adapted to the site conditions and changes them to its advantage: the precise combination of mechanisms is likely to be manifold, and varying from species to species and site to site (Torti et al. 2001, Peh et al. 2011). Prime examples are *Gilbertiodendron dewevrei* (Gérard 1960, Hart et al. 1989), and *Brachystegia laurentii* (Germain and Evrard 1956) in Central Africa, *Mora excelsa* in Guyana (Davis and Richards 1934) and Trinidad (Beard 1946), and *Dicymbe corymbosa* also in Guyana (Henkel 2003). Species without persistent recruitment, however, have been claimed to be largely successional because they were neither abundant before nor after their appearance (Connell and Lowman 1989, Hart 1990). This reasoning seems incomplete: lack of recruitment may not always be

indicating a succession per se but, as proposed here, sometimes transient dominance. Transient dominance still allows for long-term persistence when there is some disturbance and the species is shade intolerant. By contrast, there are indeed species that form monodominant stands as a culmination of succession, and a prime example is *Cynometra alexandri* in Uganda (Eggeling 1947, Sheil 2001). Or, in the case of *Mora excelsa*, Beard (1946) considered that this species had likely invaded Trinidad, its large seeds and tolerance of low light as seedlings aiding its persistence, at least temporarily. Finally, one other scenario to be considered is when a tree species may have been dominant for a long time, with conditions that favored its recruitment in the past, but now changes in the environment lead uniquely to its failure to recruit.

Studies of dominance in tropical rain forests have, perhaps unsurprisingly, been largely aimed at explaining monodominance (>80–90% basal area). There has been little attention paid to codominance or where dominance is not quite so pronounced (50–70% basal area). Forests with several more abundant species are often overlooked, or even dismissed as being less interesting: they are not composed of a single species, and they are not hyper-diverse. Nevertheless, a gradient between the two extremes does exist, and without its consideration forest ecology is certainly incomplete. Difficulties abound, however. On finding high abundance the immediate question is whether the species has a potential regeneration, i.e., are there sufficient numbers of juveniles to replace the dying adults (Condit et al. 1998)? A strong imbalance would suggest a disequilibrium situation, a case of non-persistence in the short term. An understorey with many juveniles would likely promote a view of persistence. However, any lack of small trees might only be temporary, and in the longer run, given fluctuations in recruitment, the forest could be rather constant in composition. Contrarily, relatively few juveniles may not mean a lack of, or poor, recruitment when these survive very well and also grow fast (Jones 1950, Clark and Clark 1987, 1992, Poorter et al. 1996). Below some critical relative density, recruitment has to be judged as probably leading to a decline in the species' population, at least in the short term. A key question is how to define that critical density.

Exactly how the forest changes will depend upon the rates of mortality and recruitment among the larger trees, the growth rates of juveniles, and the positive and negative effects of adults on juveniles. An intensive period of loss of just large trees might lead to a forest with fewer adults and relatively more juveniles: a slower rate of adult loss would give the opposite impression, one of poorer recruitment chances because more adults remain for longer. A forest with a relatively high proportion of trees in the middle size class, yet relatively few juveniles and few large adults, is temptingly interpreted as a cohort moving through toward dominance (Jones 1956). Working with such adult : juvenile ratios at one point in time can therefore lead to considerable uncertainty about the long-term dynamics. This said, there is no assurance either that the currently observed dynamics rates applied even approximately in the past, or will do so in the future. Persistence of a species is accordingly very difficult to assess correctly without the long-term detailed dynamics and growth data, especially in cases where the numbers of juvenile trees is neither obviously lacking nor particularly plentiful. A "middle numbers" situation makes predictability highly uncertain, with outcomes dependent on the fine interplay of several contingent internal and external factors.

Background and aims

Korup National Park (5°10′ N, 8°70′ E) lies within a Guinea–Congolean refugium, representative of the Atlantic coastal rain forest type (Letouzey 1968), and is of high conservation value (Gartlan 1992). Lying inland of Mount Cameroon, it receives ~5100 mm rain annually with one distinct dry season of 3 months (December–February) and one very strong wet season (centered around July–August). Earlier vegetation work is described by Gartlan et al. (1986), Newbery et al. (1988), and Newbery and Gartlan (1996). Newbery et al. (1998) first reported on the modal distribution of tree sizes for *M. bisulcata*, and on the relative abundances of the three main caesalps at Korup. Subsequently, Newbery et al. (2004) presented a grove map and spatial analysis for the large *M. bisulcata* trees. The present paper therefore builds upon and extends these two cornerstone studies.

In the present paper, we report on the composition, structure and 20-yr dynamics of 140 ha of the main grove complex at Korup, which is dominated by *M. bisulcata*. This involves measurements of tree growth, recruitment and mortality, and the evaluation of tree size class distributions and spatial patterns. We focus on the regeneration of *M. bisulcata* and five other caesalpinaceous species to understand forest dynamics in terms of our extended mosaic model and the notion of transient dominance.

Methods

Measurements in the P plot

The 82.5-ha P plot (Fig. 1) was set up between 15 June 1990 and 21 March 1991, and 8–30 November 1991 (median 31 January 1991). Global coordinates and elevation above sea level at the southeast corner are 0476438/0553538 and 96 m. It measures 500 × 1650 m (north-south by east-west), consisting of 330 50 × 50 m subplots (Fig. 2a). It is so called because it lies midway along the original P transect line of Gartlan et al. (1986). Plastic posts mark all subplot corners. Transect P runs along the center line in the eastern half of the plot, but deviates southward in the other half (by up to 45 m on the western edge). Subplot columns and rows were numbered 1–33 westward, and A–J southward, respec-

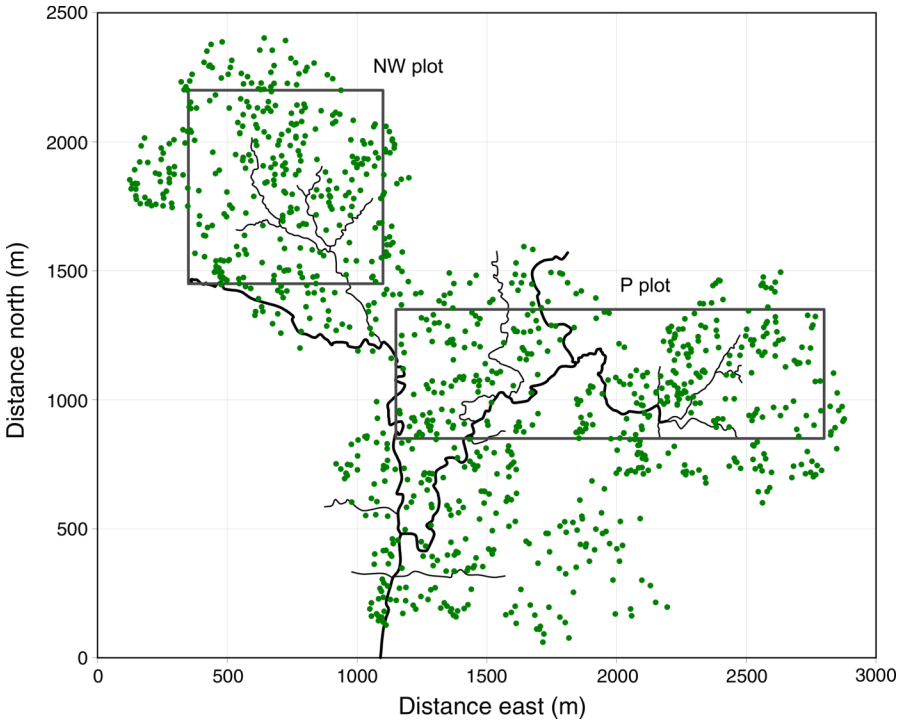

FIG. 1. Layout of the grove of large *Microberlinia bisulcata* trees in southern Korup National Park, Cameroon, and the positions of the main P and NW plots, based in part on Newbery et al. (2004). Each green dot is a tree of ≥50 cm stem diameter (above buttresses). Darker black lines are the main streams.

tively. All trees ≥50 cm stem diameter were numbered with aluminum tags, coordinates recorded, and identified to species. Diameters were derived from girth measurements with a steel tape at breast height (gbh, 1.3 m) when this was feasible. Otherwise, the point of measurement (POM) was moved higher up because of stem irregularities, or to be 10 cm above any buttresses, by using sometimes two vertical poles (with alignment and direct reading taken from a ladder) and/or Spiegel optical relascope. POMs of trees with diameters <50 cm were marked with paint. (From hereon, stem diameter will always be taken to mean diameter at breast height or, that not allowing, diameter on the next flattest section of the stem just above any buttresses or protrusions.)

Trees between 10 and <50 cm diameter were tagged in 33 subplots (one randomly selected in each column), identified and gbh measured with the tape, but not mapped (Fig. 2a). Within each subplot a north-south 5 × 50 m strip was randomly selected and counts of all stems of diameter 1 to <10 cm were made, and of these only the three main species of the large caesalps (*M. bisulcata*, *T. bifoliolata*, and *T. korupensis*: the "MTT" species) were identified and their diameters measured (with callipers). A topographic map of the P plot was made in 1991 (improved in 2004–2005), contours being based on elevations at each subplot corner post and some other points, and showing streams, swampy and periodically inundated areas, and large rocks.

The plot was remeasured between 21 February and 16 March 2005, recording which trees ≥50 cm diameter had died, and which had recruited into this size class. Blocks of 5 (A–E or F–J) × 3 (e.g., columns 1–3) subplots were visited in random order. The mean interval was thus 14.0 years. Diameters of survivors were remeasured between 23 January and 15 March 2005 using either a girth tape (and sometimes a ladder) and converted to diameters later, or a Criterion-400 ranging laser instrument (RLI; Laser Technology, Centennial, Colorado, USA), and the tree identifications were checked and revised where necessary. Diameters were taken as far as possible at the 1991 heights of measurement, or adjusted higher when buttresses had expanded upward. Some small errors in subplot alignment were corrected. From October to December 2005, dead/alive status of all trees 10 to <50 cm diameter in the 33 subplots was recorded and identifications updated. For the three main caesalpiniaceous species, all trees 10 to <50 cm diameter in the whole plot were mapped and measured during 24 January–25 March 2004 (rows B–I) and 23–25 March 2005 (rows A and J). Between 16 March and 15 April 1998 (median 1 April) diameters of surviving *T. bifoliolata* and *T. korupensis* trees 10 to <100 cm stem diameter in 1991 had been remeasured by tape at an interim census. Finally, on 5–6 May 2009, 41 large trees of *M. bisulcata* in an 8.25-ha area in the eastern half of the P plot, were remeasured for diameter above buttress using a portable RD1000 relascope (Laser Technology).

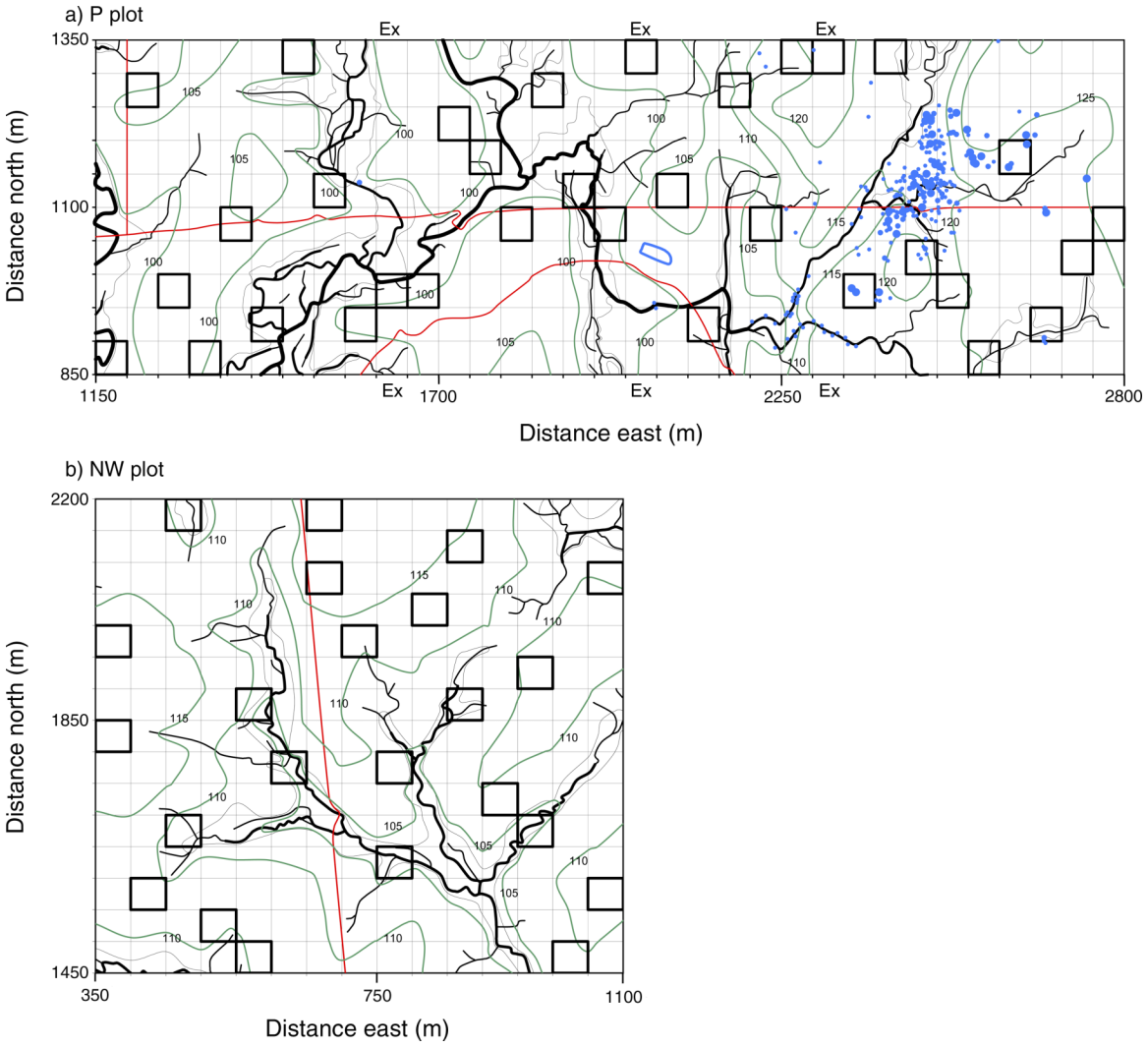

FIG. 2. Permanent plot layouts with topographic details and subplot locations: (a) P plot and (b) NW plot. Distances east and north are referenced to the map in Fig. 1. Heavy black lines and connecting fine black lines are streams; fine green lines are contours in elevation (numbers on the panels; m above sea level), fine red lines are paths; blue dots and outlines indicate major rocks or rocky areas. "Ex" marks the start of a P-plot extension. Subplots, in which trees 10 to <50 cm diameter were enumerated, are shown as heavy black squares. Grid squares are of 50 m × 50 m dimensions.

As far as possible, the 2005 heights of measurement were used, otherwise this was raised ~0.5 m on the stem if buttresses interfered.

The P plot was extended to the N and S by six extra lines of subplots (Fig. 2a). These were set up between 8 December 1999 and 4 February 2000 and varied in length from three to eight (north) and seven to 18 (south) subplots ($n = 68$ subplots; 17 ha; Appendix A), stopping when three subplots had no trees of *M. bisulcata*. A section of the southwest-most extension had an expansion eastward to include a large old gap. Stem diameters of trees ≥50 cm diameter were measured with either a tape or the optical relascope.

The resulting main data files, according to date and tree size class are denoted as P91 (large, medium), P05 (large, medium) and PE00 (large). In collating the data, frequent reference was made to the original files for 1991 and the field notebooks, also some remeasurements in 1998. Some minor corrections and revisions were needed to the 1991 P-plot data in 2005 and the methodological details are also given in Appendix A.

Measurements in the NW plot

The 56.25-ha NW plot (Fig. 1) was set up between 7 December 2002 and 25 April 2003 in a similar manner to that of the P plot. This plot is so named because it lies to the northwest of P plot. Global coordinates and elevation above sea level at the southwest corner are 0475571/0554105 and 113 m. It measures 750 × 750 m, consisting of 225 50 × 50 m subplots (Fig. 2b). The

southeast corner of this plot is 100 m north and 50 m west from the northwest corner of the P plot. Trees of ≥50 cm stem diameter were numbered, mapped, measured, and identified between 4 March and 25 April 2003. Measurement by tape was replaced by LRI estimates where direct access was not possible. In 23 subplots (Fig. 2b), between 16 October and 16 December 2004, trees 10 to <50 cm stem diameter were enumerated (as for subplots in the P plot): 15 had been selected in a Latin square design (each row and column with one subplot), with eight more from the uneven-numbered rows and columns of a second random square such that no subplots shared an edge in the final layout. All other trees with stem diameters 10 to <50 cm of the three mentioned species were mapped and measured in the whole plot between 25 March and 25 April 2003 (apart from a few exceptions later in 2003).

Recording of trees at the whole-plot level was made by taking the constituent 25 blocks of 3×3 subplots in a random order. Paint marks indicated the POMs for tape-measured trees. Trees 1 to <10 cm diameter were registered in one north-south randomly selected 10×50 m strip in each subplot, this strip being at least 10 m from north-south subplot edges. Diameters of the three selected species were measured with calipers, except for those trees just below 10 cm diameter, which were measured with a tape. A topographic map of the NW plot was made in 2003, in a similar way to that for the P plot.

Between 5 April and 8 May 2005, 50 large trees of *M. bisulcata* and all large ones of *T. bifoliolata* and *T. korupensis* (i.e., those not measured with a relascope in 2003) were revisited for status and girth measurement. Later, on 9–10 October 2009, 28 (of 168, 16.6%) trees of *M. bisulcata* were remeasured with the Criterion RD1000 relascope (6 ha of subplots in SE corner of NW plot, 10.6% of area), using the same heights on stems and bearings as in 2003. Between 6 and 17 February 2009, all large trees of these same species were revisited to record alive/dead status. Finally, in 27–30 December 2010 and 5–7 January 2011, all 634 large trees not of the three main caesalps (non-MTT) were scored for dead/alive status.

Soil sampling and recording

In the wet season of 1990 (30 August–31 October), soils were sampled from each subplot ($n = 330$ samples). At the center of each quarter of the subplot, one core to 10 cm was taken (surface litter removed), and depth of the surface organic layer recorded. Samples in each subplot were mixed and reduced in bulk, passed through a 2-mm sieve, and air dried. Chemical analyses following standard procedures were made for loss-on-ignition (LOI, organic matter), Olsen-extractable phosphorus, and ammonium-acetate exchangeable magnesium, potassium, and calcium. In the dry season of 1990–1991 (19–22 February), a further set of soil samples were collected from the subplots enumerated for trees down to 10 cm stem diameter ($n = 33$ subplots), and again in the dry season of 1992–1993 (18–23 February 1993) including an additional 17 subplots (one more at random in every second column east to west; giving $n = 50$ subplots), for the same measurements and analyses.

A stratified random sample of 17 cores were also taken along the central 100-m strip of the P plot on 2–3 November 2008, air-dried, and extracted in ammonium acetate for analysis of magnesium, potassium, and calcium. Each core was separated into 0–2 and 2–15 cm depths. On 15 December 2009, 30 samples were taken across the NW plot also in a stratified random manner, but as single 0–10 cm cores, as was done in 1991 in the P plot. The three cations were again estimated, plus LOI depth or organic layer was recorded at four locations per subplot samples and the averages found.

Taxonomic identifications

Taxonomic names in the P and NW plots were fully standardized; corrections, as new fertile material was obtained, continued until August 2006. A full species list for the plots in the grove is shown in Appendix B. Sterile and fertile voucher collections for both plots are stored at Wageningen, The Netherlands. Fertile material was distributed as follows: two duplicates for Cameroon, at Yaoundé (YA) and Limbe (SCA) Herbaria, and one each for the herbaria at Kew (K), Brussels (BR), Geneva (G), Missouri (MO), Paris (P), and Wageningen (WAG).

Tree dimensions

Total tree heights for 15 trees of *M. bisulcata* in the P plot were previously reported in Newbery et al. (2009), and heights to lower branches were taken on these and 15 others on 3 July 2010 using a clinometer. Likewise, heights were recorded for 10 randomly selected suitable trees each of *T. bifoliolata* and *T. korupensis* on 21 April 2010. From a concurrent study on seed dispersal, J. M. Norghauer (*personal communication*) kindly provided data on their crown diameters. Additionally, during 28 January–1 February 2011, 60 large trees of other species were sampled in three blocks of subplots, on dry flatter ground at the ends and center of the P plot (in rows E and F; total of 8.5 ha), for heights and crown dimensions using clinometer and compass. Strongly leaning trees, those with broken crowns, or trees that could not be seen properly, were not measured.

Remeasurement of medium-sized trees

In the P plot, the fully mapped population of medium-sized trees of *M. bisulcata* ($n = 41$ trees, one a living stump), and an ~12% sample of *T. bifoliolata* ($n = 40$ trees) and *T. korupensis* ($n = 59$ trees) were remeasured for girth on 1–4 April (median 3 April) 2008 (total $n = 140$ trees). Approximately equal sample sizes of trees from the size classes 10 to <30 and 30 to <50 cm diameter were randomly selected in a stratified way for

the *Tetraberlinia* species. They had previously been measured on 23–25 March 2004 and 24–25 January 2005, i.e., some of them during the main plot re-enumeration. Because the remeasurements were at the start of the wet season, a subsample of 38 trees was measured again on 14 May 2008. Those of *M. bisulcata* were once more measured on 21 and 27 April 2010. The complete census of medium-sized trees of the three selected species done in the NW plot in 2003 were remeasured between 5 and 25 April 2005, and those of *M. bisulcata* once again on 13 May 2008.

Tree size and maturity.—For *M. bisulcata*, the 50-cm stem diameter size is at the threshold between juvenile and adult status (Newbery et al. 1998, 2004) and trees in the diameter class 10 to <50 cm are therefore both medium sized and juvenile. However, this is mostly not true for *T. bifiololata* and *T. korupensis*, which mature at smaller sizes of ~25–30 cm diameter (J. M. Norghauer and D. M. Newbery, *unpublished manuscript*). Accordingly, the status "juvenile" is used for either considerations of forest dynamics in general or *M. bisulcata* in particular when referred to in the *Discussion*.

Aging of trees

In 2003 and 2004, 46 trees of *M. bisulcata* ≥50 cm stem diameter, selected in part at random, were cored in the P and NW plots ($n = 18$ and 28 trees, respectively). Normally cores were taken at breast height between buttresses, but in a few cases where impedance was high a point further up the stem was used. Cores were mounted and dried on wooden blocks, polished with grade-600 sanding paper, and cleaned. Previous anatomical work and C^{14} dating of six wood samples (following the procedures of Worbes and Junk [1989]) had established that the "rings," that is the bands of marginal parenchyma, are produced annually in this species. Ring widths were measured to 0.01 mm accuracy and cross-matched to a master chronology. Half of the trees ($n = 22$ trees) were either hollow (possibly due to heart rot) or the corer did not reach the central pith (mostly trees >100 cm diameter). Examination of the cores that did reach the center showed no discernable pattern of earlier-smaller vs. later-larger rings, and statistical analysis of a subset of them showed that autocorrelation was positive for the first 30–50 rings and then it became negative. The length of core missing (difference between cored length and stem radius) was thus divided by the mean growth rate of the 50 innermost rings of the cored material to obtain an estimate of the number of uncored years, and this added to the number counted to the core.

Remeasurements at Isangele Road

An additional 8.75-ha plot, located within a smaller grove just outside the southern boundary of the Park (Newbery et al. 2002), set up for a phosphorus fertilization trial in 1995 (dates of first tree measurements 25 July–24 August), was revisited on 21–23 November 2011 to record survivorship and growth of 263 medium-sized trees of "Az" species (see *Results: Medium scale within-plot floristic variation*) in three 50 × 50 m subplots. Around 30 December 2011, survival of the 33 and seven large trees of *M. bisulcata* and *T. korupensis*, respectively, in the whole plot was also recorded. There are no trees of *T. bifoliolata* in this plot.

Results

Topography and soils

Local variation in topography within P and NW plots matches well the mapped stream systems (Fig. 2), and highlights the relatively dry (well draining) vs. wet (often inundated) parts of the forest. The elevation of the P plot decreases from east to west by ~20 m, as the surface changes from drier and rocky to flatter and lower ground, crossing a small river (Fig. 2a). To the south of the plot are many permanently wet areas. The NW plot sits on a very gentle slope. It encompasses a stream system to form a complete catchment, with an outlet in the southeast of the plot (Fig. 2b).

Each subplot in each plot was indexed according to the following scale: 0, no streams; 0.5, small stream crossing <50% of subplot; 1, small stream ≥50% of subplot or large stream partly crossing; 1.5, one and a half small streams; 2, two small or one large stream; 2.5, one large and one small stream; 3, two large streams, or one large and two small streams. Proportions of subplots in these classes were very similar between plots ($\chi^2_5 = 4.28$, $P = 0.51$); averaged, they were 0, 60.5%; 0.5–1.0, 22.6%; 1.5–2.0, 11.7%; 2.5–3.0, 5.2%. Thus, ~83% of the plots' combined area was "dry" and ~17% was "wet."

Variation across the P plot in LOI and concentrations of Mg, K, and Ca were small, with CVs ranging from 5% to 18% in dry and wet seasons. For depth of organic layer and concentration of P, the variation was higher, in the range of 20–53% with large differences between seasons (Table 1). Concentrations of Mg, Ca, and P were significantly lower in the dry season compared to wet season, especially for P with a 40–45% decrease. This variation can be explained largely by differences between permanently and seasonally wet areas and the dry land, in relation to topography and drainage by rivers and streams within the plot. A principal components analysis (PCA) of the six soil ln-transformed variables of wet season 1990 accounted for 77% of the variance in the first two components (Appendix C): a scatterplot of the scores showed only four outliers (of 330 points). Component 1 can be explained by the similarly high loadings (of ~0.3) of all variables, particularly LOI and the concentrations of Mg, K, and Ca, and component 2 by the high loadings of depth of organic layer and concentration of P. The spatial variation in soil chemistry is well summarized by the plot contour map of the scores for components 1 and 2 (Appendix C). Deeper more organic soils, with higher elemental

TABLE 1. Means, 95% confidence limits (CL), and coefficient of variation (CV) of soil characteristics of the P plot in Korup sampled in the one wet ($n = 33$ samples) and two dry seasons (1990–1992, $n = 33$ and 50 samples, respectively).

	Wet 1990†			Dry 1990–1991			Dry 1991–1992		
Parameter	Mean	95% CL	CV (%)	Mean	95% CL	CV (%)	Mean	95% CL	CV (%)
Depth (mm)	5.69	3.75–8.43	50.9	4.21	2.92–5.94	48.4	6.40	5.57–7.34	20.9
LOI (%)	6.04	5.46–6.69	15.9	5.66	5.23–6.13	12.9	6.13	5.84–6.43	9.4
Mg (μg/g)	18.6	16.2–21.5	13.8	15.4**	14.2–16.7	8.5	16.7	15.3–18.1	10.4
K (μg/g)	44.0	39.6–48.9	7.8	43.4	40.8–46.1	4.6	46.2	43.2–49.4	6.2
Ca (μg/g)	42.7	34.5–53.0	16.2	33.5*	29.7–37.8	9.7	25.8***	21.8–30.5	18.0
P (μg/g)	7.26	6.28–8.40	20.6	4.35***	3.70–5.11	30.9	3.96***	3.22–4.87	52.7

Notes: Soil characteristics are depth of organic layer, loss on ignition (LOI), and the concentrations of magnesium, potassium, calcium, and phosphorus in the soils. Values were first logarithmically transformed, and then the statistics back-transformed. Dry seasons were individually compared to the wet season using the *t* test (transformed data).

† The 330 wet-season samples were fully divided into 10 exclusive subsamples of 33 by allocating at random each subplot per column to a different set and finding the average means and confidence limits of the subsamples. Confidence limits (95%) for the 330 samples: depth (5.03–6.42), LOI (5.86–6.24), Mg (17.8–19.5), K (42.6–45.4), Ca (40.0–45.6), P (6.94–7.60).

* $P \leq 0.05$; ** $P \leq 0.01$; *** $P \leq 0.001$.

concentrations, occurred in the swampy areas around rivers at low elevations, especially near 800 m east, 300 m north in the plot (Appendix C and Fig. 2a). In two isolated areas on the southern perimeter, depth and P also peaked in their values away from streams, but the contribution of component 2 overall was relatively small.

Mean concentrations of extractable Mg, K, and Ca (weighted estimates for 0–10 cm) in the P plot in 2008 were 23.0 ± 2.3, 41.9 ± 2.6, and 43.4 ± 4.8 μg/g ($n = 17$ samples), which matched closely to the wet season values of 1991 (Table 1). In the NW plot, corresponding concentrations of the three cations were 13.5 ± 0.7, 32.2 ± 1.2, and 22.8 ± 1.7 μg/g ($n = 30$ samples), these being ~50–75% lower than the P plot ones of 1991 and 2008. Mean LOI in the NW plot at 6.28 ± 0.17% was very close to that in the P plot, but depth of organic layer at 1.65 ± 0.13 mm was much less (Table 1). Soils of the NW plot were thus poorer than those of the P plot.

Ordination of large trees in main plots

Two main ordination techniques were applied in a search for internal structure to the plots' vegetation in terms of their tree species composition, and especially how *M. bisulcata* is associated with the other dominants at different scales. The first was normalized principal components analysis (n-PCA) in which samples were standardized by their norms (i.e., Euclidean distances were relativized to chord distances between samples, species abundances accordingly converted to proportions within samples), and the eigenvalues and vectors of the resulting variance/covariance matrix found. The second was nonmetric multidimensional scaling (NMS), which used a one-half matrix of chord distances between samples, and found the minimum stress for one- to five-dimensional solutions. The analyses were performed with the program PC-ORD (McCune and Grace 2002), which provides tests of significance based on randomization/permutation techniques.

0.25-ha subplot scale.—Ordination by n-PCA of subplots (50 × 50 m) for the data P91, P05, P03 (the last being a linear interpolation between P91 and P05), NW03, PNW (P03 and NW03 combined), and the PE00 (extensions to P91) resulted in solutions where the three most abundant species, *M. bisulcata*, *T. bifoliolata*, and *T. korupensis*, were highly influential. These species' scores strongly polarized the ordinations in three dimensions, leaving other species centrally clustered. Axis 1 was highly significant in each of the six cases ($P = 0.001$) but axes 2 and above were not ($P > 0.05$ and mostly $P > 0.9$). Components 1–3 nevertheless accounted for ~52–55% of the variance, axis 1 alone for 28–31%. Omitting these three dominant species led to ordinations in which the next most abundant species showed similar individualized polarization. Runs with correlation-based components (r-PCA) and correspondence analysis (CA) resulted in pronounced outliers among subplots due to unusual species occurrences, and accounted for up to only 9% of the variance. The conclusion was that the subplot scale was too small to detect associations, each subplot being occupied with one or two of the three most abundant species (3–4 stems in all per subplot). The three species, *M. bisulcata*, *T. bifoliolata*, and *T. korupensis* formed a codominant triad set apart from all other species in the plots. With such large matrices, NMS proved very slow in reaching solutions, and these were often unstable.

1-ha subplot scale.—The subplot scale in P and NW plots was increased to 1 ha by joining two-by-two 0.25-ha subplots. Since the P plot in its west-east dimension, and the NW plot in both west-east and south-north dimensions, had uneven intervals of 50 m, some edges of the plots would have had to be sacrificed. To cover most of the plots' area, two overlapping 1-ha grids were constructed for each. In the P plot the {east, north} origin was either (A) {0, 0} m or (B) {50, 0} m, so that correspondingly either the last (eastern) or first (western) columns of 0.25-ha subplots were not used ($n = 80$ subplots); and in the NW plot the origin was either (A) {0, 0} m or (B) {50, 50} m and therefore involved a diagonal, northeastern, shift in position ($n = 49$ subplots). The A-grid subplots of the P (P03) and NW (NW03) plots, and likewise the matching B-grid

PLATE 1. The main grove of *Microberlinia bisulcata* trees in southern Korup National Park, Cameroon, seen from above the middle of P plot and looking toward NW plot. Photo credit: X. M. van der Burgt.

subplots, were each combined to give two corresponding (PNW03) data sets.

Ordinations by n-PCA of the P91, P05, and NW03 data (i.e., using the two grids gave six cases) showed again very strong influences of the three most abundant species (Fig. 3): just component 1 was significant ($P = 0.001$) in each case. Percentage variance accounted for on axes 1–3 was 58–63%, and on axis 1 alone 30–37%. NMS indicated, in good agreement, only significant one-dimensional solutions in every case ($P = 0.04$–0.052), but the minimum stress values of 25.4–31.4% were far too large (the generally held criterion of a poor solution is one with stress >20%) for these to be a meaningful indication of a reliable structure and were thus unacceptable. In accordance with the dominance-rank-species analysis (see *Rank-abundance curves*), the three species *M. bisulcata*, *T. bifoliolata*, and *T. korupensis* were next omitted and the ordinations rerun. As a result, no components were significant (P of axis 1 ranging from 0.35 to 0.70) and the first three axes accounted for just ~27–36% of the total variance. Likewise, while for NMS, mostly a three-dimensional solution with P values from 0.004 to 0.112 was recommended, stress values were again rather too high at 19.2–22.3% to conclude an acceptable structure. Runs with r-PCA and CA resulted again in the characteristic "splinter" and "outlier" effects, respectively, and low variances accounted for. The combined plots' PNW03 data led to only 25–27% variance being accounted for on axes 1–3 of n-PCA, and by NMS the A- and B-grids had in common only a one-dimensional solution ($P = 0.004$) yet high minimum stress of 50%. All n-PCA solutions were numerically confirmed using a second program, Canoco 4.5 (Jongman et al. 1995).

Ordination plots were inspected for evidence of groupings of subplots and none were found. Two-way clustering and table analysis in PC-ORD (agglomerative/Ward's method; chord distance) supported this assessment. Contour plots of the n-PCA-1 and n-PCA-2 scores across the P plot had clear distributions (Appendix C) and differed between grids only slightly. They showed the dominating influence of *M. bisulcata* in the center of the eastern half, and northwest of the western half, of the P plot; and the relative balance between the codominants, *T. bifoliolata* and *T. korupensis*, from the center of P plot eastward and westward. Ternary diagrams show that subplots with predominantly one of either of the *Tetraberlinia* species, as opposed to *M. bisulcata*, were relatively quite rare; and this was much more the case in the NW than the P plot (Fig. 4), an arrangement reflecting the species ordination in Fig. 3d.

2.25-ha sub-plot scale.—The P plot was again subdivided into two alternative grids with two points of origin to allow 33 subplots of 150×150 m, and analyzed using the P91 and P05 data sets. In the NW plot, 25 subplots of the same dimensions fitted in exactly. Normalized

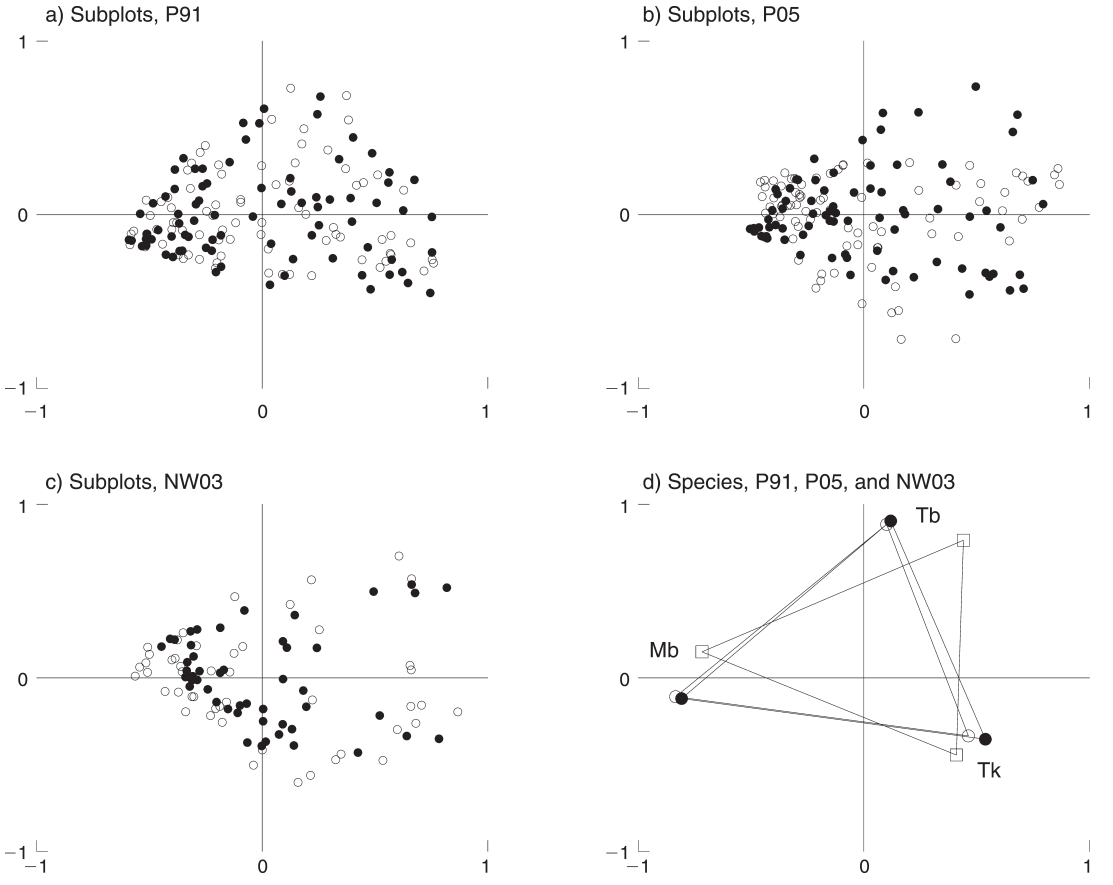

FIG. 3. Normalized-PCA ordinations showing axes 1 and 2 scores for 1-ha subplots: (a) P plot in 1991 (P91), (b) P plot in 2005 (P05), (c) NW plot in 2003 (NW03), with subplots starting at origin (grid A) shown as solid circles and 50-m offset (grid B) shown as open circles, and (d) the three main species' scores from the analyses of panels (a)–(c) together (P91, solid circles; P05, open circles; NW03, open squares; Mb, *Microberlinia bisulcata*; Tb, *Tetraberlinia bifoliolata*; and Tk, *T. korupensis*).

PCA in each case removed only axis 1 as being significant ($P = 0.001$–0.004), due to the strong effects of *M. bisulcata* and the two *Tetraberlinia* species. Unlike ordinations at the 1-ha scale, there was little structure to be seen, however, with several subplots outlying to various degrees, and poor agreement between grids A and B. At this scale, any tentative patterns appeared diffuse and unreliable.

Large trees in P and NW plots thus showed, individually or combined, no gradients involving more than the three main species. The most informative subplot scale was 1 ha. The three most abundant species formed a strong repeatable structure, but the next-ranked species added little information, their distributions and patterns appearing highly idiosyncratic. All subplots could therefore be combined for what appears, aside from local variation in proportions of the codominants, to be relatively homogeneous forest vegetation within plots.

Floristic variation in relation to environmental variables

Elevation was interpolated at the centers of the 1-ha subplots using the akima package in R (R Development Core Team 2010), and mean axis-1 and axis-2 soil PCA scores and stream index values were found from those of the four constituent 0.25-ha subplots, for the two grids (A and B) separately. Subplot scores from the n-PCA of the P plot tree data were not significantly correlated with either elevation, soil axis-1 or axis-2 scores. However, stream index was significantly correlated with n-PCA axis-1 score in both grids ($r = 0.312$ and 0.313, $df = 78$, $P = 0.005$). Using the basal-area abundances of the three main species per 1 ha there were few significant correlations with elevation, stream index, or soil axis scores: just for *M. bisulcata* there was a consistent (grids A and B) negative correlation with stream index ($r = -0.355$ and $r = -0.389$, $P \leq 0.001$) and for *T. bifoliolata* was there a consistent positive correlation with soil PCA axis 1 ($r = 0.244$, $P = 0.029$; $r = 0.320$, $P = 0.004$); i.e., there was a tendency for *M. bisulcata* and *T. bifoliolata* to be positively associated with respectively drier and nutrient-poorer soils of the plot (Appendix C).

To perform Mantel tests between main vegetation components and environmental variables (or components) in the P plot (grids A and B separately) Euclidean distance matrices were built for first the 80 1-ha subplots

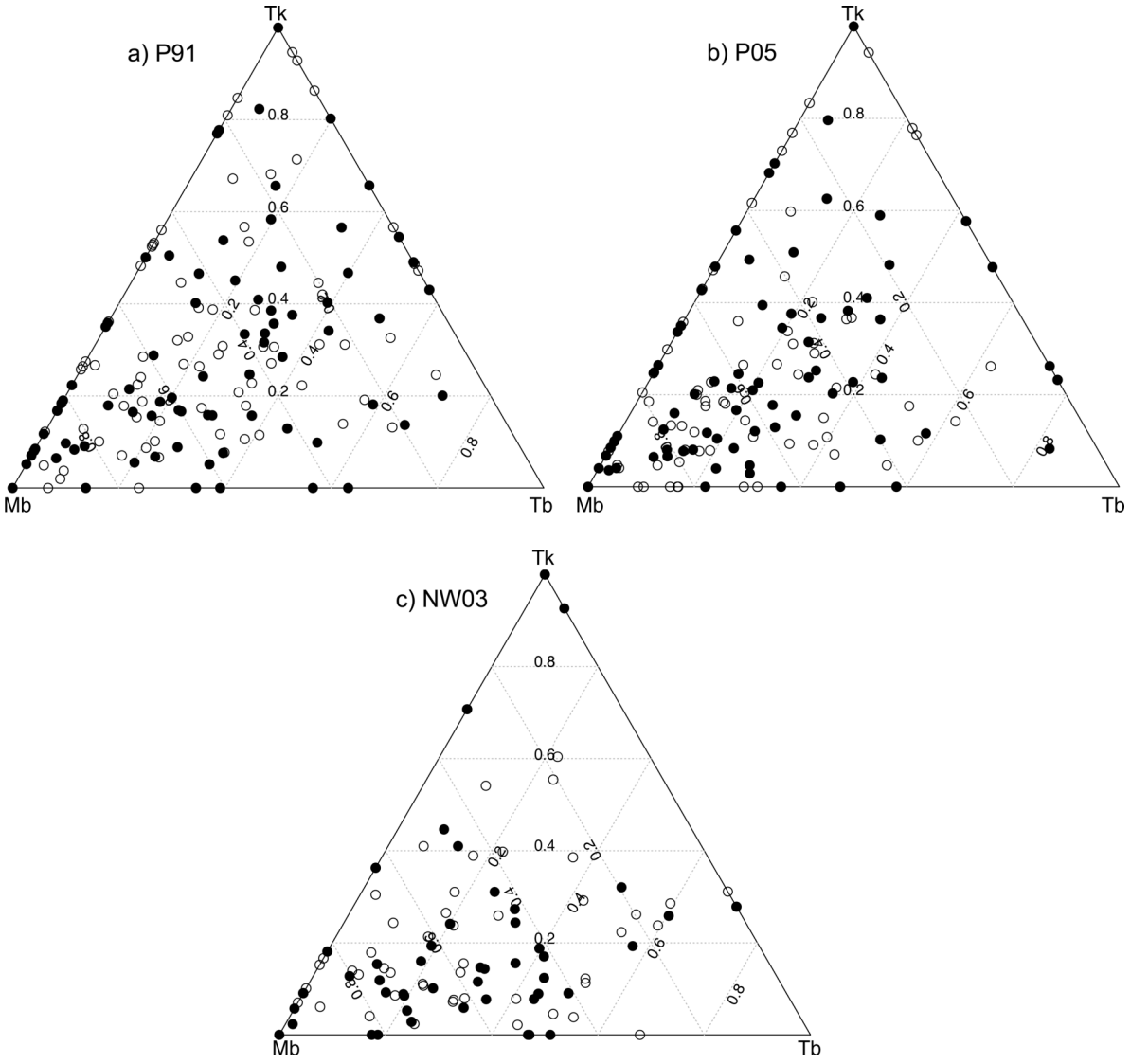

FIG. 4. The relative proportions of basal-area abundance (%) of the three main species, *Microberlinia bisulcata* (Mb), *Tetraberlinia bifoliolata* (Tb), and *T. korupensis* (Tk), in (a) P plot in 1991 (P91), (b) P plot in 2005 (P05), and (c) NW plot in 2003 (NW03) expressed as ternary diagrams. Solid and open circles are the same as in Fig. 3a–c. Vertices have the following coordinates for Mb, Tb, and Tk respectively: top (0, 0, 100), bottom right (0, 100, 0), and bottom left (100, 0, 0).

using their n-PCA components' 1–4 scores and, second, either the mapped *x*–*y* plot coordinates of the centers of subplots; or elevation, stream index, and the scores for the two soil PCA components, averaged for each ha subplot then standardized (divided by SD); or these two sets combined, with the coordinates also standardized. Both Mantel asymptotic (z) and Monte Carlo randomization tests ($n = 999$) showed no significant association with subplot coordinates ($P = 0.24$–0.61). With the four environmental variable/components there was a significant association, weak for the A grid ($P = 0.076$ and 0.044, respectively) but stronger for the B grid ($P = 0.010$ and 0.013). Taking all six variable/components led to slightly lowered significance for grid A ($P = 0.013$ and 0.070), lowered or similar for grid B ($P = 0.031$ and 0.013). There is thus some moderately strong evidence that tree compositional variation across the P plot was associated with elevation, wetness and soil chemistry when taken all together ($P \approx 0.01$–0.05).

Ordination of medium-sized trees

Ordination of the medium-sized trees (10 to <50 cm stem diameter) in the P and NW plots proceeded in a similar way to that for the large trees, first by analyzing each plot separately and then combined. Normalized (n-)PCA of the P91-medium data accounted for 30.6% and 12.8% (total 43.4%) variance on axes 1 and 2, respectively, but the randomization tests indicated that

just axis 1 was significant ($P = 0.001$) and not axis 2 ($P = 0.51$). NMS gave a two-dimensional solution with 15.3% stress ($P = 0.046$ and 0.026, for axes 1 and 2). Together this suggests just one axis being important. Two groups were clearly distinguishable along this axis ($n = 24$ and 9 subplots), and the multiresponse permutation procedure (MRPP), a nonparametric test of discrimination, indicated this to be highly significantly ($P < 0.00001$). For NW03-medium data, n-PCA accounted for 25.3% and 15.2% (total 40.5%) on axes 1 and 2, again with only axis 1 significant ($P = 0.001$), and the suggested two-dimensional NMS solution had 14.1% stress ($P = 0.001$ and 0.016). As for the P91 data, one axis was considered further and two groups ($n = 15$ and 8 subplots) were readily distinguishable (MRPP, $P < 0.00001$). The combined PNW data resulted in the first three axes being significant with n-PCA ($P = 0.001$, 0.001, and 0.002), removing 25.3%, 15.2%, and 9.7% variance, total 50.2%). NMS gave a three-dimensional solution with 12.2% stress and all axes having significance at $P = 0.001$. Four groups were found ($n = 35$, 12, 5, and 4 subplots; MRPP, $P < 0.00001$), the smaller groups of the two plot ordinations splitting differently but essentially the main differences from the *Oubanguia alata*-dominated subplots were maintained. Given the small sample sizes of two groups, solutions for each plot separately are preferred. The final ordinations, the floristic composition of the groups and the indicator species are shown in Appendix D.

Removing the dominant *O. alata* from the P91 data resulted in a considerable reduction in variance on axis 1 of n-PCA (to 14.0%) but axis 2 remained similar (at 11.0%). Randomization tests were just marginally significant ($P = 0.046$ and 0.042): no groupings of subplots was evident. By contrast, removing *O. alata* and *Crateranthus talbotii* in the NW03 data increased axis-1 n-PCA variance (to 29.3%) but reduced that on axis 2 (to 8.9%): axis 1, but not 2, was significant ($P = 0.001$ and 1.0) although the same two subplot groups were obvious. Finally, removing these two species from the PNW data greatly reduced variances on axes 1–3 (to 13.8%, 9.3%, and 6.7%: total 29.8%) and, while the randomization showed axes 1 and 2 to remain significant ($P = 0.001$ and 0.002), groupings were far less clear. Thus, to detect any significant floristic patterns among the medium trees required the dominants to be included, as they very largely determined forest structure.

In the P-plot occurrences of the two groups, *O. alata*-dominated and mixed, closely match a difference in the axis-2 values of the soil PCA ($t = 2.57$, $P = 0.020$, means: 0.11 and −0.70, respectively) suggesting that the first group is more associated with soils with relatively thinner organic layers and lower phosphorus concentrations. Groups on and off a line showed a slightly smaller but more significant difference ($t = 3.00$, $P = 0.005$; means, 0.32 and −0.56). In the NW-plot occurrences of the two groups, *O. alata*/*C. talbotii*-dominated vs. *O. alata*/mixed, exactly correspond to permanently wet vs. dry soil conditions. No other differences in PCA values were significant in P plot: the P plot had relatively fewer wet subplots although these did not show as outliers on the ordinations. Tables differentiating groups among medium trees in P and NW plots are given also in Appendix D.

Associations among commoner large-treed species

From the ranked list of species' basal-area abundances of large trees in the P03 (P plot interpolated at 2003) and NW03 (NW plot directly in 2003) combined, at the 1-ha subplot scale (separately then for grids A and B, $n = 129$ subplots), the first 20 species were retained individually and all the rest bulked into a 21st "other" species. A PCA using the correlation between species (r-PCA) was run, here with the specific aim not to involve the effect of differential abundances of the dominant and commoner species, but to highlight possible associations between species after standardization. For both grids A and B the first four axes were all significant by the randomization procedure ($n = 999$): $P = 0.010$, 0.012, 0.006, 0.004; and $P = 0.004$, 0.001, 0.011, 0.021, respectively; 39.1% and 40.3% variance). Comparing the species' scores on axes 1–4 for the two grids revealed strong correlations between axis 1 of A with axis 2 of B, and correspondingly 2 with 1, 3 with 4, and 4 with 3 (reversed) ($r = 0.730$, 0.840, 0.732, and 0.603, respectively; $df = 19$, $P < 0.001$). These matching pairs of axes' scores were averaged to produce a composite species ordination (Fig. 5). Several features emerged: (1) Despite the different order of axes extracted (with regard to species weighting on them) and their high significance, the species are remarkably well separated from one another in ordination space. (2) *M. bisulcata* was weakly and inconsistently associated over the four axes with *Bikinia le-testui*, *Hallea ledermannii*, *O. alata*, and *T. bifoliolata*. (3) *T. bifoliolata* was not close to any other species, with the possible exception of *M. bisulcata* sometimes. (4) *T. korupensis*, however, was consistently associated with *Gilbertiodendron ogoouense* and *G. newberyi* across all four axes. (5) *M. bisulcata*, *T. bifoliolata*, and *T. korupensis* were together with five other species in the negative part of axis 3 vs. 13 other species in the positive part, which included *Anthonotha fragrans*, *Berlinia bracteosa*, and *Didelotia africana*. Therefore, apart from relationship of *T. korupensis* to the two *Gilbertiodendron* species there was little strong evidence of consistent associations across the P and NW plots between the species; other species tended to be more abundant in subplots where the three codominants did not occur.

Medium scale within-plot floristic variation

Aside from the three main codominant caesalps, other species of large tree were too infrequent to examine their trends across the plots and these were considered all together as a class labeled "Az." Taking first each grid in turn, percentage basal area of the three species and Az

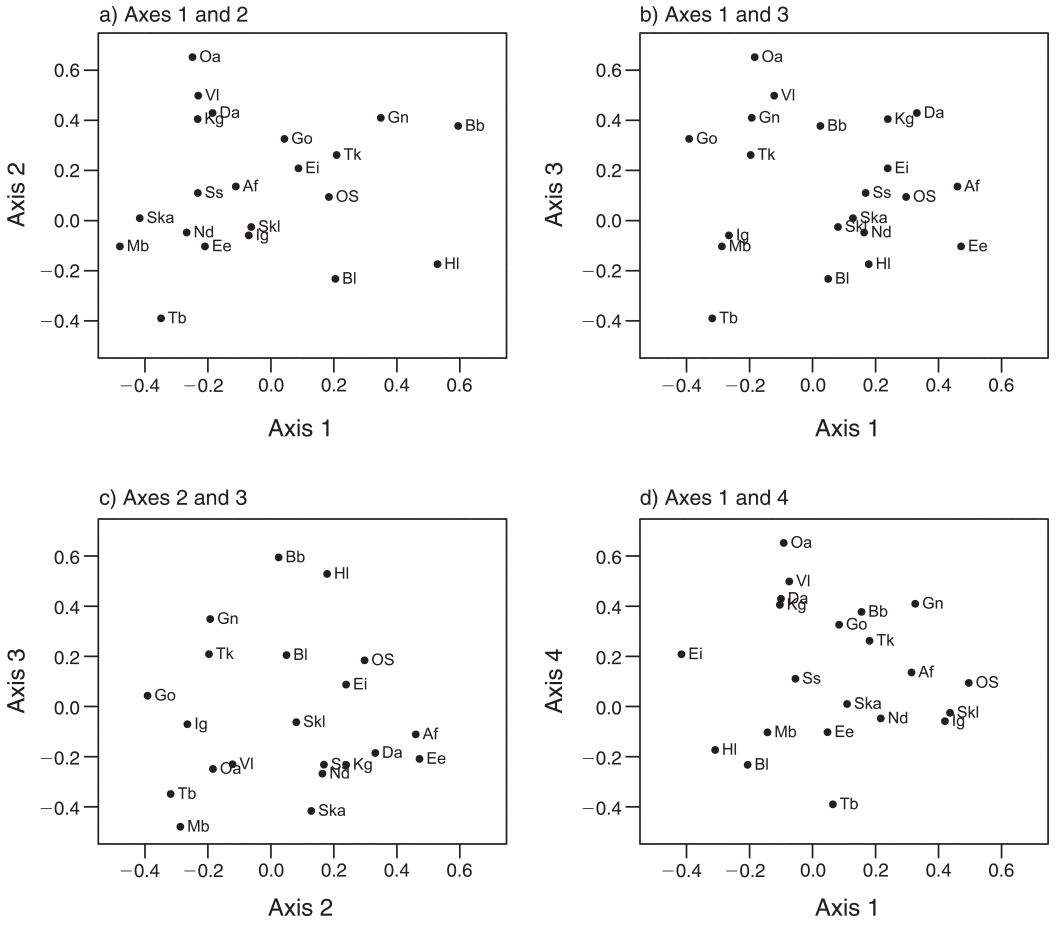

FIG. 5. Four pair-wise combinations of axis scores of the 20 most common species used in an r-PCA ordination based on basal-area abundances in 1-ha subplots of large trees interpolated for P plot as of 2003 (P03) and then combined with those of NW plot (NW03) ($n = 129$ combinations), and grouping all other species into one further "taxon." Species abbreviations are: Af, *Anthonotha fragrans*; Bb, *Berlinia bracteosa*; Bl, *Bikinia le-testui*; Da, *Didelotia africana*; Ee, *Erismadelphus exsul*; Ei, *Erythropheleum ivorense*; Gn, *Gilbertiodendron newberyi*; Go, *Gilbertiodendron ogoouense*; Hl, *Hallea ledermannii*; Ig, *Irvingia gabonensis*; Kg, *Klainedoxa gabonensis*; Mb, *Microberlinia bisulcata*, Nd, *Newtonia duparquetiana*; Oa, *Oubanguia alata*; Skl, *Scytopetalum klaineanum*; Ska, *Staudtia kamerunensis*; Ss, *Strephonema sericeum*; Tb, *Tetraberlinia bifoliolata*; Tk, *T. korupensis*; Vl, *Vitex lokundjensis*; OS, other species.

were found for each block of south-north subplots within successive 100-m west-east segments of each plot. The second percentage values for segment numbers 1–16, which overlap by 50 m in grids A and B, were averaged, a form of smoothing in the west-east direction in the P plot (and in south-north direction in the NW plot). Average elevations and stream indices were found correspondingly for these 100-m segments, with elevation in the NW plot being corrected upward by 3.63 m (an average of 3.75 m estimated by following a common edge-connecting stream, and 3.50 m from direct Garmin GPS (Garmin International, Olathe, Kansas) elevation estimates at the southeast and northeast corners of P plot and the southwest and southeast corners of NW plot (see Fig. 1) referenced to their within-plot zero elevations) to allow for difference in elevations between plots. The zero-elevation point within the P plot adjusted to be common to both it and the NW plot was accordingly 107.5 m above sea level.

The proportions of the three caesalps together increased eastward across the NW plot, declined toward the middle of the P plot, and then fluctuated to the eastern end of the P plot, returning to values close to the far west side of the NW plot (Fig. 6). *M. bisulcata* formed peaks in the middle of NW plot, western end of P plot and then two-thirds of the way along the P plot. *T. bifoliolata* had highest proportions close to where the two plots separate (western edge of the P plot and eastern edge of NW plot), while *T. korupensis* had most contribution midway along the P plot. Very approximately, where *M. bisulcata* was relatively lowest, one of the *Tetraberlinia* species was relatively highest. *M. bisulcata* peaked where the inclination was steepest but not necessarily where streams were fewest, otherwise patterns with elevation and streams were not evident at this scale (Fig. 6). Taking the P- and NW-plot segments together, the basal area of *M. bisulcata* was significantly negatively correlated with that of *T. korupensis* ($r =$

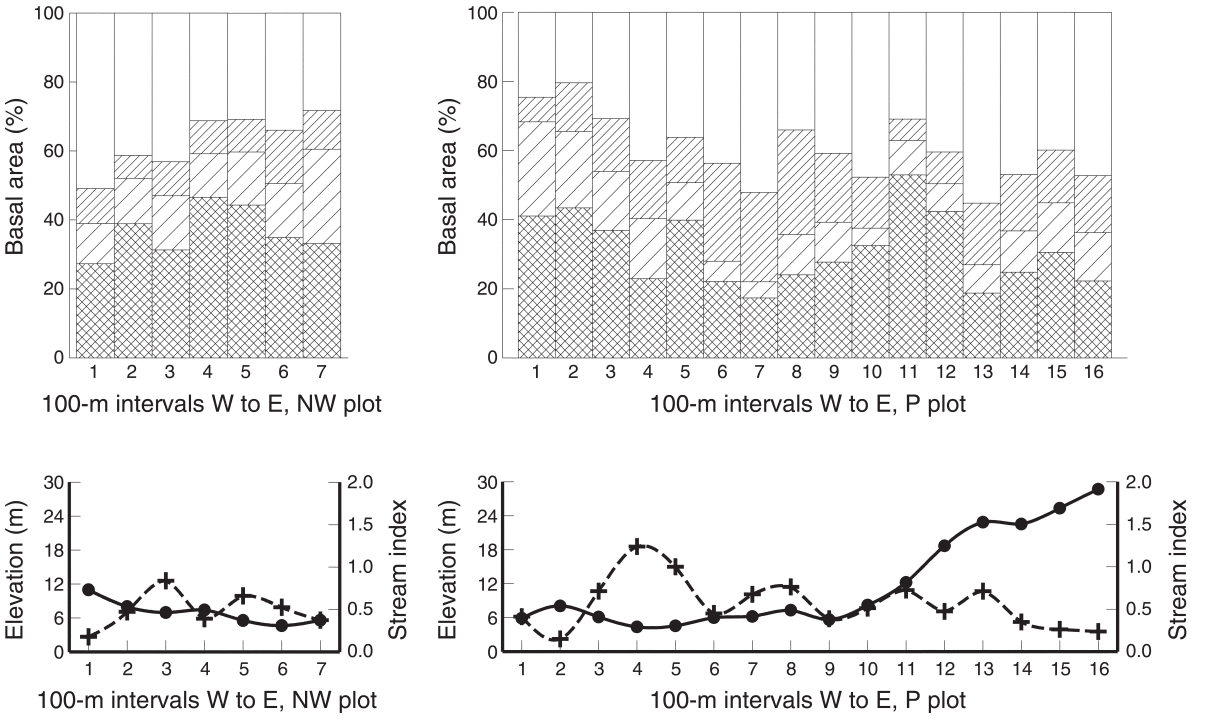

FIG. 6. Change in proportions of basal-area abundance (%) of large trees (≥50 cm stem diameter) of the three main species *Microberlinia bisulcata* (cross-hatching, lowest bar portion), *Tetraberlinia bifoliolata* (broad hatching), *T. korupensis* (fine hatching), and of all other species combined (open bars, uppermost), shown in the upper two panels as west-to-east trends within the NW and P plots (left and right); together with corresponding trends in elevation (closed circles and solid lines) and stream (density) index (crosses and dashed lines) in the lower two panels.

−0.510, df = 21, $P = 0.013$), and *T. bifoliolata* with all other species' basal area ($r = -0.708$, $P < 0.001$). Percentages of the two pairs of variables, although more strongly correlated, were not statistically independent of one another.

Population plot-maps of the three main species of interest

The focus of the paper is around the three main large caesalp species in the two plots (Fig. 7a, b). The numbers per plot, i.e., their sample sizes, shown in Table 2 indicate that these species made up almost half of all large trees but less than 3% of medium sized trees in either plot. The relative proportion of medium-sized to large trees for *M. bisulcata* was noticeably very small, and highly significantly ($P < 0.001$) less than those for the two *Tetraberlinia* species according to odds-ratio tests. Correspondingly, despite *M. bisulcata* having the most large stems in both plots its contribution to the medium size-class overall, was extremely small (~0.1%). The population sizes in Table 2 are also those used in the following section on pattern analysis.

Fine-scale spatial analysis of trees in plots

Environment.—Elevation in the P and NW plots was interpolated (akima package in R) and a pixel image at 50 × 50 m resolution built, while values of the stream index were directly imported. Scores of the first and second axes of the soils PCA were similarly treated for the P plot. After quadratic fitting on x and y, λ (tree density) was significantly positively related to elevation for *M. bisulcata* in both plots ($P \leq 0.01$), but not significantly (although positive too) for *T. bifoliolata* and *T. korupensis*. Conversely, *M. bisulcata* was significantly negatively related to the stream index in both plots at $P < 0.001$, and otherwise only *T. bifoliolata* was similarly related in the NW plot ($P < 0.02$). In the P plot, λ was positively related to soils axis 1 (decreasing nutrients) for *M. bisulcata* and *T. bifoliolata* ($P \leq 0.05$), but was nonsignificant (weakly positive) for *T. korupensis*. For soils axis 2, just *T. korupensis* was negatively related ($P \leq 0.001$). These results support the ordination analysis well: *M. bisulcata*, in particular, was highlighted as growing more on the higher ground, away from the wettest areas. The key graphics output from the following analyses are in Appendix E.

Single species.—In P and NW plots (1991 and 2003 data), the point-distance L(r) − r ($_1$Lf) and pair correlation ($_1$pcf) functions (Illian et al. 2008) were found for the large trees of the three species, with polynomial quadratic fits of intensity (λ) on x and y to correct for inhomogeneity (spatstat package version 21.1 in R; Baddeley and Turner 2005, Baddeley 2008). Changes in deviance for fits (df = 5) were high for *T.*

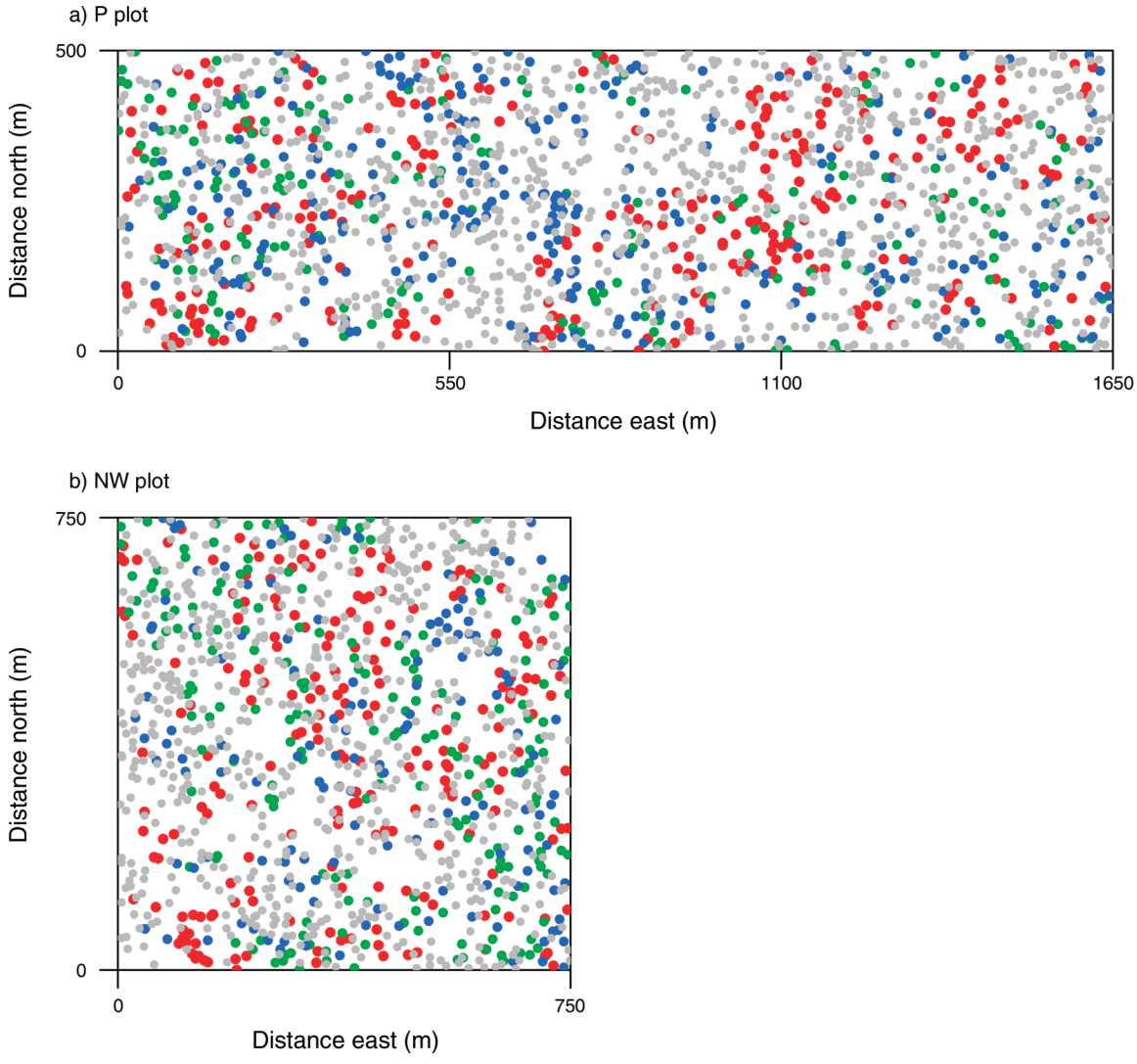

FIG. 7. Plot map distributions of large trees (≥50 cm stem diameter) of the three main species *Microberlinia bisulcata* (red), *Tetraberlinia bifoliolata* (green), *T. korupensis* (blue), and of all other species combined (dark gray) in (a) the P plot and (b) the NW plot at Korup: respective symbol sizes in the relative proportions 1.0, 0.9, 0.9–0.75 indicate approximate size ranking.

bifoliolata in both plots ($P \leq 0.01$), absent for *M. bisulcata* ($P > 0.05$) in both, and mixed for *T. korupensis* ($P \leq 0.01$ in P plot, $P > 0.05$ in NW plot). (Linear fits were insufficient, but polynomial cubic and kernal estimators overfitted.) Monte Carlo simulations ($n = 99$) provided point-wise tests of departure from randomness ($\alpha = 0.02$); a minimum distance between trees was set a priori at 15 m. *M. bisulcata* showed evidence of aggregation up to 60 m (also at $P = 0.002$) in the P plot and likewise up to 40 m in the NW plot using the $_1$Lf; this was supported by $_1$pcf, though just at 10–30 m in the P and NW plots ($P = 0.002$ and 0.02, respectively). Neither of the other species showed significant departures from randomness. For *M. bisulcata*, the result reflects its tendency to grow in small groups of 2–5 trees. Analysis of the medium-sized trees, in a parallel way to that for large trees, revealed that just *T. bifoliolata* in the P plot was marginally significantly aggregated at a scale of 10–25 m by both functions ($P = 0.02$–0.05). There was therefore little evidence of spatial patterning of the caesalp medium-sized trees in the plots.

Species pairs.—Species were paired and the bivariate functions $L_{ij}(r) - r$ ($_2$Lf) and pair correlation ($_2$pcf) found (i and j being the two species), allowing again for inhomogeneity using quadratic fits of intensity (λ_i, λ_j) on mark (i.e., positions x and y). Simulations were achieved by random relabeling of trees of each species. In the P plot, cubic polynomials improved the correction for inhomogeneity, ensuring that departures outside the simulation envelope returned within it by $r = 150$ m. *M. bisulcata* was significantly repulsed from *T. bifoliolata* and from *T. korupensis*, at distances of up to 80–100 m in the P plot according to the $_2$Lf ($P = 0.002$) and 30–40 m with $_2$pcf ($P = 0.02$–0.01); and this outcome was

TABLE 2. Numbers and relative contributions (RC) of large (≥50 cm) and medium (10 to <50 cm) stem-diameter trees in the P and NW plots for the three main caesalpiniaceous species at Korup (*Microberlinia bisulcata*, *Tetraberlinia bifoliolata*, and *T. korupensis*), with tests of significance of the relative proportions of *Tetraberlinia* spp. compared with those of *M. bisulcata*.

	Trees in stem diameter class										
	10 to <50 cm		≥50 cm		≥10 cm	≥100 cm		Odds ratio		Wald's	
	No. trees	RC (%)	No. trees	RC (%)	No. trees	No. trees	Odds	Ratio	95% CL	*z* statistic	*P*
P plot											
M. bisulcata	41	0.13	294	17.81	335	170	7.170	—		—	
T. bifoliolata	344	1.09	195	11.81	539	37	0.567	12.65	8.73–18.33	13.41	<0.001
T. korupensis	522	1.65	279	16.89	801	42	0.534	13.42	9.38–19.18	14.23	<0.001
Other species	30 673	97.13	883	53.48	31 556	46					
Totals	31 580†		1651								
NW plot											
M. bisulcata	24	0.09	219	18.34	243	129	9.122				
T. bifoliolata	322	1.27	197	16.50	519	23	0.612	14.91	9.44–23.56	11.58	<0.001
T. korupensis	438	1.73	144	12.06	582	9	0.329	27.75	17.49–44.04	14.11	<0.001
Other species	24 524	96.90	634	53.10	25 158	21					
Totals	25 308†		1194								

Notes: Relative contribution (RC) is the percentage contribution to the total. Odds = (proportion of trees ≥50 cm)/(proportion of trees 10 to <50 cm). Odds ratios (OR) are the odds of *T. bifoliolata* (Tb) and *T. korupensis* (Tk) each compared to that of *M. bisulcata* (Mb) as reference category (hence, there is no OR for Mb). Wald *z* statistic *P* values for Tb/Mb and Tk/Mb, P- and NW-plot data combined: OR = 13.41(10.07 − 17.86), $z = 17.75$ ($P < 0.001$); and OR = 17.91(13.51 − 23.75), $z = 20.02$ ($P < 0.001$), respectively.

† Estimated by scaling up from subplot sampling (see Appendix F: Tables F2a and F2b).

paralleled in the NW plot with the very similar ranges for *r* and the same *P* values. For the two *Tetraberlinia* species, there was no evidence of spatial interaction. The outcome largely reflects *T. bifoliolata* and *T. korupensis* growing apart from and around the smaller groups of *M. bisulcata*.

Size classes.—For each of the three species in the two plots, large trees were divided into two size classes of those less than and those greater than or equal to median stem diameter. Simulations for $_2$Lf and $_2$pcf (quadratic correction for inhomogeneity as for species pairs) were achieved by randomly shifting the locations of trees in the smaller size class. Size classes were positively significantly associated in the P plot at only $P = 0.05$ yet at very similar scales for all three species, namely 30–40 m for $_2$Lf and 15–30 m for $_2$pcf. In the NW plot, patterns were similar to those in the P plot but just below significance ($P > 0.05$). Therefore, the tendency for large trees to occur around very large trees was stronger in the P than NW plot.

Medium-large tree interactions, same species.—The functions $_2$Lf and $_2$pcf were found for medium and large trees of the same species, in the two plots separately, and correcting for inhomogeneity. Positions of the large trees were held fixed and those of the medium trees independently randomized many times under MC simulation. In nearly all cases, the cubic polynomial fit was much higher, and more effective at removing trends, than the quadratic fit. On that basis, $_2$Lf showed a significant negative (repulsive) association in the P plot for *M. bisulcata* at the scale 20–40 m ($P < 0.02$), and this was supported by $_2$pcf at 10–30 m ($P < 0.02$). There was a slight positive association for *M. bisulcata* in the NW plot, however, at the scale 70–100 m ($P = 0.05$) using $_2$Lf, but it was not significant with $_2$pcf. For *T. bifoliolata* in the P plot, $_2$Lf showed positive associations at 25–100 m ($P < 0.05$) and in the NW plot at 30–120 m ($P < 0.02$), correspondingly for $_2$pcf at 20–40 m and ($P < 0.05$) and 20–50 m ($P < 0.02$). For *T. korupensis*, there were no significant associations for either function or either plot ($P > 0.05$). Where $_2$pcf is used as confirmation to $_2$Lf then, to conclude, medium *M. bisulcata* trees were repelled from larger ones in the P plot up to ~40 m (but not in the NW plot); and medium *T. bifoliolata* trees were attracted to large trees in both plots up to ~100 m.

Medium-large tree interactions, different species.—The same approach was followed to test for associations between small trees of one species with large trees of each of the other two (6 species combinations × 2 plots). Medium trees of *T. bifoliolata* were significantly negative associated with large trees of *M. bisulcata* in just the P plot (20–100 m for $_2$Lf, $P < 0.01$; but 10–25 m for $_2$pcf, $P < 0.05$). Conversely, medium trees of *T. korupensis* were significantly negatively associated with large trees of *M. bisulcata* in just the NW plot (10–40 m for $_2$Lf, $P < 0.02$; but 10–25 m for $_2$pcf, $P < 0.02$). Less strong was the result that medium *M. bisulcata* trees were positively associated with large trees of *T. korupensis*, in P plot (10–50 m for $_2$Lf, $P < 0.05$; but $_2$pcf was nonsignificant). The other nine combinations showed no significant bivariate patterns. Hence, the robust conclusion is that medium trees of *T. bifoliolata* in the P plot, and of *T. korupensis* in the NW plot, were both repelled from large *M. bisulcata* trees up to ~25 m.

TABLE 3. The first 73 species in rank descending order of basal-area abundance (BA) in the composite 140-ha sample of the Korup grove for trees ≥10 cm stem diameter (≥5.0 m^2/100 ha), together with their tree densities (composite number).

Species	Composite number				BA (m^2/100 ha)
	10 to <50	50 to <100	≥100	All	
Microberlinia bisulcata	110	216	300	626	360.3
Oubanguia alata	7810	102	0	7912	275.4
Tetraberlinia korupensis	1030	373	52	1455	182.5
Tetraberlinia bifoliolata	840	333	61	1234	177.4
Crateranthus talbotii	2810	1	0	2811	63.8
Klaineanthus gabonii	1750	14	0	1764	60.8
Strephonema sericeum	490	121	2	613	51.9
Diospyros gabunensis	2520	0	0	2520	51.6
Irvingia gabonensis	330	127	1	458	46.6
Didelotia africana	440	97	1	538	41.1
Hymenostegia afzelii	1380	0	0	1380	37.4
Dichostemma glaucescens	2400	0	0	2400	35.4
Strombosia pustulata	1520	0	0	1520	34.1
Diospyros iturensis	3190	0	0	3190	33.9
Oubanguia africana	780	20	0	800	33.2
Gilbertiodendron demonstrans	1740	0	0	1740	31.2
Vitex lokundjensis	60	78	6	144	30.5
Amanoa bracteosa	630	22	0	652	29.9
Cola rostrata	1550	0	0	1550	26.2
Bikinia le-testui	60	35	15	110	24.4
Cola lateritia	430	16	0	446	24.2
Amanoa strobilacea	440	25	0	465	23.6
Berlinia bracteosa	180	43	2	225	21.7
Garcinia staudtii	1750	0	0	1750	21.6
Anthonotha fragrans	160	46	1	207	21.5
Uapaca staudtii	660	2	0	662	20.9
Baphia leptostemma	830	3	0	833	20.5
Coula edulis	360	16	0	376	18.7
Mammea africana	360	12	0	372	18.5
Gilbertiodendron ogoouense	80	35	4	119	17.0
Erythrophleum ivorense	20	28	6	54	16.8
Scytopetalum klaineanum	250	32	0	282	16.3
Cola verticillata	260	11	0	271	16.2
Diospyros gracilescens	160	9	0	169	13.7
Strombosiopsis tetrandra	390	8	0	398	13.7
Hallea ledermannii	60	48	0	108	13.4
Vangueriella nigricans	740	0	0	740	13.2
Talbotiella korupensis	440	1	0	441	13.0
Newtonia duparquetiana	130	35	0	165	12.9
Gilbertiodendron newberyi	30	12	8	50	12.2
Magnistipula glaberrima	500	0	0	500	11.7
Berlinia auriculata	640	0	0	640	11.6
Staudtia kamerunensis	50	29	2	81	11.3
Manilkara lososiana	620	1	0	621	11.2
Xylopia aethiopica	230	3	0	233	10.5
Erismadelphus exsul	60	25	0	85	9.6
Endodesmia calophylloides	110	13	0	123	9.4
Symphonia globulifera	150	9	0	159	9.3
Diogoa retivenia	650	0	0	650	9.2
Garcinia gnetoides	890	0	0	890	8.9
Nauclea vanderguchtii	120	4	0	124	8.8
Dialium pachyphyllum	300	0	0	300	8.2
Carapa parviflora	500	0	0	500	8.2
Hymenostegia bakeriana	80	18	0	98	8.1
Anisophyllea purpurascens	180	8	0	188	7.8
Vitex grandifolia	250	0	0	250	7.3
Warneckea austro-occidentalis	380	0	0	380	7.2
Calpocalyx dinklagei	430	0	0	430	6.7
Didelotia afzelii	270	0	0	270	6.7
Diospyros hoyleana	630	0	0	630	6.7
Afzelia bella	100	16	0	116	6.5
Hypodaphnis zenkeri	90	4	0	94	6.5
Oncoba glauca	120	5	0	125	6.3
Alstonia boonei	10	19	0	29	5.9
Klainedoxa gabonensis	0	7	5	12	5.6
Anisophyllea polyneura	140	3	0	143	5.6
Annickia affinis	210	0	0	210	5.5

TABLE 3. Continued.

Species	Composite number				BA (m^2/100 ha)
	10 to <50	50 to <100	≥100	All	
Dialium guineense	90	11	0	101	5.4
Newtonia griffoniana	30	20	0	50	5.4
Scytopetalum tieghemii	80	3	0	83	5.3
Crudia ledermannii	40	10	0	50	5.2
Klainedoxa trillesii	10	9	1	20	5.1
Anthocleista vogelii	130	1	0	131	5.0
Totals (73 species)	47 260	2139	467	49 866	2229
Density (trees/ha)	337.6	15.3	3.3	356.2	NA
Totals (all species)	57 450	2395	480	60 325	2477

Notes: The composite number for tree density is the number per 140 ha, with exact counts for trees ≥50 cm diameter, scaled-up 10-fold for smaller trees. The abundances of the remaining, less abundant, 172 species are listed in Appendix G. NA stands for not applicable.

Combined abundance table

The six data sets (P91, P05, PE00 and NW03 for large trees, and P91 and NW03 for medium-sized trees) contained 252 species. Of these, 14 were recognized as taxa to genus level only and three to family level only (Appendix B). These last represented 1.6% of all trees, and with 0.4% completely unknown, identification to the species level was 98.0%. Density (trees/plot) and basal area (m^2/ha) abundances of species in each of these six sets were separately tabulated: the large- and medium-sized tree lists are given in Appendix F: Table F1a–d and Table F2a–b. Large and medium-sized trees were also combined for P91 and NW03 separately by scaling up the estimates for medium-sized trees in the subplots to the whole-plot areas of the large trees. For the P plot, this was simply a 10.0-fold factor; for NW03 the corresponding factor was 9.783-fold (Appendix F: Table F2c–d). Numbers of trees were found in increasing 10-cm diameter classes for each of the resulting eight data sets.

Because the ordination results suggested little multi-species heterogeneity, gradients, or clustering, both within and between plots, compositional data were combined on a 140-ha basis. This was achieved in the following way. The medium tree data came from 8.25 and 5.75 ha in the P and NW plots, respectively, summing to 14 ha. The large-tree whole-plot areas were correspondingly 82.5 and 56.25 ha, summing to 138.75 ha. To make up the latter's shortfall of 1.25 ha, i.e., to bring the sampled area for large trees to 140 ha, five subplots from the PE00 extensions were added, one each closest to the P-plot perimeter in each of the extensions that had trees of *M. bisulcata*. Scaling up the 14 ha of medium-sized tree data 10-fold allowed an optimal presentation of 140 ha of grove complex. Table 3 shows the first 72 species (ranked by basal-area abundance) that had ≥5 m^2/100 ha; with the remaining 173 species continued in Appendix G. That there were 245 species in this sample, seven less than in the six data sets together, was due to not all of the PE00 subplots being used to form the 140-ha sample.

The degree of similarity in species' rank abundances between P and NW plots was remarkable (Fig. 8). Taking density and then basal-area abundances in turn, and comparing P91 with NW03 or P05 with NW03, abundances were first ranked and species matched for the first plot's data and this then repeated with the second plot's ranking. Percent similarity, PS (or 1 − [Bray and Curtis Index]) was found incrementally for lists running from rank 1 to n (maximum, 60) and the average PS per rank found. Plotted on a ln–ln basis, PS declined linearly with rank in all four cases (2 plots × 2 abundance measures; Fig. 8; $P < 0.0001$; $R^2 > 97\%$). A similar analysis using the medium tree data for P91 and NW03 showed no such relationship; it had a mixed and complex cubic-like form with much scatter.

The most abundant (73) species in the 140-ha sample represented 82.7% of the total density and 90.0% of the total basal area of trees ≥10 cm diameter. In the 10 to <50, 50 to <100, and ≥100-cm size classes, the corresponding proportions were 82.3%, 89.3%, and 97.3% (Table 3, Appendix G). Frequencies of species in abundance classes (i.e., numbers of trees/species), for large and medium-sized trees in P91 and NW03 (not shown), declined approximately linearly and showed no modal values among the large trees, but there was a hint of a mode at class 2 for the medium trees. Fits of the log-normal model were poor (P of deviance of fit [approximately χ^2-distributed], 0.42–0.97). The most likely reason is that the area sampled, for the other large tree species especially, was not sufficiently large and, aside from the obvious taxonomic problems of rarer taxa, this was a main reason to focus on the abundant tree species in the plots.

Rank-abundance curves

Ranked abundances of species of both large and medium-sized trees in the P and NW plots (Fig. 9) fitted the Zipf-Mandelbrot (Z-M) model very well for basal area, also well for density of medium trees but rather less well for the density of large trees (Table 4; Appendix H, using the ECFIT maximum likelihood procedure in GenStat [version 13 (Payne et al. 2009)]). The model is

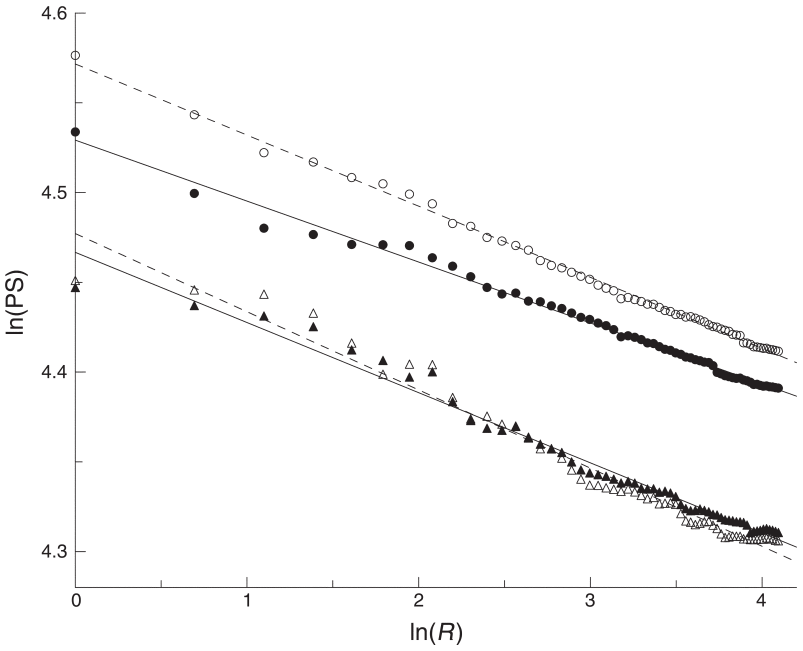

FIG. 8. Percentage similarity (PS) in density (den; triangles) and in basal-area (ba; circles) abundance of large trees (≥50 cm stem diameter) in the P plot in 1991 (P91, solid symbols) or in 2005 (P05, open symbols), and the NW plot in 2003, for increasing numbers of species as defined by their respective density and basal-area ranking (R; highest to lowest per plot and date). Linear regression fits (all cases $P < 0.001$): $\ln(PS_{den\_P91}) = 4.47 - 0.039 \ln(R)$, $r^2 = 0.981$; $\ln(PS_{den\_P05}) = 4.48 - 0.044 \ln(R)$, $r^2 = 0.972$; $\ln(PS_{ba\_P91}) = 4.53 - 0.034 \ln(R)$, $r^2 = 0.992$; $\ln(PS_{ba\_P05}) = 4.57 - 0.040 \ln(R)$, $r^2 = 0.997$.

given by $\eta_i = c/(i + \beta)^{\gamma}$, where c is a constant ($=\eta_1$), i is the species rank, and β and γ are parameters. Best fits excluded the rare tail species (as defined in Table 4) but good fits were also obtained for all species, their estimates of γ being similar although those for β were slightly higher. Table 4 shows that γ was different from 1.0 (the simpler Zipf model), and except in one case β was different from 0.0. The less good fits in Appendix H: Fig. H1a, b concern the first eight species. For basal areas of large trees *M. bisulcata*, *T. bifoliolata*, and *T. korupensis* fall well on the line, but then follows a step down to the 12 next-ranked species in the P plot; in the NW plot, the step down to the next 15 species is less pronounced and the series is broken into three parts. It would be hard to conceive of a model that could accommodate these "steps." Nevertheless, the segments straddle the line with species before and after fitting very well for the P plot, a little less so for the NW plot. (The species associated with the points are those listed in the tables in Appendix F). Simpson's index of dominance, D ($1 - D$ being also an index of diversity with emphasis of the most abundant species) was higher for basal area than density abundances, and higher for large than medium-sized trees, in both plots (Table 5). The NW plot showed higher dominance than the P plot for large trees, but the converse was the case for medium-sized trees.

In the P plot for large trees, the three most abundant species appeared in the order *M. bisulcata*, *T. korupensis*, and then *T. bifoliolata*, while in the NW plot, the latter two are reversed in position. Of the next 12 in P91, eight are among the next 15 in the NW03, showing a high degree of dominance consistency. For medium-sized trees in the P plot, one species alone, *O. alata*, was outstandingly dominant (Fig. 9) but in the NW plot it was accompanied by the abundant subdominant, *C. talbotii*. After *O. alata* in the P plot, of the 14 next most abundant species, eight of them occurred within the 14 next in the NW plot, again demonstrating a considerable concordance. Removing the three large-tree dominants, and the one or two medium dominants, in P91 and NW03, led to much improved fits of the Zipf-Mandelbrot model.

Given that the Z-M model represents a "natural order of things" these dominants are superdominants, i.e., dominant at proportions above what might be expected. Polynomial (cubic) regressions were fitted to the expected frequencies ($\log_{10}$-transformed) of first 15 species from the Z-M models vs. rank on the above data sets lacking their corresponding dominants. Fits were almost perfect, with adjusted R^2 values of 100%. The equations were used to extrapolate the curves obtained to the left of, and including for reference, rank 1, i.e., what would be expected for "ranks" 0, −1, and −2, where 1, 2, or 3 dominant species had been removed. The expected frequencies, after back-transformation, were compared with the observed ones (Fig. 10). Since the fits of the Z-M model to the data without dominants had ~1/10th the residual deviances compared to the fits to data with them, the former were taken as the "base

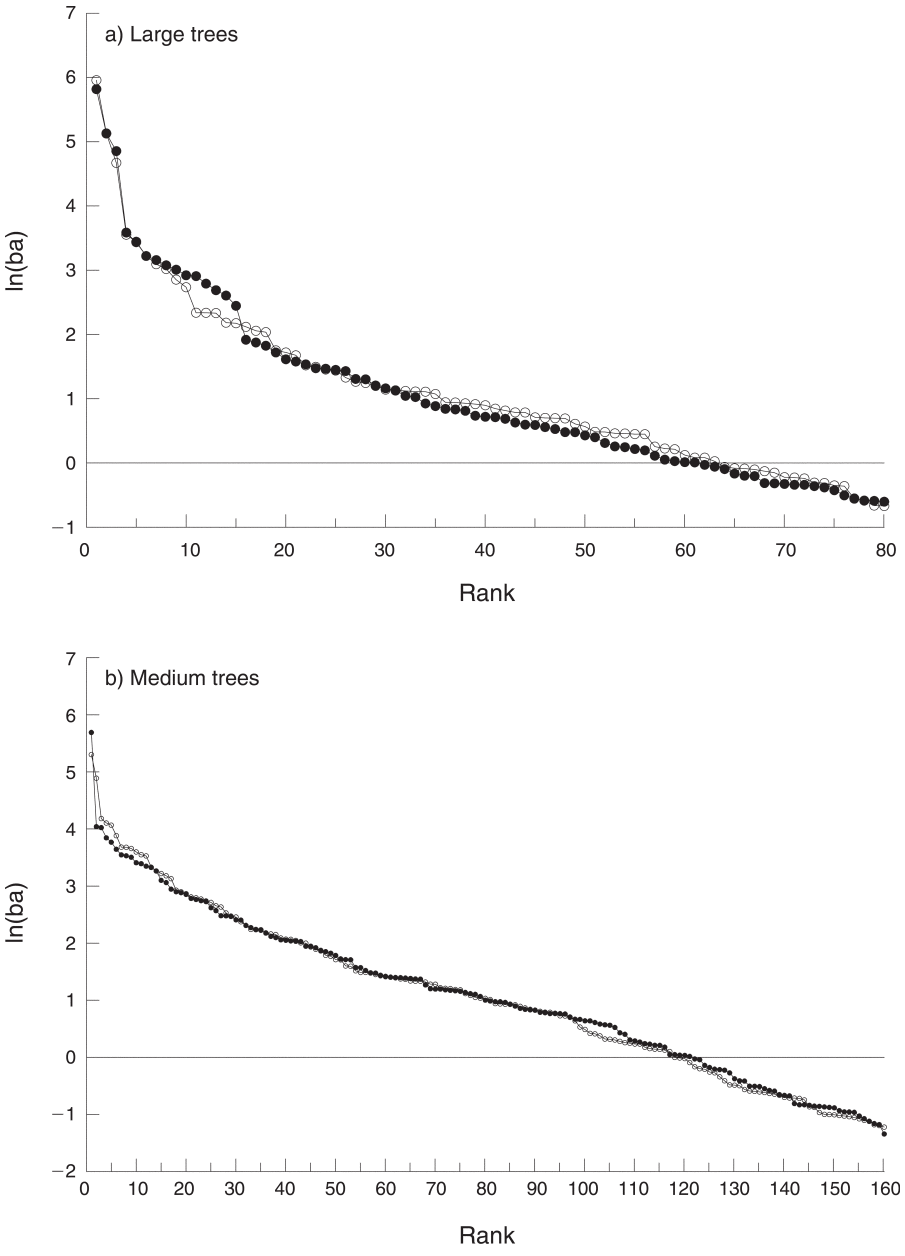

FIG. 9. Rank basal-area abundance curves for (a) large (≥50-cm stem diameter) and (b) medium-sized (10 to <50-cm) trees in the P plot in 1991 (solid circles) and in the NW plot in 2003 (open circles).

ordering of species": the mean value of ln (observed/expected) for the classes concerned is termed here the degree of overdominance (Dod). The Dod-value was higher for basal area than density abundance, and highest for large and medium-sized trees in the P plot (Table 5).

Size-class distributions

All trees ≥10 cm diameter.—The relationship between ln(number of stems per 10-cm or stem diameter class) was sigmoidal for both the P (1991) and the NW (2003) plots (Fig. 11). Beyond 150 cm diameter, frequencies per class became very small and variable. On removing the three main caesalp species, the curves noticeably straightened (although not so much when removing just *M. bisulcata*). Removing *O. alata* had little effect, however, on the change in overall shape.

Main caesalps ≥10 cm diameter.—The three caesalp species mapped down to 10 cm stem diameter across the whole-plot areas allowed a complete assessment of their size-class distributions above this limit, especially for those species with few medium-sized stems. For the P plot, medium-sized trees (10 to <50 cm diameter) recorded in 2004 were combined with adults (≥50 cm)

TABLE 4. Fitted parameters (γ and β) to the Zipf-Mandelbrot model (mean ± SE), with residual deviances (dev.), for large and medium trees in P and NW plots and both tree density and basal-area abundances, with and without dominant species (see Appendix H).

Abundance measure	With dominant species				Without dominant species			
	γ	β	df	dev.	γ	β	df	dev.
Density (number/plot)								
Large, ≥5								
P 1991	1.72 ± 0.12	2.40 ± 0.55	38	57.3	1.90 ± 0.41	8.84 ± 3.91	35	8.82
NW 2003	1.61 ± 0.15	1.91 ± 0.60	30	43.8	1.55 ± 0.47	6.57 ± 3.91	27	5.67
Medium, ≥10								
P 1991	0.82 ± 0.03	−0.29 ± 0.10	56	68.8	1.38 ± 0.14	7.62 ± 1.96	55	10.78
NW 2003	1.43 ± 0.11	4.42 ± 0.90	48	14.9	1.53 ± 0.19	8.00 ± 2.35	46	8.31
Basal area (m^2/100 ha)								
Large, ≥1.0								
P 1991	1.56 ± 0.08	0.49 ± 0.21	58	42.0	2.34 ± 0.61	13.48 ± 6.76	55	6.72
NW 2003	1.42 ± 0.07	0.01 ± 0.14	60	23.9	1.53 ± 0.30	5.87 ± 3.07	57	2.06
Medium, ≥5.0								
P 1991	0.63 ± 0.03	−0.82 ± 0.05	50	41.6	1.85 ± 0.56	18.89 ± 10.06	49	1.74
NW 2003	0.96 ± 0.06	0.59 ± 0.35	48	19.4	1.85 ± 0.49	15.97 ± 7.80	46	2.51

Note: Threshold abundances are shown after the size class name in the left-most column.

remeasured in 2005 (P05) and, for the NW plot, medium-sized trees of 2005 were combined with adults of 2003 (NW03), these being the closest matches in census timing. *M. bisulcata*, *T. korupensis*, and *T. bifoliolata* had similarly shaped distributions in the P and NW plots, with *M. bisulcata* showing a pronounced and characteristic mode around 100–120 cm diameter, very few stems ~40 cm, yet the numbers increasing slightly toward 10 cm ($\chi^2_{15} = 19.2$, $P = 0.20$; Fig. 12a). Indeed, the numbers of trees of *M. bisulcata* in the four successive 10-cm diameter classes between 10 and 50 cm in the P plot were 16, 15, 7, and 3 and, for the NW plot, the numbers were correspondingly 10, 6, 5, and 3. In marked contrast, the two *Tetraberlinia* species showed strong decreases in their frequencies between the 10- and 20-cm classes, and then a gradual tailing off toward the larger size classes (Fig. 12b, c). The *Tetraberlinia* species did differ slightly in their relative frequencies across classes between plots, but not significantly so (*T. korupensis*, $\chi^2_{10} = 21.4$, $P = 0.019$; *T. bifoliolata*, $\chi^2_{10} = 22.5$, $P = 0.013$).

Main caesalps 1 to <10 cm diameter.—In the 33 strips (5 × 50 m) in the P plot in 1991, there were 4, 146, and 76 saplings of *M. bisulcata*, *T. bifoliolata*, and *T. korupensis*, respectively, with corresponding densities of 4.8, 177.0, and 92.1 trees/ha (as reported in Newbery et al. [1998]). In the 23 strips (10 × 50 m) in the NW plot in 2003, there were 4, 163, and 147 saplings of *M. bisulcata*, *T. bifoliolata*, and *T. korupensis*, respectively, with corresponding densities of 3.5, 141.7, and 127.8 trees/ha. Counts per 250-m^2 strip area did not differ significantly for *T. bifoliolata* and *T. korupensis* (GLM with Poisson error model and log-link function, quasi-$F_{1,54} = 0.73$ and 2.08, respectively, $P > 0.15$; for *M. bisulcata*, there were too few saplings to make a test). Densities in 1-cm diameter classes decreased more steeply for *T. bifoliolata* than for *T. korupensis* but in a rather similar manner in both plots (Fig. 13). Mean diameters were quite similar in the two plots for each species: *M. bisulcata* (2.16 vs. 2.23 cm), *T. bifoliolata* (1.91 vs. 2.13 cm), and *T. korupensis* (2.66 vs. 2.70 cm). The extreme lack of *M. bisulcata* saplings in both plots, in comparison to the two other species, is very apparent from Fig. 13.

Other large-treed species.—Among the 73 most abundant species in the composite 140-ha list (Table

TABLE 5. Simpson's diversity index and bootstrapped standard errors for large and medium trees in P and NW plots and both tree density and basal-area abundances, with and without dominant species; and the degree of overdominance (Dod) as calculated by the Zipf-Mandelbrot model (see Appendix H).

Abundance measure	Simpson's *D*		Dod†
	With dominants	Without dominants	
Density (number/plot)			
Large			
P 1991	8.47 ± 0.40	3.75 ± 0.21	0.293
NW 2003	8.51 ± 0.41	3.52 ± 0.26	0.306
Medium			
P 1991	4.64 ± 0.19	2.41 ± 0.08	0.427
NW 2003	3.51 ± 0.13	2.64 ± 0.10	0.080
Basal area (m^2/100 ha)			
Large			
P 1991	15.37 ± 0.89	3.95 ± 0.30	0.561
NW 2003	17.92 ± 1.07	3.75 ± 0.31	0.455
Medium			
P 1991	5.62 ± 0.44	2.08 ± 0.09	0.674
NW 2003	3.95 ± 0.22	2.33 ± 0.10	0.317

Note: Values for Simpson's *D* are means ± SE and have been multiplied by 100.

† When observed abundance equals expected, Dod = 0.0.

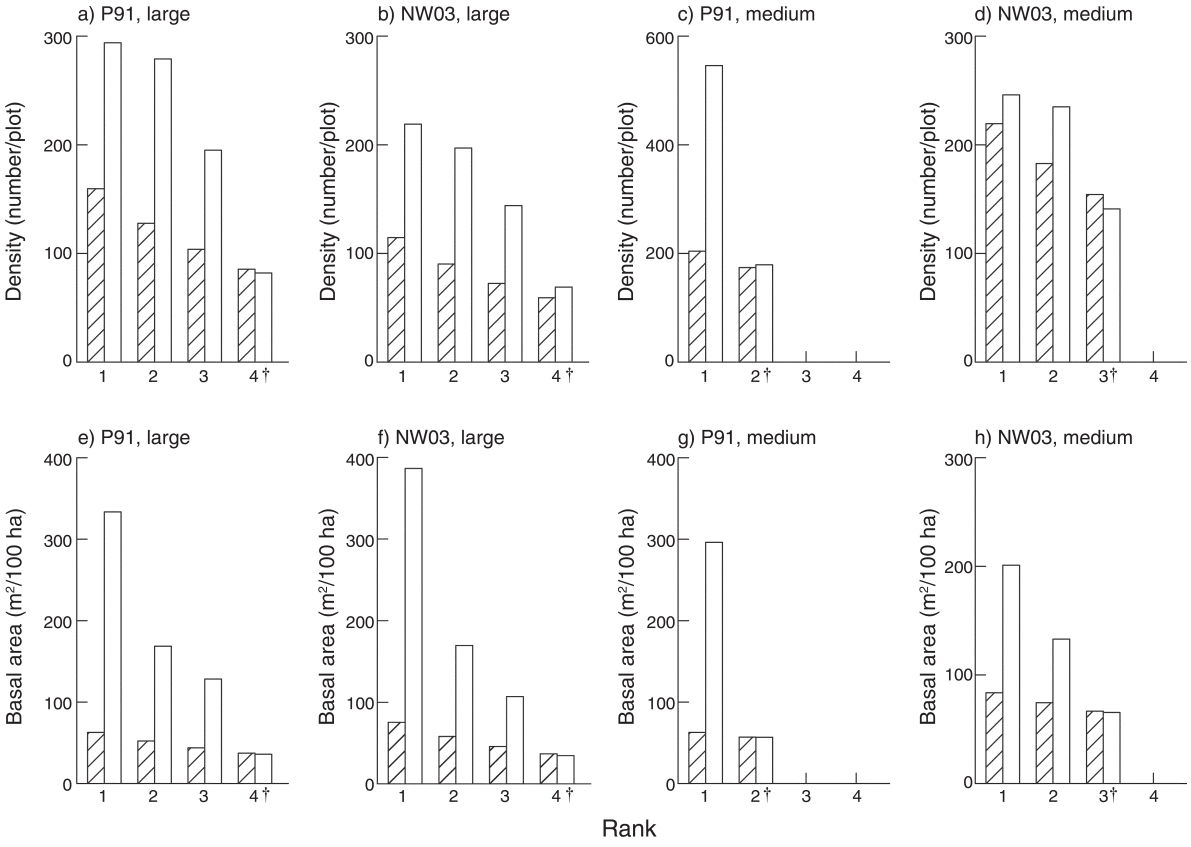

FIG. 10. Degree of overdominance (DoD) shown by comparisons of observed abundances of tree species (open bars) and those predicted from fitted Zipf-Mandelbrot models based on species beyond the indicated number first-ranked (rank greater than that marked with dagger †; hatched bars), for the eight combinations of plot (P, NW), abundance variable (density, basal area) and tree size class (large, medium).

3), 23 had ≥20 trees with stem diameters ≥50 cm. Leaving the three above-analyzed caesalps aside, the diameter frequencies of trees ≥10 cm belonging to the other 20 were examined using six 20-cm classes (10 to <30, 30 to <50, . . . , ≥110 cm; Fig. 14). Nine species (*Bikinia le-testui*, *Erismadelphus exsul*, *Erythrophleum ivorense*, *Gilbertiodendron ogoouense*, *G. newberyi* (new species to Korup [van der Burgt et al. 2012]), *Hallea ledermannii*, *Newtonia griffoniana*, *Staudtia kamerunensis*, *Vitex lokundjensis*) had flat, or near-to-flat, distributions; while the other 11 had decreasing numbers with increasing size (Fig. 14). The two species in each of the two genera *Amanoa* and *Oubanguia* had many more trees in the 10 to <30 and 30 to <50-cm classes than higher ones because they are characteristically understorey–subcanopy species, while the other seven are main canopy species. Together with *M. bisulcata* the proportion of species with very few small compared to large trees is 10/23 or 43.5%.

Population dynamics

Large trees.—Of the 1651 (20.0 trees/ha) large trees in the P plot recorded in 1991, 300 (18.2%) had died by 2005 and 249 (15.1%) had recruited into the ≥50-cm stem diameter class (Table 6), leading to annualized mortality and recruitment rates of 1.42 and 1.22% per year respectively, and a population of 1600 (19.4 trees/ha) in 2005. (The formulae are given in Table 6.) The first 25 ranked species with ≥10 trees in the plot in 1991 made up 86% of the trees in all, and their mortality and recruitment rates (taken together) were slightly less than those for the plot overall (Table 6). In particular, the recruitment rate of the 88 other rarer species together was three times higher than that of the commoner species. Correspondingly, the turnover rate of the rarer species was twice that of the more common species, leading to an overall plot value of 1.22% per year. The common species had decreasing population sizes over the 14 years, while the rarer species had increasing population sizes (Table 6). Of the large trees, none was left undetermined.

Among the 25 commoner species of large trees, annual mortality rate (m_a) ranged from 0.0 to 6.34% per year, this last value (for *N. duparquetiana*) being a distinct outlier since the next highest value was with 2.85% per year (Table 6). Apart from the zero rate (for *C. verticillata* with only $n = 10$ trees), *M. bisulcata*, the dominant species in P plot, had a very low rate of 0.22%

per year, and large trees of the dominant species in the medium size class *O. alata* had an even lower rate at 0.11% per year. The contrast between the m_a of *M. bisulcata* and that of a group of other main ectomycorrhizal species, viz. the two *Tetraberlinia* species, *D. africana*, and *B. le-testui* (2.05–2.85% per year) is very striking (an ~10-fold difference). Other ectomycorrhizal species, *A. bella*, *A. fragrans*, *B. bracteosa*, and the two *Gilbertiodendron* species had lower values (0.37–1.86% per year), nevertheless, still much higher than for *M. bisulcata* (an approximately fivefold difference on average). The non-ectomycorrhizal species showed quite variable rates but tended to be placed toward the lower end of the m_a range.

Annual recruitment rates (r_a) had a much less consistent pattern than mortality rates, indeed r_a was poorly correlated with m_a ($r = -0.086$, df = 22, excluding the outlier mentioned; $P = 0.69$). Aside from two species with zero rates (with $n = 10$–13 trees), *M. bisulcata* had the lowest r_a of 0.17% per year. All other rates were >0.50, ranging up to 2.66 (*Amanoa bracteosa*), and then finally the outlying 5.17% per year for *N. duparquetiana* (Table 6). Values of r_a varied widely across the other main ectomycorrhizal species (0.34–1.40% per year). Interestingly, the two *Tetraberlinia* species had r_a values less than half their m_a values; and the dominant medium-sized tree species, *O. alata*, had a relatively very high r_a (1.79% per year) compared with its very low m_a (an ~16-fold difference). As a consequence of these two dynamic rates, *M. bisulcata* had the lowest turnover rate of all (0.20% per year), and the other grouped main ectomycorrhizal species among the highest (0.84–1.74% per year). Thus, while *M. bisulcata* was remaining remarkably stable with near-zero population change from 1991 to 2005, the two *Tetraberlinia* species, *D. africana*, *B. le-testui*, and *A. bella* were declining (Table 6). Most of the other species, those less numerous among the 25, were conversely increasing over the census period.

Omitting *M. bisulcata*, the rates of all 112 other species, taken together, increased appreciably because both the rates for *M. bisulcata* were so low and it was the commonest species (Table 6). Finally, neither m_a, r_a, nor turnover were significantly correlated with $\ln(n_{91})$ (the number of trees alive in 1991; $r = 0.176$, $P = 0.41$; $r = -0.359$, $P = 0.085$; $r = -0.089$, $P = 0.68$, respectively), showing that the situation of *M. bisulcata* was unlikely to have been due to its high abundance per se.

Confirmatory data for the three most abundant species' m_a rates was obtained from the NW plot. In the period 2003–2009 (5.86 yr), three of 215 *M. bisulcata*, 14 of 183 *T. bifoliolata*, and 15 of 130 *T. korupensis* trees died; the rates were correspondingly 0.23%, 1.25%, and 1.85% per year. The agreement with the P-plot results (Table 6) for *M. bisulcata* was excellent: for the two *Tetraberlinia* species, m_a rates were, however, 60–70% those in the P plot. Of the 634 large trees of the other (Az) species, 41 had died by the start of 2011 (7.75 yr) giving a m_a of 0.86% per year. Furthermore, from the restart of phenological recording on 1 January 2010, two of 63 large *M. bisulcata* trees in the P plot had died since a mean date of 17 February 2005 ($m_a = 0.66\%$ per year). The smaller plot at Isangele Road revealed similar results too. One of 33 and four of seven trees of *M. bisulcata* and *T. korupensis*, respectively, died in the 16.39-yr interval, giving m_a values of 0.19% and 3.36% per year.

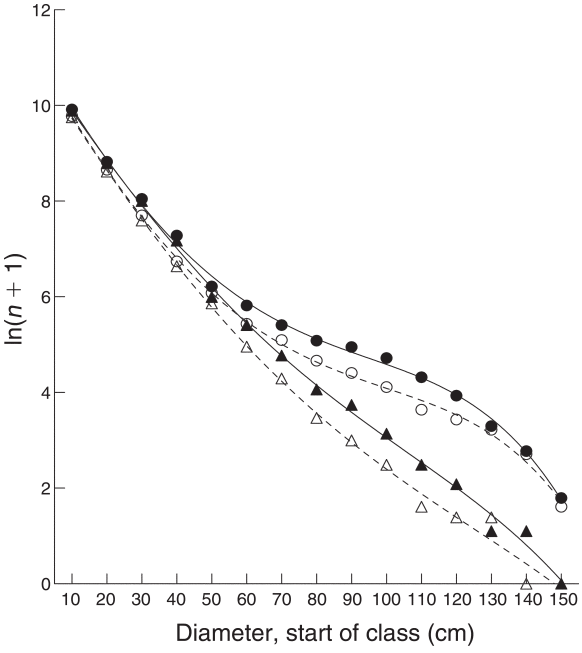

FIG. 11. Frequency distributions (ln-transformed, f) of number of trees ≥10 cm stem diameter (n) of all species in increasing 10-cm diameter classes (d, midpoint) in the P and NW plots at Korup (all; solid and open circles, respectively) and after removal of the three main species (MTT; solid and open triangles). Quartic-equation regression fits (all cases $P < 0.001$; $r^2 = 0.998$–0.999): $f_{P,all} = 11.14 - 1.244d + 0.0461d^2 + 0.00448d^3 - 0.00032d^4$; $f_{NW,all} = 10.97 - 1.240d + 0.0332d^2 + 0.00547d^3 - 0.000328d^4$; $f_{P,MTT} = 10.95 - 1.085d + 0.0151d^2 + 0.00315d^3 - 0.00017d^4$; and $f_{NW,MTT} = 10.87 - 1.163d + 0.0216d^2 + 0.00206d^3 - 0.000105d^4$.

Medium trees.—For medium trees in the subplots, the sample of 3168 (384 trees/ha) trees in 1991 had 507 (16.0%) deaths by 2005 giving an overall mortality rate of 1.17% per year (Table 7). Among the 33 first-ranked commoner species with ≥20 trees in the subplots in 1991 (making 75.5% of the sample) the mortality rate was very slightly less at 1.12% per year. The other 153 rarer species included an entry for undetermined species. These last were the 24 unnamed trees in 1991 that had died by 2005, mostly recorded as missing and no tag recovered. It is possible that a few of them belonged to common species though the likelihood is low because common species were the best identifiable in 1991. Mortality rates ranged from zero to 3.13% per year, then the more exceptional value of 5.65% per year for *Calpocalyx dinklagei*. *Oubanguia alata* had the fourth

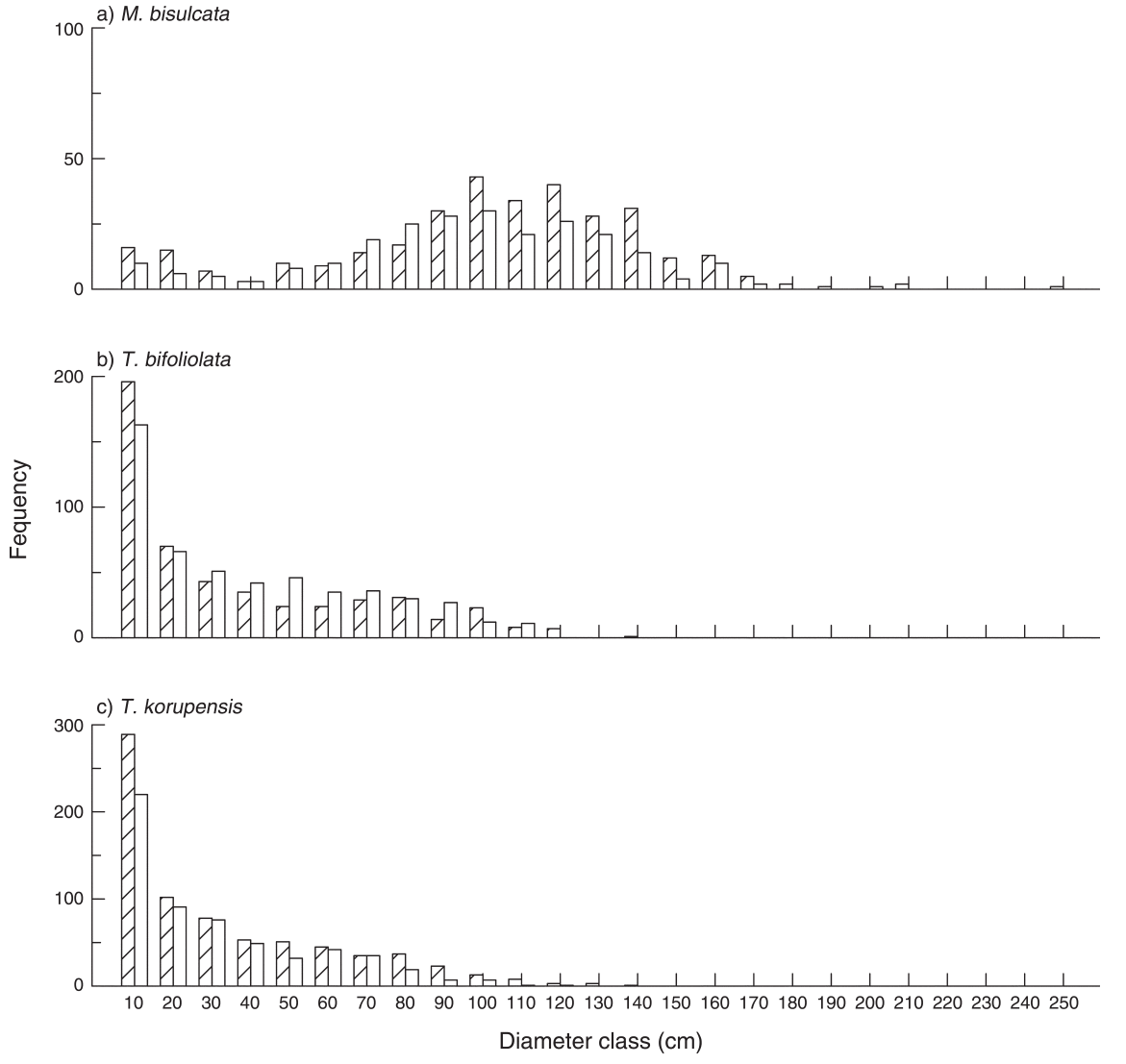

FIG. 12. Frequency distributions of trees ≥10 cm stem diameter of the three main species: (a) *Microberlinia bisulcata*, (b) *Tetraberlinia bifoliolata*, and (c) *T. korupensis*, in increasing 10-cm diameter classes in the P (hatched) and NW plots (open bars).

lowest m_a rate, but this rate of 0.39% per year is important given the clear dominance of *O. alata*. Although *M. bisulcata* trees were too few ($n = 6$ trees) for Table 6 as such, none died by 2005 so the m_a was 0.00% per year. *T. bifoliolata* and *T. korupensis* had above-average m_a rates (1.82% and 1.32% per year, Table 7), less than those for their large trees and among them in the reverse order. *C. talbotii*, codominant and abundant in the NW plot, here in P plot had a close-to-average m_a rate (Table 6). Omitting *O. alata* resulted in an m_a rate higher than that for all species together and almost identical to the value for the rarer species (Table 7). The m_a rate across the 33 common species was again not significantly correlated with $\ln(n_{91})$ ($r = -0.125$, df = 31, $P = 0.49$).

From the subsets of medium trees 10 to <50 cm stem diameter of the three main species in the P plot revisited for growth between 2004 and 2008, two of 40 *M. bisulcata* ($m_a = 1.33\%$ per year), none of 40 *T. bifoliolata* ($m_a = 0.00\%$ per year), and three of 59 *T. korupensis* ($m_a = 1.34\%$ per year), had died. From the repeat of the 2003 census of the NW plot in 2005, for the same size class, none of the 24 trees of *M. bisulcata* died ($m_a = 0.00\%$ per year), but seven of 329 *T. bifoliolata* (1.06% per year) and nine of 447 *T. korupensis* (1.00% per year) did die. At Isangele Road, among the medium-sized trees of Az species, m_a was 0.95% per year. In this plot's subplots, there were no medium-sized trees of *M. bisulcata* recorded in 1995, just four of *T. korupensis*, and none of *T. bifoliolata*.

Mortality and recruitment with tree size.—Within the large trees, mortality rates (m_a) in the 50 to <100-cm and ≥100-cm stem diameter classes in the P plot were, respectively, 0.12% and 0.30% per year for *M. bisulcata*,

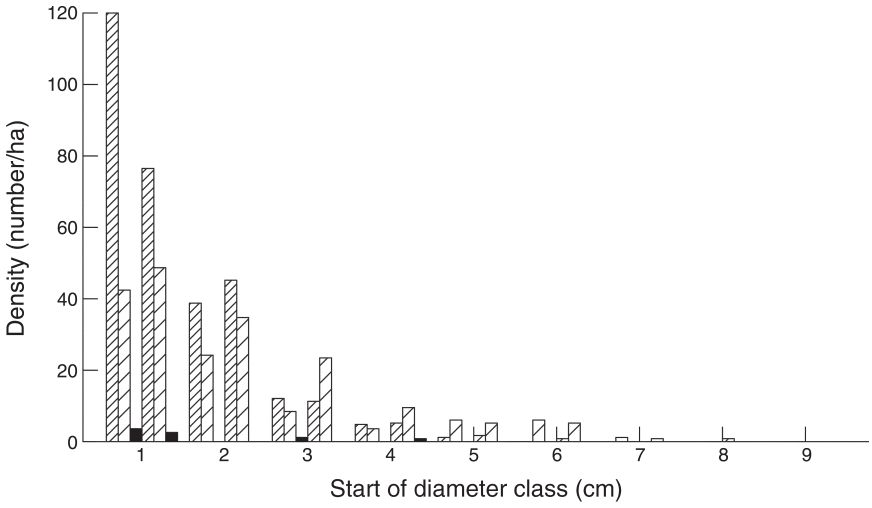

FIG. 13. Frequency distributions of 1 to <10-cm stem diameter trees of the three main species in increasing 1-cm diameter classes in the P plots (bars 1–3, left) and NW plots (4–6, right). Key: *Microberlinia bisulcata*, solid bars; *Tetraberlinia bifoliolata*, fine-hatched bars; and *T. korupensis*, broad-hatched bars.

1.83% and 3.05% per year for *T. bifoliolata*, 2.51% and 4.21% per year for *T. korupensis*, and 1.29% and 2.34% per year for all other (Az) species. The rise between increasing size classes was much higher for *M. bisulcata* (2.59-fold) than the other two species and Az (1.66–1.82-fold). Nevertheless, taking all species together the corresponding rates were very similar at 1.43% and 1.38% per year. In the P plot, 57, 16, 7, and 13 trees of *M. bisulcata*, *T. bifoliolata*, *T. korupensis*, and all other species, respectively, that were 50 to <100-cm in 1991 recruited into the ≥100-cm stem diameter class by 2005 (see Table 2 for numbers in 1991), leading to corresponding r_a estimates of 2.08%, 2.60%, 1.11%, and 1.79% per year (1.98% per year taken all together).

Tree growth rates

M. bisulcata grew much faster than the other two species in the P plot but not so much more than in the NW plot (Table 8). Weighted mean stem absolute growth rate (agr) and relative growth rate (rgr) values were close to 2.0–2.5-fold higher for *M. bisulcata* than for *T. bifoliolata* and *T. korupensis* in the 10–50-cm diameter class in the P plot, significantly so for the period 2004–2008 ($F_{2,131} = 20.0$ and 24.1, respectively; both $P < 0.001$). In the P plot, differences were similar for larger size classes, but in the NW plot, the rates of *M. bisulcata* were barely higher than those of *T. bifoliolata* and *T. korupensis* for trees 50 to <100 cm diameter although approximately twice what they were together for trees ≥100 cm (Table 8). Rates for *M. bisulcata* were markedly lower in the NW than the P plot. In the P plot, trees 50 to <100 cm diameter grew much faster than those ≥100 cm, while in NW plot, this was the converse case.

On combining estimates of agr for medium and large trees and regressing on stem diameter (large, 1991–2005; medium, 2004–2008), *M. bisulcata* and *T. bifoliolata* showed reasonably good quadratic fits (Fig. 15; $P < 0.02$) but for *T. korupensis*, the fit was less strong ($P < 0.1$). A remarkable feature of these data is the very large variation in agr, especially in the diameter range 50–100 (125) cm, with agr varying between approximately −0.2 and 3.5 cm/yr. Notable decreases were seen for trees >100 cm diameter. The scarcity of trees of *M. bisulcata* with diameters 30–60 cm is again apparent (Fig. 15a).

In the recheck of a mixed subsample of medium-sized trees of the three species after the start of the rains in 2008 (over a 41-day interval), the diameter increment was 0.019 ± 0.011 cm (mean ± SE), or ~0.2 mm ($n = 36$ trees; two erroneously high negative values omitted). Growth rates of 10–50 cm diameter *M. bisulcata* trees in the P plot showed particularly good agreement between the different periods measured (Table 8).

Judged from the slight time trends and the SEs on the means, in the 50 to <100-cm and ≥100-cm diameter classes, *T. bifoliolata* and *T. korupensis* differed little in agr between plots (Table 8). *M. bisulcata*, however, can be compared more closely by calculating interpolated (in one case slightly extrapolated) values from the mid-period dates of two rates in the P plot, which match exactly the mid-period dates of the NW-plot estimates. For 10 to <50-cm trees (at 29 October 2006), the agr values in the P and NW plots were 0.801 and 0.612 cm/yr, respectively; rgr was correspondingly 3.179 and 2.330 $cm \cdot m^{-1} \cdot yr^{-1}$; for 50 to <100-cm trees (at 14 April 2004) agr values were 1.352 and 0.525 cm/yr and rgr values were 1.910 and 0.713 $cm \cdot m^{-1} \cdot yr^{-1}$; and for ≥100-cm trees (also 14 April 2004), the agr values were 1.583 and 0.556 cm/yr and rgr values were 1.184 and 0.525 $cm \cdot m^{-1} \cdot yr^{-1}$. Or correspondingly, in a more simple way, for the latest periods measured up to 2009, agr was 1.365 and 0.965 cm/yr and rgr was 1.612 and 0.845

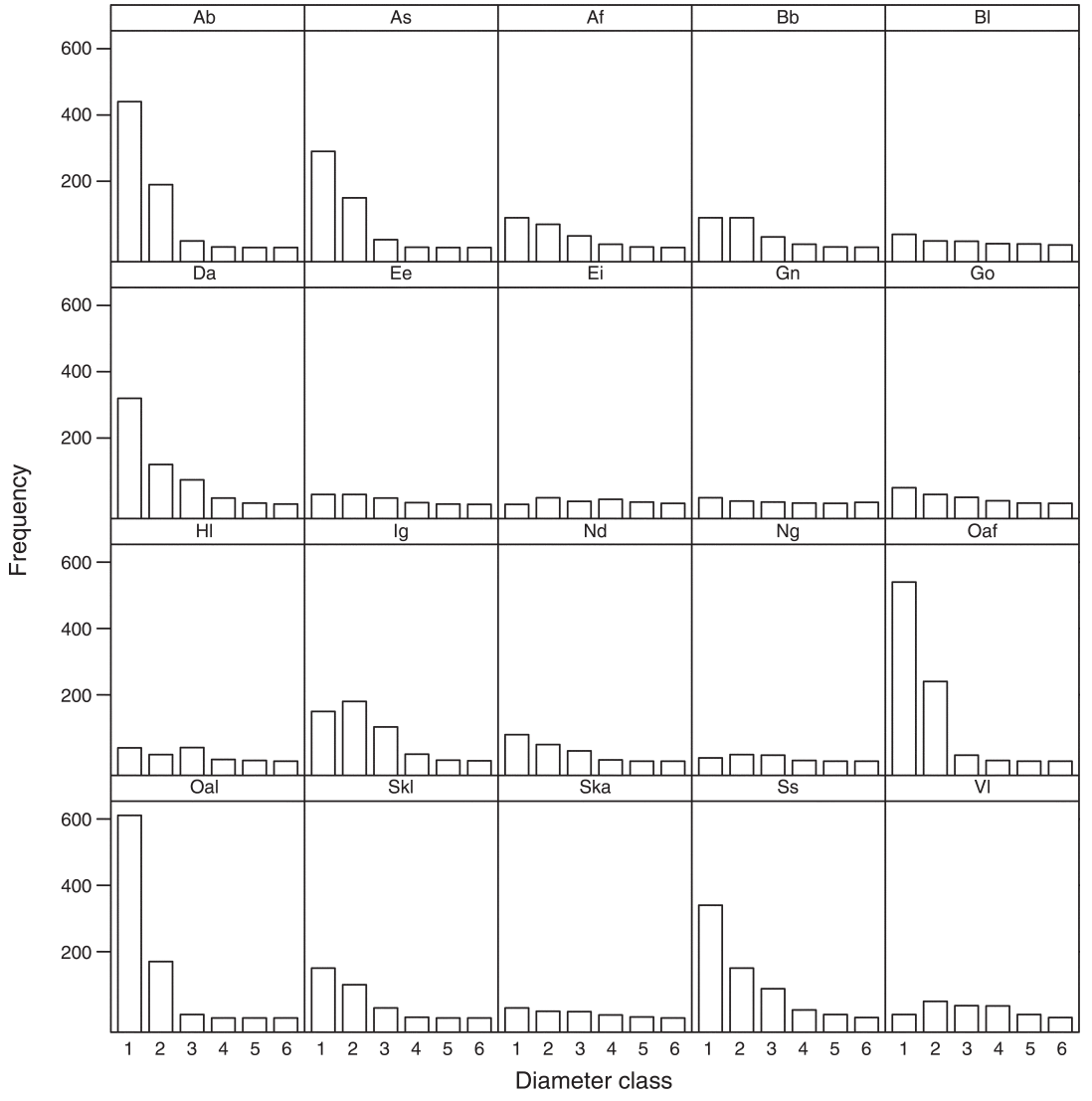

FIG. 14. Frequency distributions of size classes (number per 140 ha, as in Table 3) of the 20 other most abundant large tree species in P and NW plots combined (i.e., those next ranked after the three codominants). Species abbreviations can be found in the legend to Fig. 5 and, in addition: Ab, *Amanoa bracteosa*; As, *Amanoa strobilacea*; Ng, *Newtonia griffoniana*; and Oaf, *Oubanguia africana*. Diameter size classes are 1, 10 to <30 cm; 2, 30 to < 50 cm; 3, 50 to <70 cm; 4, 70 to <90 cm; 5, 90 to <110 cm; 6, ≥110 cm. Note that for *O. alata* (Oal) frequency has been multiplied by 0.1, in order to have a similar scale for all species.

$cm \cdot m^{-1} \cdot yr^{-1}$ for the P and NW plots, respectively (Table 8).

Thus, while the smallest trees of *M. bisulcata* showed only small differences, the large ones had over twofold higher growth rates in the P than the NW plot. Interestingly, within the P plot, across the 9-year interval covering mid-period dates March 1998–March 2007 (Table 8), agr and rgr were falling in the 10 to <50-cm diameter class, staying fairly constant or slightly rising in the 50 to <100-cm class, but sharply increasing in the ≥100 cm class. The smaller difference between plots for the smallest size class, compared with the larger ones, is in part explained by that declining rate over time for *M. bisulcata*.

For Az species, just those trees ≥50 cm diameter in the P plot where the stem was remeasured at the same POM in 1991 and 2005 were considered (458/731, one strong negative outlier removed; i.e., 62.6% of trees with "valid" increments). Within this class, the very large trees were few in number ($n = 13$ trees, or 2.84%) so large and very large trees were combined (in contrast to the MTT comparisons in Table 8). Mean (± SE) agr and rgr were 0.200 ± 0.013 cm/yr (quartiles and median; 0.043, 0.141, 0.309) and 0.299 ± 0.018 $cm \cdot m^{-1} \cdot yr^{-1}$ (0.067, 0.227, 0.445), respectively. In terms of agr, *M. bisulcata* grew on average 4–5× faster, and the *Tetraberlinia* species twice as fast, than the Az species (Table 8). In terms of rgr, the corresponding rates were 3–6× and 2×

TABLE 6. Mortality (m_a) and recruitment (r_a) of trees ≥50 cm stem diameter of the most abundant species (≥10 trees), expressed as annualized rates in the P plot at Korup over a 14-year interval (1991–2005), together with population sizes and changes.

Species	Number in plot				Rates (%/yr)			Population change (%)
	n_{91}	n_d	n_r	n_{05}	m_a	r_a	TO	
Microberlinia bisulcata	294	9	7	292	0.22	0.17	0.20	−0.7
Tetraberlinia korupensis	279	90	30	219	2.74	0.73	1.74	−21.5
Tetraberlinia bifoliolata	195	49	15	161	2.05	0.53	1.29	−17.4
Strephonema sericeum	82	15	11	78	1.43	0.90	1.17	−4.9
Oubanguia alata	64	1	18	81	0.11	1.79	0.95	26.6
Didelotia africana	61	20	3	44	2.80	0.34	1.57	−27.9
Vitex lokundjensis	59	4	4	59	0.50	0.47	0.48	0.0
Irvingia gabonensis	58	7	3	54	0.91	0.36	0.64	−6.9
Berlinia bracteosa	42	8	9	43	1.50	1.40	1.45	2.4
Hallea ledermannii	35	2	5	38	0.42	0.96	0.69	8.6
Erythrophleum ivorense	30	4	3	29	1.02	0.68	0.85	−3.3
Gilbertiodendron ogoouense	26	3	4	27	0.87	1.03	0.95	3.8
Anthonotha fragrans	25	2	6	29	0.59	1.55	1.07	16.0
Gilbertiodendron newberyi	20	1	4	23	0.37	1.31	0.84	15.0
Amanoa bracteosa	18	5	8	21	2.30	2.66	2.48	16.7
Bikinia le-testui	18	6	3	15	2.85	1.11	1.98	−16.7
Cola lateritia	14	2	4	16	1.10	1.81	1.45	14.3
Newtonia duparquetiana	15	9	11	17	6.34	4.01	5.17	13.3
Alstonia boonei	14	1	3	16	0.53	1.40	0.96	14.3
Afzelia bella	13	3	0	10	1.86	0.00	0.93	−23.1
Scytopetalum klaineanum	12	2	4	14	1.29	2.08	1.68	16.7
Coula edulis	11	1	3	13	0.68	1.74	1.21	18.2
Cola verticillata	10	0	1	11	0.00	0.68	0.34	10.0
Crudia ledermannii	10	2	0	8	1.58	0.00	0.79	−20.0
Hymenostegia bakeriana	10	1	2	11	0.75	1.31	1.03	10.0
First 25 species	1415	247	161	1329	1.36	0.77	1.07	−6.1
Remaining 88 species	236	53	88	271	1.80	2.29	2.04	14.8
All 113 species	1651	300	249	1600	1.42	1.01	1.22	−3.1
All except *M. bisculcata* (112 species)	1357	291	242	1308	1.71	1.19	1.45	−3.6
Az (110 species)†	883	152	197	928	1.34	1.45	1.39	5.1

Notes: Mortality rate is calculated as $m_a = [1 - (1 - [n_d/n_{91}])^{1/t}] \times 100$, recruitment rate is calculated as $r_a = [(1 + [n_r/n_{91}])^{1/t} - 1] \times 100$, t is time interval (yr), n_{91} and n_{05} are the numbers of trees alive in 1991 and 2005, and n_d and n_r are the numbers dying and recruiting in the interval. Turnover (TO) is the average of m_a and r_a, and percentage change in population size is with respect to n_{91}.

† Az refers to all species except *M. bisulcata*, *T. bifoliolata*, and *T. korupensis*.

faster. This demonstrated the comparatively very fast growth of large trees of *M. bisulcata*, yet also the still relatively fast growth of the *Tetraberlinia* species.

Among the 20 more abundant Az species of large trees in P plot (Fig. 14, Table 6), agr (1991–2005) was similar to that of *T. bifoliolata* and *T. korupensis* for five of them (*A. fragrans* 0.279 ± 0.067 cm/yr, $n = 12$ trees; *B. bracteosa* 0.216 ± 0.050 cm/yr, $n = 15$; *D. africana* 0.196 ± 0.027 cm/yr, $n = 39$; *G. newberyi* 0.281 ± 0.056 cm/yr, $n = 14$; and *G. ogoouense* 0.309 ± 0.059 cm/yr, $n = 18$), but much higher and similar to that of *M. bisulcata* for the sixth (*B. le-testui* 1.063 ± 0.163 cm/yr, $n = 4$ trees; diameter range 73–108 cm; cf. Table 8). (One strongly negative value for each of *G. ogoouense* and *B. le-testui* was omitted.)

Medium-sized trees in the P plot were not remeasured but the trees at Isangele Road, over the interval of 16.29 years, serve as good substitutes. Here, the mean (± SE) agr was 0.117 ± 0.010 cm/yr (0.047, 0.075, 0.134) and rgr 0.618 ± 0.050 cm·m^{-1}·yr^{-1} (0.235, 0.399, 0.723). Comparing again with Table 8, agr of *M. bisulcata* was ~8×, and that of *Tetraberlinia* species ~3×, higher than that of the Az species; and for rgr, the corresponding multiples were ~5× and 2×. *M. bisulcata* therefore showed relatively faster growth rates than Az species in the smaller than in the larger size classes, while for the *Tetraberlinia* species the rates were similar across the classes. Among the medium-sized trees of the Az species, agr and rgr were also positively skewed (medians approximately two-thirds of the means) so modal *M. bisulcata* vs. Az species rates may have even led to ratios as high as 10× and 7× between them.

Tree dimensions and canopy height

Total tree heights in the P plot, for large emergent individuals, were similar for the three main caesalps: *M. bisulcata*, 44.3 ± 1.4 m (mean ± SE, $n = 15$ trees); *T. bifoliolata*, 48.1 ± 3.1 m ($n = 10$); and *T. korupensis* 46.0 ± 3.6 m ($n = 10$). Heights to the lowest branch were more different: *M. bisulcata*, 17.8 ± 0.6 m ($n = 30$); *T. bifoliolata*, 20.8 ± 1.4 m ($n = 10$); and *T. korupensis*, 23.0 ± 1.3 m ($n = 10$). The corresponding average crown diameters, however, were very different for *M. bisulcata* vs. the other species: *M. bisulcata*, 26.2 ± 0.8 m ($n = 114$); *T. bifoliolata*, 14.5 ± 0.7 m ($n = 76$); and *T. korupensis*, 16.0 ± 0.8 m ($n = 47$) (J. M. Norghauer,

TABLE 7. Mortality (m_a, %/yr) of trees 10 to <50-cm stem diameter of the most abundant species (≥20 trees), in the P plot at Korup over a 14-year interval (1991–2005), together with population sizes.

Species	n_{91}	n_d	m_a
Oubanguia alata	546	31	0.39
Diospyros iturensis	181	22	0.87
Diospyros gabunensis	144	22	1.12
Hymenostegia afzelii	124	15	0.87
Gilbertiodendron demonstrans	121	25	1.55
Cola rostrata	99	6	0.42
Dichostemma glaucescens	99	35	2.91
Klaineanthus gabonii	96	35	3.02
Strombosia pustulata	91	13	1.04
Diogoa retivenia	65	3	0.32
Amanoa bracteosa	62	14	1.72
Tetraberlinia korupensis	56	10	1.32
Baphia leptostemma	50	10	1.50
Garcinia staudtii	48	15	2.50
Strephonema sericeum	44	6	0.99
Tetraberlinia bifoliolata	42	10	1.82
Cola lateritia	41	1	0.17
Vangueriella nigricans	40	15	3.13
Berlinia auriculata	37	2	0.38
Uapaca staudtii	37	10	2.11
Crateranthus talbotii	35	6	1.26
Talbotiella korupensis	35	1	0.20
Piptostigma pilosum	34	7	1.55
Magnistipula glaberrima	33	5	1.11
Diospyros hoyleana	31	4	0.93
Soyauxia gabonensis	30	8	2.08
Carapa parviflora	29	5	1.27
Didelotia africana	28	4	1.04
Calpocalyx dinklagei	26	15	5.65
Mammea africana	24	6	1.93
Strombosiopsis tetrandra	23	1	0.30
Coula edulis	20	4	1.50
Dialium pachyphyllum	20	0	0.00
First 33 species	2391	366	1.12
Remaining 153 species†	777	141	1.35
All 186 species†	3168	507	1.17
All except *O. alata* (185 species)	2622	476	1.35
Az (183 species)	3040	104	1.11
Microberlinia bisulcata	6	0	0.00

Notes: The rate for *Microberlinia bisulcata* is appended for comparison. Az is defined as in Table 6.

† Includes the undetermined trees ($n = 24$).

personal communication). Thus while *M. bisulcata* is not quite as tall as either *T. bifoliolata* and *T. korupensis*, its crown, which is similarly deep to theirs on average, was three times larger in vertical projection. Put otherwise, three *T. bifoliolata*/*T. korupensis* trees fill the same ground space as does one *M. bisulcata*.

The sample of 60 trees of other species included 25 species, of which the two most frequent were *Strephonema sericeum* ($n = 8$ trees) and *Didelotia africana* ($n = 6$ trees). Their mean (±SE) top heights were 33.81 ± 1.25 m, and corresponding heights to lower branch 17.71 ± 0.79 m. Mean crown diameter was 13.09 ± 0.69 m. While top height and height to lowest branch were strongly correlated ($r = 0.776$, df = 58, $P < 0.001$), the former and crown diameter was less so ($r = 0.572$, df = 58, $P < 0.001$), indicating much more variability in crown diameter than crown depth across species. Some species reached the maximum heights of the three main caesalps (upper quartile = 37.8 m) though on average they were shorter. Crown diameters were similar to those of two *Tetraberlinia* species but very rarely reached those typical *M. bisulcata*.

Estimation of tree ages

Because coring was done at slightly different times from when tree diameters were recorded, the latter were adjusted using mean diameter growth rates in the plots. For the P plot, this meant a downward correction (from 2005 to 2003 [–1.8 cm] or 2004 [–0.9 cm]), and for the NW plot, an upward correction (from 2003 to 2004 for 12 of 31 trees [+0.5]; the others being cored and measured in 2003). The sample was reduced on three grounds: (1) In the NW plot several cored trees were close together and thus likely not spatially independent. In a group of eight, five were therefore removed to achieve a maximal spacing of the three remaining, and in two other groups of three trees the middle one was dropped. (2) Six trees (in the NW plot) that required >100 rings (years) to be estimated to the center were excluded on grounds of their ages being judged too unreliable. (3) Two obvious outliers in the P plot, with large diameters (165–189 cm) relative to their low ages (141–142 yr) were removed. This led to a calibration set of $n = 31$ trees. And while no trees estimated to be over 250 yr were sampled anyway in the P plot, the procedure excluded those six in the NW plot that did. The resulting linear regression (age range 50–250 yr; Fig. 16) was diam = $35.7 + 0.353 \times$ age ($F_{1,29} = 24.82$; $P < 0.001$, $R^2 = 44.3\%$; diam stands for diameter). Lines were not fitted separately for each plot because of the different age distributions sampled, and the different degrees to which hollow trees were encountered. When the "closely clustering" trees were kept in the sample, the regression parameters changed little but the fit was poorer (diam = $34.4 + 0.340 \times$ age, $F_{1,36} = 20.72$; $P < 0.001$, $R^2 = 34.8\%$).

Extending the relationship back to the graphical origin, trees evidently grew much faster in diameter in their first 50 years of life (at ~1 cm/yr) than later on (0.34 cm/yr). More data would certainly have allowed the fitting of a complete curve: there is a hint of perhaps a sigmoidal shape, rates between 150 and 225 yr appearing much faster than before or after this period. As trees became older, their diameters became increasingly variable too, with trees of 200 yr age having any diameter between ~50 and 150 cm (an expected mean of 106 cm). Modal tree diameter for both plots was 100–120 cm (Fig. 12), which suggests an *average* age close to 200 yr. The majority of present grove's trees of *M. bisulcata* most probably therefore arose ca. 1795.

Mean tree annual increments were found for 1980–2003 (24 yr; Fig. 17). After omitting the two outliers and seven clustered trees, those trees with ages 150–250 yr were selected to achieve a similar representation of sampling within the two plots. Means of mean (radial) increment did not differ significantly between the plots (P, 1.47 ± 0.24 mm, $n = 9$; NW, 1.72 ± 0.25 mm, $n = 11$;

TABLE 8. Absolute (agr) and relative (rgr) growth rates in stem diameter of trees (mean ± SE) of three main caesalpiniaceous tree species, *Microberlinia bisulcata*, *Tetraberlinia bifoliolata*, and *T. korupensis*, in two size classes for various time intervals (int) between 1991 and 2010 in the P and NW plots at Korup.

Species	Period	int (yr)	*n*	agr (cm/yr) Rate	agr (cm/yr) *b*	agr (cm/yr) *P*	rgr (cm·m^{-1}·yr^{-1}) Rate	rgr (cm·m^{-1}·yr^{-1}) *b*	rgr (cm·m^{-1}·yr^{-1}) *P*
P plot									
10 to <50 cm diameter									
M. bisulcata	2004–2008	3.85	38	0.846 ± 0.091	0.0161	0.071	3.360 ± 0.368	NS	0.190
	2008–2010	2.05	34	0.863 ± 0.126	0.0248	**0.031**	3.047 ± 0.468	NS	0.951
	wtd mean			0.854			3.210		
T. bifoliolata	1991–1998	7.61	39	0.330 ± 0.039	0.0113	**0.001**	1.357 ± 0.155	NS	0.710
	2004–2008	3.76	40	0.413 ± 0.061	0.0127	**0.015**	1.565 ± 0.219	NS	0.856
	wtd mean			0.372			1.462		
T. korupensis	1991–1998	7.61	59	0.310 ± 0.050	NS	0.859	1.405 ± 0.229	−0.033	0.062
	2004–2008	3.86	56	0.310 ± 0.040	0.0062	0.059	1.142 ± 0.133	−0.189	0.084
	wtd mean			0.310			1.277		
50 to <100 cm diameter									
M. bisulcata	1991–2005	13.94	121	1.027 ± 0.105	NS	0.342	1.083 ± 0.105	−0.0179	0.026
	2000–2001	1.00	25	1.338 ± 0.129	NS	0.317	2.248 ± 0.217	−0.050	0.058
	2005–2009	4.21	13	1.365 ± 0.298	NS	0.472	1.612 ± 0.313	NS	0.682
	wtd mean			1.347			2.030		
T. bifoliolata	1991–2005	14.02	121	0.557 ± 0.050	−0.0069	0.065	0.740 ± 0.060	−0.0182	**<0.001**
	1991–1998	7.61	144	0.504 ± 0.033	NS	0.807	0.693 ± 0.046	−0.011	**0.002**
	wtd mean			0.528			0.714		
T. korupensis	1991–2005	14.01	166	0.435 ± 0.031	NS	0.775	0.600 ± 0.041	−0.0081	**0.008**
	1991–1998	7.61	197	0.385 ± 0.024	NS	0.209	0.542 ± 0.032	−0.004	0.090
	wtd mean			0.408			0.569		
≥100 cm diameter									
M. bisulcata	1991–2005	13.70	161	0.824 ± 0.084	NS	0.193	0.614 ± 0.065	−0.0067	**0.030**
	2005–2009	4.22	27	1.987 ± 0.298	NS	0.671	1.487 ± 0.228	NS	0.225
	wtd mean			0.991			0.739		
T. bifoliolata	1991–2005	14.06	23	0.347 ± 0.062	NS	0.588	0.303 ± 0.053	NS	0.983
T. korupensis	1991–2005	14.08	22	0.406 ± 0.092	NS	0.474	0.356 ± 0.081	NS	0.355
NW plot									
10 to <50 cm diameter									
M. bisulcata	2003–2005	2.01	23	0.873 ± 0.114	NS	0.250	3.844 ± 0.465	NS	0.130
	2005–2008	3.08	23	0.612 ± 0.089	0.0244	**0.002**	2.330 ± 0.270	NS	0.373
	wtd mean			0.743			3.087		
T. bifoliolata	2003–2005	2.00	325	0.364 ± 0.021	0.0172	**<0.001**	1.481 ± 0.083	0.0127	0.086
T. korupensis	2003–2005	2.01	441	0.257 ± 0.016	0.0136	**<0.001**	1.057 ± 0.063	NS	0.106
50 to <100 cm diameter									
M. bisulcata	2003–2005	2.04	43	0.525 ± 0.050	NS	0.903	0.713 ± 0.074	NS	0.114
T. bifoliolata	2003–2005	2.01	168	0.498 ± 0.027	NS†	0.480	0.718 ± 0.039	−0.0112†	**<0.001**
T. korupensis	2003–2005	2.01	129	0.433 ± 0.035	−0.0061†	**0.041**	0.653 ± 0.057	−0.0186†	**<0.001**
≥100 cm diameter									
M. bisulcata	2003–2005	2.04	7	0.556 ± 0.127	NS	0.756	0.525 ± 0.115	NS	0.652
	2003–2009	6.57	28	0.965 ± 0.060	0.0064	0.005	0.845 ± 0.047	NS	0.553
	wtd mean			*0.883*			*0.781*		
T. bifoliolata	2003–2005	2.02	21	0.466 ± 0.078	NS	0.837	0.425 ± 0.071	NS	0.580
T. korupensis	2003–2005	2.01	7	0.391 ± 0.136	NS	0.410	0.364 ± 0.125	NS	0.596

Notes: Slopes (*b*) of the linear regression of agr or rgr on diameter (cm) at the start of the period are shown where they were significant at $P < 0.1$, otherwise as NS; those more strongly significant at $P < 0.02$ have their *P* values in boldface type. Where there were two or more estimates for a species in a size class, sample-size-weighted (wtd) means are also given.

† One strongly outlying value removed for each species.

$t = -0.75$, adjusted df = 17, $P = 0.465$; corresponding mean ages and diameters were 191 and 187 yr, 120 and 94 cm). Mean annual increments for each of the nine selected trees in P plot for 1991–2003 (13 yr) were found to be weakly positively correlated with their mean annual radial increments found directly from the 1991 and 2005 enumerations ($r = 0.587$, df = 8, $P < 0.1$). Trees that were cored (i.e., at points between buttresses, close to breast height) grew on average at 1.67 ± 0.28 mm/yr, while diameter-read trees (at points necessarily above buttresses) did so at 2.33 ± 1.31 mm/yr (paired $t = 0.57$, df = 8, $P = 0.59$). Two additional results are: (1) The six recruits (into the ≥50-cm class by 2005) sampled in the P plot had 24-yr mean (radial; ±SE) increments of 3.92 ± 0.88 mm/yr (age = 74.0 ± 9.3 yr, diam = 54.6 ± 1.6 cm; reliable estimates since tree centers were reached).

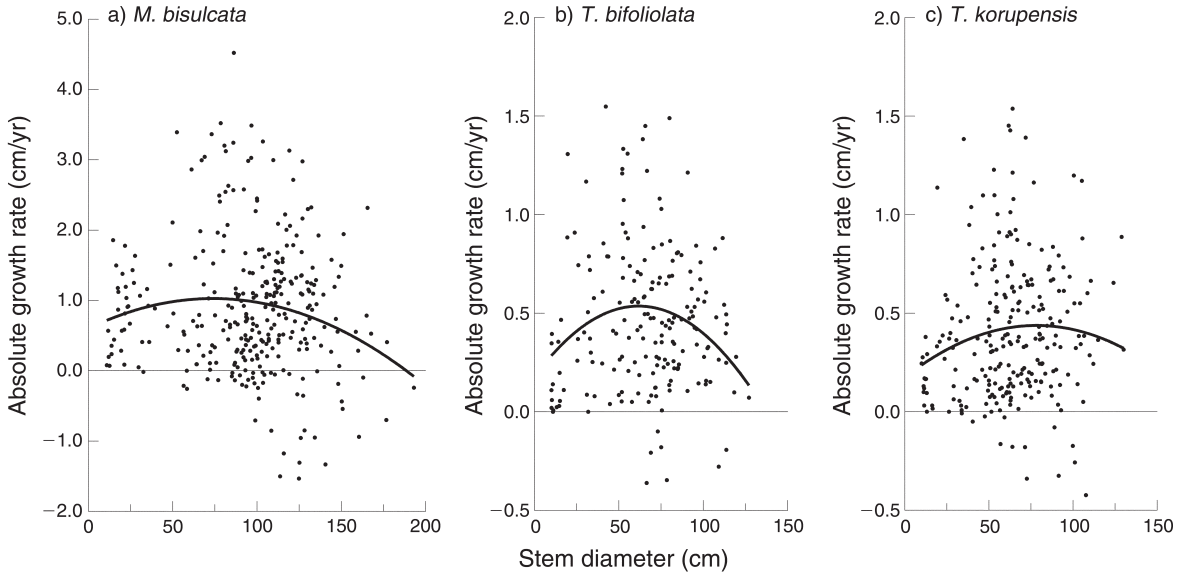

FIG. 15. The dependence of absolute growth rate (agr) in stem diameter on stem diameter (diam) in the P plot, combining estimates for medium-sized (10 to <50 cm) and large (≥100 cm) trees (points) and fitted by quadratic regression (lines), for (a) *Microberlinia bisulcata* (agr = 0.6017 + 0.01152[diam] − 0.000078[diam^2]; $F_{2,311} = 4.20$; $P = 0.016$, $R^2 = 2.0\%$; four outliers and two points for trees with diameters >200 cm omitted); (b) *Tetraberlinia bifoliolata* (agr = 0.1772 + 0.01163[diam] − 0.000094[diam^2]; $F_{2,181} = 5.23$; $P = 0.006$, $R^2 = 4.4\%$; four outliers omitted; and (c) *T. korupensis* (agr = 0.1739 + 0.00674[diam] − 0.000043[diam^2]; $F_{2,244} = 2.61$; $P = 0.076$, $R^2 = 1.3\%$; three outliers omitted).

(2) The four very large trees in the NW plot had increments of 1.50 ± 0.48 mm/yr (age = 380 ± 50 yr, diam = 152.9 ± 11.1 cm; less reliable because heartwood was lacking at their centers).

Trees in the P and NW plots grew at very similar rates between 1980 and 1993; but their increments increased in the NW plot while in the P plot, after little change until 1998, they showed a pronounced peak in 1999–2000 (Fig. 17). This peak was caused primarily by four particular trees responding concordantly. Radial increment in both plots between 1984 (the year in which climate recording started at Bulu) and 2003, of the selected subset of trees, was significantly positively correlated with dry season radiation in the current year (P plot, $r = 0.499$, df = 18, $P = 0.025$; NW plot, $r = 0.644$, df = 18, $P = 0.002$) and with mean daily dry-season radiation in the previous year (P plot, $r = 0.484$, df = 17, $P = 0.038$; NW plot, $r = 0.636$, df = 17, $P = 0.003$). Nonsignificant correlations were recorded between radiation in the other three seasons (early, mid, and late-wet), and with rainfall in any season, current or lagged ($P > 0.05$).

Radial increments from cores cannot be equated to those gained from direct stem girth measurements because the former were obtained at points lower down *between* buttresses and the latter at points well *above* them on the straight stem bole. For a 50-yr-old tree with a diameter of 50 cm, the mean growth rate of 0.34 cm/yr was to be matched up with 1.03 and 0.82 cm/yr for trees 50 to <100 and ≥100 cm diameter, respectively, measured between 1991 and 2005 in the P plot. The horizontally viewed "circumference" around buttresses at ~1 m height is obviously many-fold that of the bole at a height of 3–5 m: the wood form and density would also be different at these points.

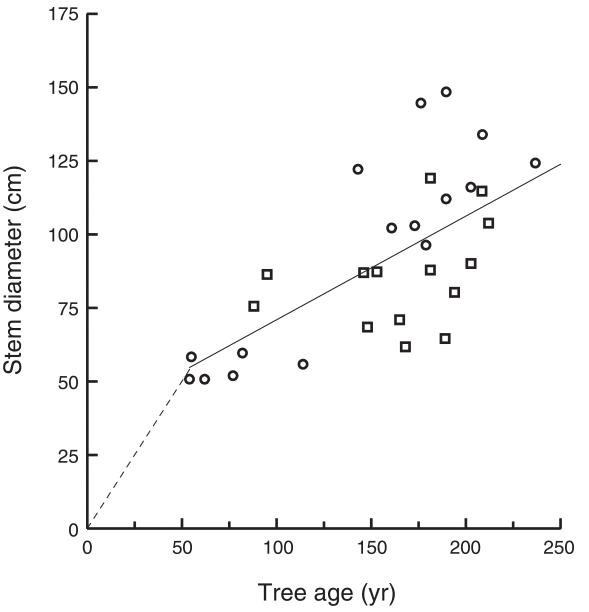

FIG. 16. Relationship between stem diameter (above buttress) and age of 31 trees of *Microberlinia bisulcata* at Korup (open circles, P plot; open squares, NW plot). The solid line is the fitted linear regression, and the dashed line is an interpolation to the origin.

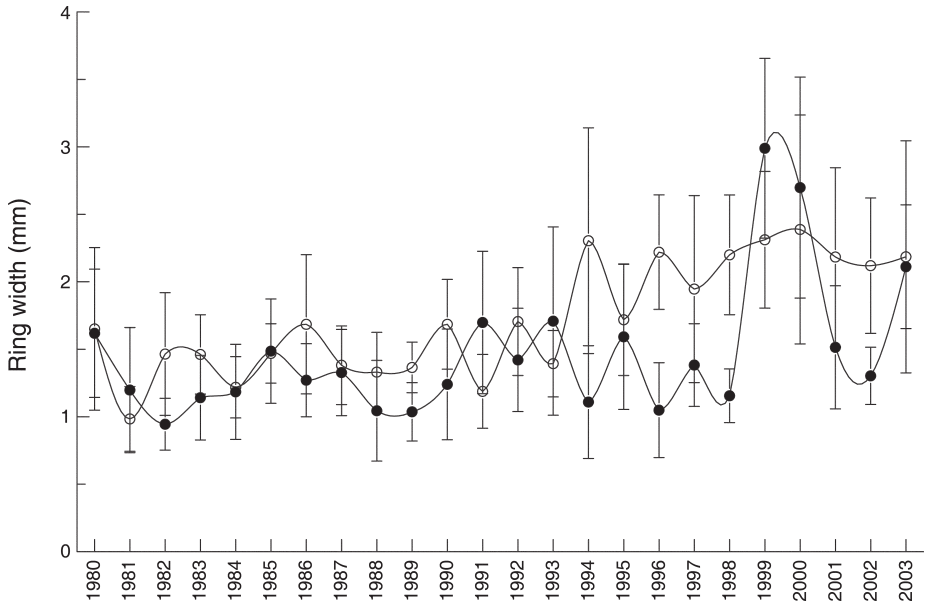

FIG. 17. Change in stem-wood ring width (mean ± SE) over the last 24 years recorded for *Microberlinia bisulcata* trees, with estimated ages 150–250 yr at Korup (solid circles, P plot, $n = 9$ replicates; open circles, NW plot, $n = 11$ replicates). The curves are spline fits.

Construction of a transition matrix and projected grove dynamics

A population transition matrix ($\mathbf{A}_{\mathrm{Mb}}$) consisting of the three size classes medium (10 to <50 cm), large (50 to <100 cm) and very large (≥100 cm) stem diameters was constructed for *M. bisulcata* (Mb) in the P plot. Empirically estimated mortality, recruitment, and absolute growth rates (found for these classes specifically, see Appendix I) allowed the terms P_{ii}, the probability of an individual to stay in a class i; G_{ij}, the probability that it moves from class i to the next larger one j; and F_{ji}, the relative replacement potential of the larger classes j by the smallest one i. Details of the calculations are laid out in Appendix I. For *M. bisulcata*, the starting vector of numbers of trees in the size classes, $n_0(t)$, was [41, 80, 212] in 2005 (medium-sized trees, 2003). The population transition matrix was

$$\mathbf{A}_{\mathrm{Mb}} = \begin{bmatrix} 0.97538 & 0.00412 & 0.00412 \\ 0.00393 & 0.97146 & 0 \\ 0 & 0.02086 & 0.99700 \end{bmatrix}.$$

The very low recruitment rate into 50–<100-cm class accords with the density of trees in the 10-cm class just <50 cm, i.e., those 40–50 cm. In the enumeration, there were only three individuals in this class and seven 30–40 cm, so growing at even ~1 cm/yr, 7–8 of these might cross into the large class after 14 years, a count very close to that found in 2005 (Table 6). Recruitment into the medium size class was found from growth rates in the 10 to <20-cm class and applying the *Gf* estimate of Kohyama and Takada (1998).

A similar approach was adopted for the two *Tetraberlinia* species in order to find P_{11}, G_{12}, P_{23}, G_{23}, and P_{33} for them from the m_{a} and r_{a} rates (Appendix I). For *T. bifoliolata* (Tb), $n_0(t)$ was [344, 122, 39], and for *T. korupensis* (Tk), $n_0(t)$ was [522, 191, 28] in 2005. The population transition matrices for these species were

$$\mathbf{A}_{\mathrm{Tb}} = \begin{bmatrix} 0.98785 & 0.03322 & 0.03322 \\ 0.00650 & 0.97479 & 0 \\ 0 & 0.02600 & 0.96955 \end{bmatrix}$$

$$\mathbf{A}_{\mathrm{Tk}} = \begin{bmatrix} 0.98270 & 0.02749 & 0.02749 \\ 0.00855 & 0.97281 & 0 \\ 0 & 0.01107 & 0.95790 \end{bmatrix}.$$

The modeling could not be applied to the NW plot since m_{a} and r_{a} estimates were lacking there.

Matrix dimension was limited to three because there are presently too few reliable data available for 1 to <10-cm diameter trees of *M. bisulcata*: the large–very large (size at maturity) threshold was appropriate for *M. bisulcata* and applied to the *Tetraberlinia* species to enable comparison.

Populations of the three species in 2005 were projected to 25 and 50 yr using the package popbio in R, based upon the assumption that these transition matrices remained constant. The model predicts that numbers of medium-sized trees of *M. bisulcata* would increase slightly while the numbers of large trees decrease and correspondingly those of very large trees increase, albeit less steeply (Fig. 18). Effectively, large *M. bisulcata* trees would be simply growing into even larger ones due to very low attendant mortality and

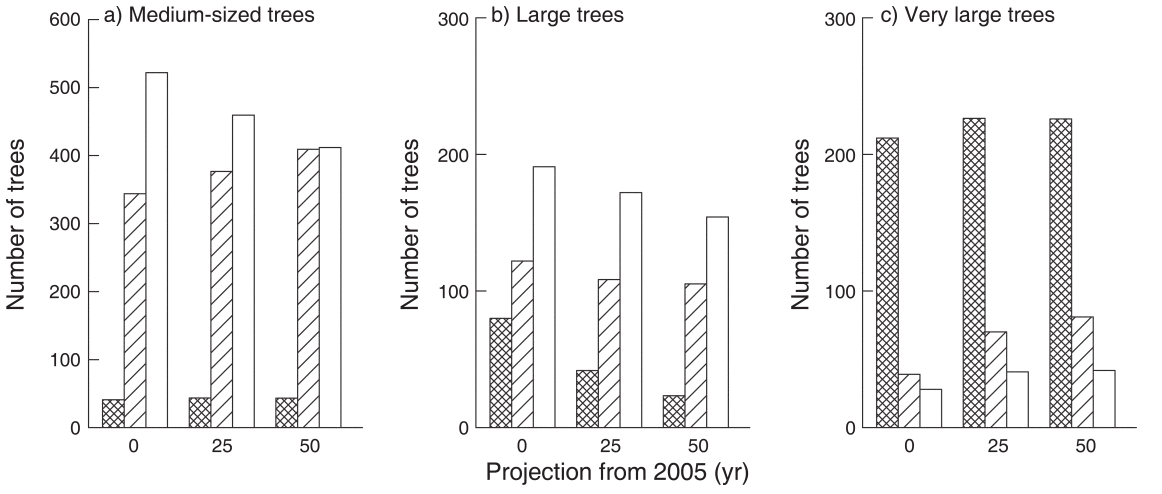

FIG. 18. Changes in the numbers of (a) medium (10 to <50 cm), (b) large (50 to <100 cm), and (c) very large (≥100 cm) stem diameter trees of *Microberlinia bisulcata* (cross-hatched bars), *Tetraberlinia bifoliolata* (hatched bars), and *T. korupensis* (open bars), in the P plot at Korup, as projected using matrices of 1991–2005 transition probabilities 25 and 50 years on from 2005.

relatively high growth rates, while recruitment of large trees remained low. The *Tetraberlinia* species would appear to behave more similarly to one another, but differently from *M. bisulcata* (Fig. 18), both with declining numbers of medium trees, yet for *T. bifoliolata* numbers of large trees declining and those of very large trees varying little; conversely, large trees of *T. korupensis* stay almost constant but their numbers of very large trees increase. Reruns of the projections for *T. bifoliolata* and *T. korupensis* allowing for a minimum diameter at maturity of 30 cm scarcely altered the outcomes.

Total numbers of trees ≥50 cm diameter (i.e., large plus very large trees) of the three species are projected to decline over 50 years by 5.9% from 672 to 632 in the P plot. While the relative proportion for *M. bisulcata* would decrease from 43.5% to 39.5%, that of *T. bifoliolata* would correspondingly increase from 24.0% to 29.5% and of *T. korupensis* would decrease only slightly from 32.6% to 31.0%. Examining the three size classes more carefully, medium-sized *M. bisulcata* would remain very few and unchanging, large trees would decline but very large trees would remain very many and slightly increasing: a shift from large to very large over time (Fig. 18). The two *Tetraberlinia* behave quite differently, however. While medium-sized and very large trees of *T. bifoliolata* would increase, their numbers of large trees would remain near constant. By contrast, medium-sized and large trees of *T. korupensis* would decrease, yet their number of very large trees would remain constant. This suggests a general progression of *T. bifoliolata* and regression of *T. korupensis*. With repeated projections, *M. bisulcata* would come to disproportionally occupy more canopy space and biomass with its very large stem and crown sizes, increasing its dominance not by numbers, but by having relatively more very large trees. A forest grove increasingly dominated by older and larger *M. bisulcata* trees appears to be the likely near-future outcome, based on the dynamics rates measured 1991–2008.

The projection model can be used to investigate hypothetical scenarios. If the very large trees of *M. bisulcata* should begin to die at faster rates (grove collapse) over the next 50 years, would the growth of medium-sized and large trees be sufficient to replace them? Changing this size class' survival probability to reflect increasing mortality from 0.3% (the empirical value), to 0.65% per year, then from 1% to 5% per year in 1% steps, revealed a steep exponential decline in the number of very large trees (down to $n = 30$ trees at $m_a =$ 5% per year; cf. 226 in 2005, i.e., just 13% remaining; Fig. 19). Numbers of large trees vs. m_a of very large trees remains quite constant at 42 (25 yr) and 23 (50 yr), whereas medium-sized trees decline correspondingly from 44 to 36 and from 59 to 57 (Fig. 19). Allowing for a 72% higher rate of recruitment into the medium-tree class (see Appendix I for details), raises the numbers of medium-sized trees fairly uniformly by 10–20 (at 50 years) but it had virtually no effect on the numbers of large and very large trees (Fig. 19). Alternatively, increasing the recruitment rate of trees from the medium to the large size class, by a similar degree (Appendix I) simply depletes the numbers in the medium class, and barely increases those in the large size class (Fig. 19). These results suggest that, in the short term at least, the large and very large trees of *M. bisulcata* in the grove will be unable to replace themselves, even when recruitment into medium and large classes is raised to levels that trees can realistically at maximum achieve in their growth rates, and thus the present population structure is not sustainable within the life time of typical adult trees (given current conditions).

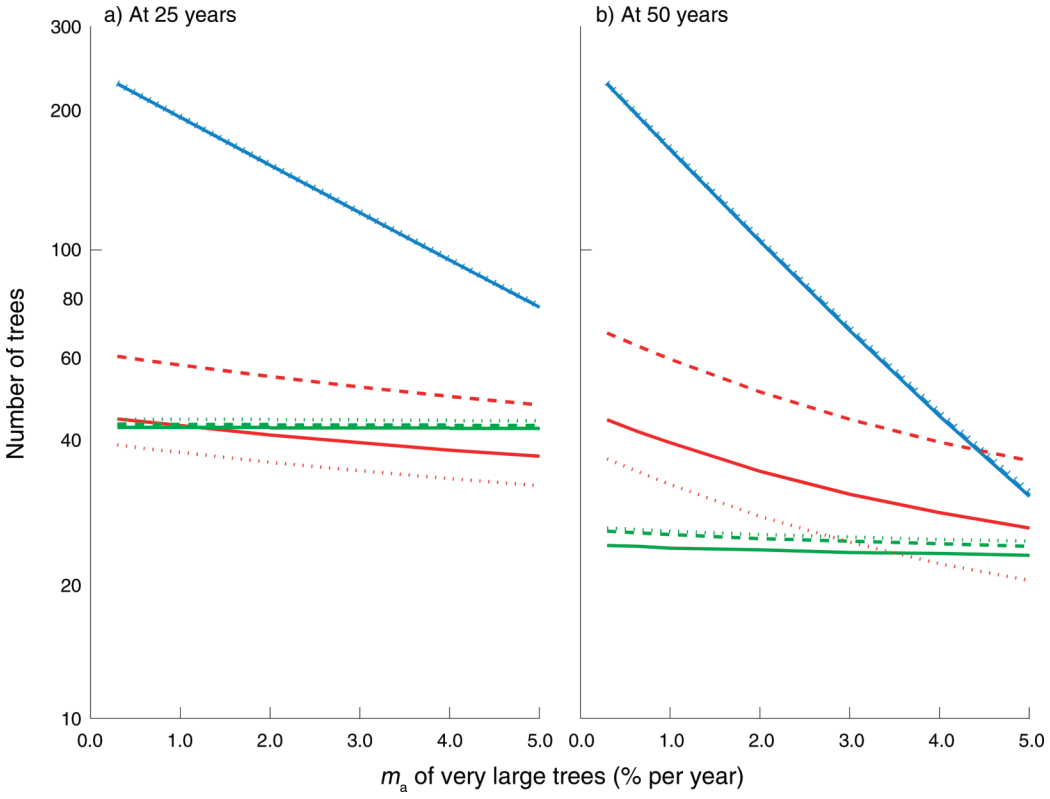

FIG. 19. Predicted changes in numbers of very large (blue lines), large (green lines), and medium-sized (red lines) trees of *M. bisulcata* in the P plot at Korup if the annual mortality rate (m_a) of very large trees were to increase from the observed 0.3–5.0% per year, over the next (a) 25 years and (b) 50 years. The dashed and dotted lines, for comparison, show the effect of increased recruitment into the medium and large size class (by ~72%), respectively. The solid, dashed, and dotted blue lines and some of the green lines are almost identical, hence their overlap.

DISCUSSION

Structure and dynamics

Within the *M. bisulcata*-dominated grove complex studied here at Korup, the forest was found to be highly homogeneous in its structure and species composition at the ~50–100-ha scale. The two codominants, *T. bifoliolata* and *T. korupensis*, were widespread, while the other less abundant species of large tree were interspersed almost at random. The two large sample plots (82.5 and 56.25 ha) differed primarily in two respects concerning the trees' environment: the P plot had parts (in its eastern half) with higher elevation ground than that recorded in the NW plot, and the soils of the P plot were overall slightly richer in nutrients than those of the NW plot. *Microberlinia bisulcata*, and to a lesser extent *T. bifoliolata*, tended to be positively associated with the higher-elevation (drier) and more nutrient poor areas of the plots, while *T. korupensis* showed the opposite result, occurring more on the lower (in part wetter) and more nutrient rich soils. This was seen for the main east–west trends in tree abundances across the complex and was supported by the ordination and spatial pattern analyses of large trees' locations within the plots. The medium-sized (subcanopy) trees were strongly dominated, in both plots, by one species, *O. alata*, remarkable because of its high and even local abundance; but also by a more clustered codominant *C. talbotii* in the NW plot. Apart from the obvious localized effects of permanently wet swampy conditions around streams, there were no clear species associations that might lead to any form of classification of the vegetation on well-drained ground within the grove complex. The combined, and scaled-up, composite sample of 140-ha for trees ≥10 cm stem diameter gives a reliable quantitative description of the *M. bisulcata*-dominated forest community. Nevertheless, from the stem diameter distributions, a very pronounced relative lack of small stems of *M. bisulcata*, compared to *T. bifoliolata* and *T. korupensis*, was registered.

The spatial distributions of the three large codominants complement one another in the plots. There was considerable local fine-scale (~2–5 ha) heterogeneity among the mixing of the main species. Large *M. bisulcata* were significantly clustered, particularly with large trees being attracted to very large ones, but large trees of the two *Tetraberlinia* species were absent: medium-sized trees of all three species occurred at random. Consequently, large *T. bifoliolata* and *T. korupensis* were being repelled from large *M. bisulcata*,

effectively occurring in the forest where *M. bisulcata* was absent. Likewise, medium *M. bisulcata* trees were repelled from their adults (in the P but not the NW plot), yet medium *T. bifoliolata* (but not *T. korupensis*) was attracted to its adults (i.e., both occurred away from large *M. bisulcata*). Large *M. bisulcata* repelled medium *T. bifoliolata* in the P plot and medium *T. korupensis* in the NW plot. The other (Az) species, making up approximately the fourth quarter of the large trees, were filling the remaining places. Thus, *M. bisulcata* led to one or both of the codominants, as well as its own medium-sized trees, being "displaced," which can be interpreted as indirect evidence of its considerable competitive influence. The most likely mechanism behind that competitive dominance is not simply the numerical abundance of *M. bisulcata* (which was roughly on a par with each of the *Tetraberlinia* species), but the species' much greater size and biomass, expressed in terms of a combination of its height typical of a main canopy-emergent tree, and its very wide canopy spread and extensive lateral buttresses and rooting extent (Newbery et al. 2009), than nearly all other tree species at Korup. *Microberlinia bisulcata* "sets the scene," biotically and abiotically, above- and belowground. In the P plot, the stronger repulsion effect of large *M. bisulcata* on other smaller trees than in the NW plot may be explained by a stronger competitive influence with the higher soil resources in the P compared with the NW plot. The species' relative abundance fits to the Zipf-Mandelbrot model showed strong overdominance of especially *M. bisulcata*, but also of *T. bifoliolata* and *T. korupensis*.

The current dynamics of the grove forest are particularly distinct from most other, more species rich, lowland rain forests that have been studied. The overall m_a and r_a rates of the large trees (at 1.42 and 1.22% per year, respectively) were low by those global tropical norms of ~1.8–2.0% (Swaine et al. 1987), as was the average m_a rate (1.17% per year) for the medium-sized trees. In both cases, this was largely due to the very low rates contributed by the dominant species (*M. bisulcata* at 0.22 and 0.17% per year; and *O. alata* at 0.39% per year for m_a; the latter even lower for its near maximum-sized trees >50 cm, at 0.11% per year). Slow dynamics were clearly associated with the (over)dominance. In stark contrast, the m_a rates for the large-tree codominants, *T. bifoliolata* and *T. korupensis*, were close to 10-fold higher than those of *M. bisulcata* (2.05–2.74% per year), these being over twice the mean forest rate; and even though their r_a rates were around the mean (0.70–1.06% per year). In the subcanopy, however, several less abundant species did have rates higher than *O. alata*. These P-plot results were supported by the NW-plot results except that Az species in the NW plot had lower m_a rates than in the P plot. Sample sizes were rather too small to reliably estimate mortality of medium-sized *M. bisulcata* (twice zero on first-time estimates for the P and NW plots, but 1.33% for the second P-plot estimate); in general *T. bifoliolata* and *T. korupensis* had lower rates of m_a as medium compared with large trees, in the range 0.0–1.82% per year.

Considering stem growth, *M. bisulcata*, but not *T. bifoliolata* and *T. korupensis*, trees had higher rates in the P than the NW plot. For both large (50 to <100-cm) and very large (≥100-cm) diameter trees in the P plot, *M. bisulcata* grew over twofold faster than *T. bifoliolata* and *T. korupensis*, but this was only the case for very large trees in the NW plot. Indeed, over recent years larger trees of *M. bisulcata* were growing relatively faster than small and medium-sized ones. The relatively faster growth rate in the P plot than in the NW plot, combined with the spatial statistics results, suggests that the large *M. bisulcata* trees may have been suppressing the intermediate trees of all three codominants and hence their survival. That *M. bisulcata* grew approximately fourfold faster than the other Az species, and the two *Tetraberlinia* twofold as fast, attests to the success of these three species at the site and hence an explanation for their co-dominance. Interestingly, the increment analysis of the stem cores from *M. bisulcata* were strongly positively correlated with dry season radiation, suggesting an annual controlling effect of climate on tree growth rate.

Two other studies where large tree growth rates from individual species in primary forest were reported based directly on stem sizes *and* using adequate sample sizes afford comparisons with Korup. Clark and Clark (1996) measured stem diameter growth rates (above buttresses; trees >70 cm diameter, 7-yr period) of 0.19, 0.26, 0.36, and 0.52 cm/yr for *Dipteryx panamensis*, *Lecythis ampla*, *Hieronyma alchorneoides*, and *Pithecellobium elegans*, respectively (n = 27–60 trees). Makana et al. (2011), recording trees ≥50-cm diameter in four 10-ha plots at Ituri, Zaïre, reported mean stem diameter growth rates of 0.26, 0.35, 0.59, and 0.15 cm/yr for *Cynometra alexandri*, *Gilbertiodendron dewevrei*, *Julbernardia seretii*, and *Zanthoxylum gilletii*, respectively (corresponding densities of 6, 19, 4, and 1.5 trees/ha). A few other scattered values for various species, often smaller in stem diameter, and based on much smaller sample sizes, are to be found in the non-managed-forest literature, lying largely in this range 0.2–0.5 cm/yr. Hence the mean growth rates (agr) for *T. bifoliolata* and *T. korupensis* fit well within this range, but those for *M. bisulcata* are obviously much higher.

As strongly implied by forest structure, the dynamics data suggest too, that among the large trees there exists a four-part system made up of trees of (1) *M. bisulcata*, (2) *T. bifoliolata*, (3) *T. korupensis*, and (4) the rest (Az). *M. bisulcata* remained stable, constant, and dominating while the *Tetraberlinia* species grew around it with heightened turnover rates, and the other species filled the remaining space. *M. bisulcata* large trees enforced their recent dominance by still having substantially high growth rates, this leading under near-future projections to more and larger *M. bisulcata* trees, at the cost of a

reduction, and shift in composition, of the codominants, and other species. The differences between plots do not permit any causal inferences to be drawn, however, because while faster growth in the P than NW plot might have been due to the generally higher nutrients in P (and its more elevated and better draining ground), the improved nutrient status could, conversely, have been the result of better growth causing higher nutrient turnover rates. From previous work at Korup, it is likely that while both processes operate, trees have affected the soils more than vice versa. The increasing biomass of *M. bisulcata* means that competition between the *Tetraberlinia* species is being intensified over time: these indications and the projections suggest that *T. korupensis* will gradually replace *T. bifoliolata*.

The major overdominant status of *M. bisulcata*, as many large to very large trees in the canopy and emergent layers of the forest groves at Korup, as well as the combined ectomycorrhizal guild dominance of it and the two codominant *Tetraberlinia* species, must have a large dampening influence on the degree of heterogeneity of the abiotic habitat, above- and belowground, in which the other less abundant species occur. The resulting homogeneity, enhanced by a tight nutrient cycle, would provide for very few other edaphic niches. Clearly the high competitive effect of *M. bisulcata* on its neighbors, which are less well adapted to the low nutrient soils of Korup, is central. *Tetraberlinia bifoliolata* and *T. korupensis* share the same hyphae network and cycling as *M. bisulcata*, so they are positioned (if there exists some form of competitive hierarchy) between those larger, faster-growing, *M. bisulcata* and the other mostly non-ectomycorrhizal species. The benefits of the nutrient cycling pathways created by *M. bisulcata* are, in the main, largely self-accruing since this species occupies so much of the canopy and forest floor space; the *Tetraberlinia* species may be able to benefit marginally through the shared below-ground ectomycorrhizal network, but this gain is probably outweighed by strong competition for light above ground. The last must especially be important when the *Tetraberlinia* species are of medium sizes, since as large trees they can form crowns (albeit comparatively smaller), that are as high as those of *M. bisulcata*. Likewise, small to medium-sized *M. bisulcata* trees necessarily grow away from under their parents' crowns and, being very few in number anyway, they too need to find spaces in which to reach the canopy. Thus, as *M. bisulcata* continues to dominate the grove it not only suppresses species as neighbors of its guild, but it also severely limits its own recruitment into the larger tree size classes, which would prepare the way for continuous replacement when, inevitably, these old forest giants en masse begin to disintegrate and fall due to extreme mechanical loading and/or a major environmental disturbance.

Despite the difficulties in estimating ages of the very large *M. bisulcata* trees (most were hollow), dating showed that trees of a similar age could be of very different sizes, and conversely after a given time trees could differ markedly in size. Gaining a precise age structure of the whole grove is therefore not possible by stem coring. Neighborhood competition, substrate differences, light microclimate, and avoidance of damage all likely contributed to differences in juvenile growth and survival, although once mature (~50 cm diameter) the substrate conditions (soil depth, drainage, lack of rocks [impinging on the efficacy of the nutrient cycle]) probably have the main influence on onward growth and canopy expansion. The populations across subgroves and plots varied considerably in age structure at a local scale, so much so that identifying cohorts originating from past events is very difficult. Waves of enhanced recruitment may have happened in past centuries but their signature was subsequently blurred by the large variance in growth rates. Nevertheless, one distinctive mode in tree size at around 110-cm stem diameter, and a corresponding average age of 200 years, is evident and suggests a type of stabilization in which tree sizes converge over time. Through competition, symbiotic guild interdependence, intense packing and resource use, populations of different dates of origin may have worked toward a common emergent grove structure. The current lack of small (young) stems across the grove remains characteristically pronounced, whatever the vagaries of past recruitment, even though it is clear that once established juvenile trees can grow very fast, likely aided then especially by their ectomycorrhizas.

Insights into recent and past dynamics

Two underlying motivating questions about these caesalp groves have been (1) will they stay constant in structure and composition and (2) how did they arrive at their current configuration? The first question concerns the future and can be broken down into: (1a) Can the recently observed dynamics maintain the present structure? (1b) If not, what other processes would be required to do so? The second question concerns the past and leads to: (2a) Under what conditions would the recently observed dynamics have led to the present structure and composition? (2b) If these are unfeasible, what different dynamics would have achieved it? The new structural and dynamics data in this paper provide some partial answers.

Whether an ecosystem is assessed to be in a relatively constant (steady) state, depends on the time scale considered. What may appear for a short while (e.g., over a few decades) as an increasing or decreasing trend could be part of a long-term cycle, and when viewed over a much longer span of time (say centuries) it could be indeed quasi-constant. The structure of the Korup grove system has been observed for only ~20 years, yet its trees live to typically 200–250 years. It is an important caveat that analysis, models, and interpretation of forest structure and inferred long-term dynamics at Korup are resting on dynamic variables measured

during a recent 20-year period: it is simply not known empirically how these would have differed in the past (as the grove established, for instance) or how they will differ in the future (as perhaps the grove declines with or without a new period of disturbance operating).

Disturbances coming as all old trees dying one day (as the population model assumes) will mean relatively few sparsely distributed juveniles and a less dense stand until they are mature. Alternatively, a more drastic externally driven event, where many trees die together, will lead to a strong pulse in recruitment with longer lag. The former would probably lead to a flatter humped size distribution (more ages/sizes spread out) and the latter more peaked dominance pushing the few juveniles already existing before them to become the very large trees in the future, i.e., those beyond the modal peak. The second situation appears to prevail in Korup presently.

Size or age-class distributions, combined with growth rates, can give a good indication of what may be happening. Lack of smaller trees, as is obviously the case here for *M. bisulcata*, may not necessarily mean that the adults that die are not replaceable if those conspecific juveniles are numerous enough, have a very high survivorship rate and can grow very fast through the size classes. They would need to come on behind the advancing mode of large trees at a much faster rate than those large trees can grow. The matrix modeling tested this and showed, based on current dynamics, that recruitment into the very-large tree class could continue based on the stock of large trees (close to and above the modal size) but the juvenile trees are simply too few and cannot grow fast enough to replace the large ones: in time a hiatus would occur with ever more very large trees, few large ones and similar numbers of medium ones. The mode would simply be displaced to the right on the size axis, and with greater skew, effectively a bimodal distribution of very old and young trees. This is a pattern not infrequently seen in other species exhibiting characteristics of transient dominance.

It is unrealistic to imagine, however, that many of the very large trees would survive a further 50 years given our age–size data set. Our observations in the field reveal too that the largest (likely oldest) ones simply fall apart under their own loads, first by loss of the huge branches and then full tree decline. Several examples were observed in the field in the last 5–7 years (D. M. Newbery, *personal observation*). We do expect the m_a rate to increase though, and if suddenly an environmental (perhaps climate-assisted) disturbance occurred, that m_a would increase even higher still. The projection model scenarios showed that even a 0.5% per year mortality of the very large trees (and allowing the large trees to continue with no losses), with scarcely any replacement affordable from those large trees, would lead to a major decline in the population, thinning the stand of trees $\geq$50-cm stem diameter from 292 to 80 (by 73%) and, interestingly, leaving the medium (10 to $<$50 cm), large, and very large trees in close to a 40:40:40 set of ratios. The numbers of medium-sized trees, growing at maximum likely growth rates, would be insufficient to replace them. At the same time, declining numbers of medium-sized *T. bifoliolata* and *T. korupensis* is accompanied by increases in their large tree numbers. For all three species, the unstable interplay between growth and mortality is therefore central to the outcome of stand dynamics. Such conditions, though, would drastically alter the plot environment, creating huge gaps that, on the one hand, would favor the enhancement of *M. bisulcata* in the smallest size classes yet, on the other hand, given the dense packing of *M. bisulcata* in the grove, leading to some damage of medium and large trees under these falling giants. Thunderstorms with lightening are common at Korup but they appear to affect the mortality of the emergent *M. bisulcata* trees, with their large domed crowns, very little. From coring, we have shown that the largest trees are almost all hollow and water filled, so their stems may be acting as protecting electrical conductors.

Long-lived pioneers?

The majority of tree species that have been called long-lived pioneers are strongly shade intolerant when young, and depend on major disturbances to provide the open lighted conditions to which they respond well in terms of growth. As a consequence, since gaps need to be large to be effective, these trees form single-species patches of moderate to large areas. They may give way to shade-tolerant species eventually if regeneration of the new dominant is not persistent. This type of pioneer has to be contrasted with the short-lived one that, under the classical model of succession applied to tropical rain forests, grows for a short period of time in gaps and is replaced in turn by longer-living secondary species and eventually mature forest species of the canopy. In the past, medium-term pioneer species have been mostly labeled "secondary species," while arguably there is a continuum of life spans across light-responding pioneers, these albeit more frequently occurring at the shorter rather than longer end of the longevity scale. Our concern here, *M. bisulcata* in mind, is mainly with these long livers that can attain large sizes and dominate large areas of forest, even if that dominance turns out to be transitory.

Examples of long-lived pioneers forming large canopy or emergent-sized trees are several and have attracted attention because of the seeming paradox that a fast growing light-responding species when young can still make trees of substantial mass and stature in a forest. In the Pacific northwest of North America, *Pseudotsuga menziesii* forms stands of large old trees (up to 500 years in age) but often with poor in situ recruitment, and relies on major gap-generating disturbances to regenerate (Ishii and Ford 2002). *Pinus palustris*, in Georgia, USA, shows strongly oscillating population abundances, spatially and temporarily, which lag major multi-decadal forest disturbances, and lead to a wide range

in juvenile-adult ratios while across the landscape species cover stays fairly constant (Platt et al. 1988). Again, in mountains of California, USA, *Sequoiadendron giganteum*, as very old and large trees, displays a distinct grove structure, as a heterogenous mosaic of size classes, where fires are needed to release the highly shade-intolerant seedlings (Stephenson 1994). *Liriodendron tulipifera*, in the North American Appalachian Mountains, forms large patches in coves but only when large gaps have been formed by disturbance to release its shade-intolerant seedlings (Busing 1995). This last species can attain remarkable growth rates and trees of 200 plus years in age: its unconventional status led Huston and Smith (1987) to mislabel, in our view, *L. tulipifera* as a "superspecies" in their simple trade-off model for pioneer (short-lived) vs. canopy (long-lived) tree species. This polarization of "types" is prominent in the classification of forest tree species by Swaine and Whitmore (1988).

In the temperate rain forests of the southern hemisphere, most species of *Nothofagus* are shade intolerant as seedlings and require disturbance to recruit and grow to large canopy trees. This happens largely in situ, and often results in monodominance locally (Veblen et al. 1996, Pollmann and Veblen 2004). Pollmann (2004) showed an interesting example of *N. alpina* in Chile, which has a modal, or bell-shaped, size frequency distribution and no regeneration (like *M. bisulcata*) where disturbance is lacking, but at a site with known past disturbance, waves of recruitment led to two peaks of medium-sized trees. Likewise, *N. gunnii*, in Australia (Read and Brown 1996), has very limited recruitment in all the stands examined where it is locally abundant, and without recent disturbance looks set to die out locally (again a case matching *M. bisulcata*). By contrast, in the rain forests of Papua New Guinea, where different *Nothofagus* species often form monospecific stands, regeneration appeared to be high for most of them, in the form of the forester's classical reversed-J curve for frequencies of tree sizes (Read et al. 2000); in New Caledonia, different again but more close to temperate *Nothofagus* dynamics, many species were modal in size frequencies, some with and some without small-tree recruitment (Read et al. 1990).

Read et al. (1990) produced a synthetic graphical model for the different forms of *Nothofagus* forest dynamics that clearly shows how transient dominance (they did not use this term) can occur in relation to disturbance regime. *Nothofagus gunnii*, for instance, has a modal distribution with failing regeneration which, if rectified by disturbance release, would result in a future (i.e., *lagged*) peak in abundance at the site. This could happen by death of old trees (our autogenic process) or by external factors (the allogenic process), the former likely leading to flatter broader modal distribution and the latter to a more peaked narrower distribution (i.e., varying degrees of transitional dominance according to our extended mosaic model; see *Introduction*). Interestingly, in Papua New Guinea, *Nothofagus* forests tend to form mosaics of dominance but not monodominance and, in New Caledonia, the opposite happens (Read et al. 1990, 2000). *Nothofagus* species (Fagaceae) are ectomycorrhizal (Veblen et al. 1996) like *Microberlinia*, *Tetraberlinia*, *Berlinia*, and others in the Amherstieae of the Caesalpiniaceae (Newbery et al. 1988, 1997). Other tropical examples are hard to find, but one notable case is *Shorea albida* (Anderson 1964). This species is near monodominant in peat swamps of Sarawak, and has highly shade-intolerant seedlings, whose recruitment is released by lightning strikes that regularly kill up to 70 mature trees in large patches, and from these come a new local cohort of juveniles. *Swietenia macrophylla* in the Amazon also has light-demanding seedlings but its populations are far sparser and do not form aggregations, although they are related to gaps after disturbance (Gullison et al. 1996).

Several authors have stressed the essential rule in connection with the long-lived pioneer strategy, that intervals between disturbances should be longer than the average time to reach maturity but shorter than average large-tree longevity. Matching this window to environmental stochasticity, in the form of an evolutionarily stable strategy, might be difficult. On the one hand, it may explain the wide patchiness of species like *Pinus palustris* and *Sequoiadendron giganteum* when the synchronization fails (contemporaneously at least), or the more structured changes of *Pseudotsuga menziesii* and *Liriodendron tulipifera* when it does. On the other hand, disturbances coming at times away from the averages for maturity and death, might be less effective and set the forest back less than when they occur close to its most susceptible stage. Long-lived pioneers do present a fascinating problem for the forest ecologist, somewhat exceptional to the norm of most species (Huston and Smith 1987), and rather analogous to the understanding of the biennial life history strategy for grasses and herbs sitting part way between that of annuals and perennials. Ford and Ishii (2001) specifically applied their "synthetic ecological method" to understanding the position of long-lived pioneers.

Since the timing of disturbances can be expected to be stochastic, that is largely unpredictable, so also will be their effects on recruitment and patch or grove development, resulting in a cyclic mosaic as suggested by Aubréville (1938) and Watt (1947), and evidenced by the examples mentioned above. For Cameroonian coastal forests, this matches well with what Letouzey (1968, 1985) carefully described for caesalps, various states of good and poor regeneration, more or less well formed patches and sometimes near monodominance locally, and otherwise scattered adults. The mosaic theory need not rest on ex situ processes of regeneration alone but could readily accommodate in situ ones, or indeed a shifting gradient between both processes depending on extent of species' dispersal and edaphic selection factors. Possibly, Aubréville (1938) was also

seeing in situ cases with long intervals between peaks in dominance?

At Korup, the southern part of the Park is quite uniform edaphically and the most important factor in the ex situ vs. in situ discussion is the dispersal of *M. bisulcata*. A characteristic of many long-lived pioneers that form patches or local dominance is their poor dispersal. However, there are other long-lived pioneers that are very well dispersed, usually by wind, and this leads to their scattered occurrence in smaller (tree fall) gaps than those already described for dominant and aggregated species. A good example is *Weinmannia trichosperma* in Chile, which can attain considerable longevity (Lusk 1999): this species fits van Steenis's (1958) concept of "nomads" in the rain forest. Likewise, the species referred to by Alexandre (1989) as "géante anémochore" are long-lived pioneers, and further examples of *Ceiba pentandra* and *Entandrophragma* spp., quoted by Hallé et al. (1978), are also wind dispersed. Schulz (1960) also highlighted two species in Suriname, *Goupia glabra* and *Simarouba amara*, which require lighted gaps yet are long living. They showed clear deficiencies in their numbers of small and medium-sized trees. At Korup, an equivalent example would be *Vitex lokundjensis* (formerly *V. ferruginea*; Gartlan et al. 1986, Green and Newbery 2001*b*). In the same vein, we would not characterize *M. bisulcata* as a "giant invader," as Turner (2000: 246) implied, first because that would mean much longer distance dispersal than we have observed at the time of a major event, and second because *M. bisulcata* is scattered around the region even outside the Park to the south and east, and was quite well distributed in the previous century as far south as Tiko before logging removed it (Jentsch 1911). Basically, *M. bisulcata* is not a pioneer, in any real sense of the word: it is simply a species with shade-intolerant seedlings that can grow to very large trees when sufficiently and repeatedly lighted.

Hawthorne (1996) introduced "... the 'non-pioneer light-demander' (NPLD) guild, on the basis of their assumed tolerance of or requirement for shade as seedling, but with a requirement for gaps to survive *beyond* the sapling stage" (our emphasis), for trees in Ghanaian forests; but again the first characteristic does not fit with species such as *M. bisulcata* either. These NPLDs are close to typical shade-tolerant canopy species. Examples quoted are *Khaya*, *Ceiba*, *Entandrophragma*, *Piptadeniastrum*, *Albizia*, *Terminalia*, and *Pycnanthus* and, according to Hawthorne (1995), all but the last one are wind-dispersed species. These are not the same as long-lived pioneers as often defined because of they are not, apparently, intolerant of shade as seedlings. *Pycnanthus* produces animal dispersed seeds and had a recorded low relative frequency of juveniles to adults, unusual for the main Ghanaian trees species. Sheil et al. (2006) point out in an analysis of the same Ghanaian tree inventory data that the relationship between maximum tree size and degree of shade tolerance of juveniles was weak, admitting that *some* large tree species are shade-intolerant and require light from early on.

Two contrasts can be made between species, such as *M. bisulcata*, which are very shade intolerant but light responsive when seedlings and saplings, yet grow fast as trees to produce dominant stands of very large individuals, and (1) the many tree-gap-dependent canopy species, which are found scattered at low abundance across forests and (2) fast growing species of usually smaller stature that can dominate patches of secondary forest. As an example of the first case, Wright et al. (2003) highlighted *Jacaranda copaia*, in Panamanian forest, having large trees (up to ~85 cm stem diameter) but very few recruits. They interpreted this situation as part of the expected spectrum of many possible tree life histories, and not necessarily as an indication of potential failure to replace. For the second case, Worbes et al. (2003), for example, recorded local dominance of old secondary forest in Cameroon by *Triplochiton scleroxylon* (mean age ~110 years) but with very few juveniles, and argued for is having long-lived pioneer status within the succession. Both cases involve relatively fast-growing species reaching moderately large sizes of medium longevity, but they lack the non-successional primary-forest dominance shown by *M. bisulcata* at Korup.

Theoretical synthesis

A. S. Watt's (1947) seminal work has left an enduring and valuable influence on vegetation ecology for over 60 years. He was at that time aware of Aubréville's (1938) ideas and integrated them into his paper expounding a new theory of dynamics. It remained for Richards (1952) to synthesize these two authors' ideas further for tropical rain forest ecology, laying emphasis on local dominance, adaptation to habitat, and edaphic processes. Since then there has been surprisingly little advancement of a theory for dynamics of low-diversity tropical forests. With the idea of transient dominance we hope to reset the direction, and to explain ecological phenomena in a way better testable in terms of physical and physiological processes. Moreover, statistical "laws of nature," exemplified by the Zipf-Mandelbrot model for relative species' abundances (Frontier 1985), suggest that in complex interacting systems with multiply compounding exponential processes (Newman 2005), numerical dominance is to be expected unless external factors, such as disturbance, intervene. This highlights again, as Watt (1947) himself showed well, the importance of deaths of patches of large trees, coming regularly or irregularly with varying frequency and intensity. This notion links forest dynamics to its driver, environmental stochasticity, which creates a strong selective force on tree species' life histories and populations.

It has long been a paradigm in vegetation ecology that disturbance leads to succession, and different species

find niches in the different stages (Pickett et al. 2007). For tropical rain forest that has been typified by pioneer, secondary, and primary (climax) species (Whitmore 1982). However, there is no deterministic rule yet shown that applies to all forests, and predictions concerning succession are accordingly often vague and inaccurate. Universal traits are hard to find, and ecology has come to recognize that such a putative sequence is a complex continuum, often lacking representatives at its start and/or its end. There may be primary forest tree species that are not part of a succession per se at all. Such is the case made here for light-demanding (as juveniles) long-lived (as adults) tree species in Africa. One excellent example, the subject of this paper, is *Microberlinia bisulcata*. There are strong reasons, too, in believing that there are many other similar tree species that have been poorly observed, less well reported or not properly researched. These species can no longer be regarded as uncomfortable exceptions, or "misfits," to a too-simple model of forest regeneration. They force a paradigm change toward a wider theory that admits more routes for forest regrowth in the face of a variable and disturbance-rich environment.

Modal tree-size frequency distributions appear more commonly among African tropical large-tree species' populations than on other continents, and certainly they are pronounced in the western Central Africa region (Gartlan et al. 1986, Newbery and Gartlan 1996, Newbery et al. 1998, 2004), lending much support to the theory of Aubréville (1938). In a previous analysis, we have called these the "group 5" species (Newbery and Gartlan 1996; see Condit et al. 1998), and it is just one step to link these observations generally to the idea of transient dominance. As Richards (1952, 1996) often indicated, Africa was and is "the odd man out," but it can sometimes give interesting perspectives on wider processes of dynamics, as shown for Korup.

There are some notable examples of strongly disturbance-induced modal size distributions from other forest sites. For the tropics, Baker et al. (2005) reported seasonally dry evergreen forests in Thailand with *Hopea odorata* having a modal stem diameter of ~1 m at 230 yr, and six further species with modal ages of 100–180 yr. This was interpreted as a complex set of responses to several catastrophic disturbances (cyclones and fire among others) in the previous centuries. Our model for Korup, though, envisages less strong and more frequent disturbances (Newbery et al. 2004), occurring as clusters over periods of perhaps 20–30 yr that would allow the mentioned onward ratchet-like recruitment of *M. bisulcata* saplings. This appears to fit quite well with what is known of past rainfall in Africa (Nicholson et al. [2012] for a recent synthesis), with more pronounced drying in 1800–1815 and 1825–1840 for central and west Africa. We estimated our modal tree age to be ~200 yr and a start of the grove just before 1800: reliable climate records are not available before 1800 (Nicholson et al. 2012).

The theory of transient dominance that we propose builds on the Watt-Aubréville-Richards framework by suggesting that some species come to dominate large patches of forest (or groves), their regeneration temporarily failing in situ, and after their decline (slowly or precipitously) in response to external disturbance they regain their earlier level of abundance. A perfectly synchronized cycle would appear near impossible, but a cycle entrained by feedbacks in response to environmental stochasticity is indeed a plausible hypothesis. This suggests that the cycle (Watt), spatially realized (Aubréville) and further enforced by edaphic selection (Richards), is essentially unstable. Presumably climatic disturbances have occurred over the past millennia to enable species such a *M. bisulcata* to become selected, and to have the life history traits that it shows. Otherwise it is difficult, given our direct knowledge of its size distribution, growth rate, and physiological traits, to envisage how it could complete its life cycle. That dominance may be transient and not permanent allows for a much deeper, and more interesting, understanding of the forests of western Central Africa.

Acknowledgments

The Ministries of Forests and Wildlife (MINFOF) and Scientific Research and Innovation (MINRESI) kindly granted permission to carry out the research; the Forest Research Centre at Kumba, then later IRAD at Ekona and finally University of Buea provided over 20 years of continuous support. We thank E. Abeto, W. Bischoff, P. Ekundo, M. Elangwe, M. Eyakwe, P. Fraser, J. Green, M. Jackson, S. Lorenz, C. Okha, C. Oponde, P. Mezili, F. Namata, J. Naweya, S. Ngibili, J. Norghauer, C. Praz, S. Schwan, N. Songwe, P. Taylor, and F. Zeugin for field assistance between 1990 and 2010; F. Tchuenteu, M. White, and M. Zimmermann for laboratory assistance in the soil analyses; and J. M. Norghauer for commenting on the manuscript. The setting-up and first P-plot enumeration was funded by an EU contract SDT2*0246 (1990–1994, with the Institute for World Forestry, Hamburg, Germany [T. W. Schneider]), its remeasurement and the start of the NW plot, later by Swiss National Fond grant #3100-066655 (2002–2006), and all subsequent work by the University of Bern. We thank the two reviewers for their valuable comments on the manuscript.

Literature Cited

Alexandre, D. Y. 1989. Dynamique de la régéneration naturelle en fôret dense de Côte d'Ivoire. Editions d'ORSTOM, Paris, France.

Anderson, J. A. R. 1964. Observations on climatic damage in peat swamp forest in Sarawak. Empire Forestry Review 43:145–158.

Aubréville, A. 1938. La forêt coloniale: les forêts de l'Afrique occidentale française. Société d'Editions Géographiques, Maritimes et Coloniales, Paris, France.

Baddeley, A. 2008. Analyzing spatial point patterns in R. Workshop notes. Version 3, CSIRO and the University of Western Australia, Perth, Australia.

Baddeley, A., and R. Turner. 2005. Spatstat: an R package for analyzing spatial point patterns. Journal of Statistical Software 12:1–41.

Baker, P. J., S. Bunyavejchewin, C. D. Oliver, and P. S. Ashton. 2005. Disturbance history and historical stand dynamics of a seasonal tropical forest in western Thailand. Ecological Monographs 75:317–343.

Beard, J. S. 1946. The Mora forests of Trinidad, British West-Indies. Journal of Ecology 33:173–192.
Busing, R. T. 1995. Disturbance and the population dynamics of *Liriodendron tulipifera*: simulations with a spatial model of forest succession. Journal of Ecology 83:45–53.
Clark, D. A., and D. B. Clark. 1992. Life-history diversity of canopy and emergent trees in a neotropical rain-forest. Ecological Monographs 62:315–344.
Clark, D. B., and D. A. Clark. 1987. Population ecology and microhabitat distribution of *Dipteryx panamensis*, a neotropical rain forest emergent tree. Biotropica 19:236–244.
Clark, D. B., and D. A. Clark. 1996. Abundance, growth and mortality of very large trees in neotropical lowland rain forest. Forest Ecology and Management 80:235–244.
Condit, R., R. Sukumar, S. P. Hubbell, and R. B. Foster. 1998. Predicting population trends from size distributions: a direct test in a tropical tree community. American Naturalist 152:495–509.
Connell, J. H., and M. D. Lowman. 1989. Low-diversity tropical rain forests: some possible mechanisms for their existence. American Naturalist 134:88–119.
Connell, J. H., and R. O. Slatyer. 1977. Mechanisms of succession in natural communities and their role in community stability and organization. American Naturalist 111:1119–1144.
Davis, T. W. A., and P. W. Richards. 1934. The vegetation of Moraballi Creek, British Guiana: an ecological study of a limited area of tropical rain forest. Part II. Journal of Ecology 22:106–155.
Eggeling, W. J. 1947. Observations on the ecology of the Budongo rain forest, Uganda. Journal of Ecology 34:20–87.
Finegan, B. 1984. Forest succession. Nature 312:109–114.
Ford, E. D., and H. Ishii. 2001. The method of synthesis in ecology. Oikos 93:153–160.
Frontier, S. 1985. Diversity and structure in aquatic ecosystems. Oceanography and Marine Biology Annual Review 23:253–312.
Gartlan, J. S. 1992. Cameroon. Pages 110–118 *in* J. A. Sayer, C. S. Harcourt, and N. M. Collins, editors. The conservation atlas of tropical forests: Africa. Macmillan Publishers, London, UK.
Gartlan, J. S., D. M. Newbery, D. W. Thomas, and P. G. Waterman. 1986. The influence of topography and soil phosphorus on the vegetation of Korup Forest Reserve, Cameroun. Vegetatio 65:131–148.
Gérard, P. 1960. Etude écologique de la forêt dense à *Gilbertiodendron dewevrei* dans la région de l'Uele. Publications de l'Institut National pour l'Etude Agronomique du Congo; Série scientifique 87:1–159.
Germain, R., and C. Evrard. 1956. Etude écologique et phytosociologique de la forêt à *Brachystegia laurentii*. Publications de l'Institut National pour l'Etude Agronomique du Congo Belge. INEAC, Yangambi, Belgian Congo.
Green, J. J., and D. M. Newbery. 2001*a*. Light and seed size affect establishment of grove-forming ectomycorrhizal rain forest tree species. New Phytologist 151:271–289.
Green, J. J., and D. M. Newbery. 2001*b*. Shade and leaf loss affect establishment of grove-forming rain forest tree species. New Phytologist 151:291–309.
Green, J. J., and D. M. Newbery. 2002. Reproductive investment and seedling survival of the mast-fruiting rain forest tree, *Microberlinia bisulcata* A. Chév. Plant Ecology 162:169–183.
Gullison, R. E., S. N. Panfil, J. J. Strouse, and S. P. Hubbell. 1996. Ecology and management of mahogany (*Swietenia macrophylla* King) in the Chimanes Forest, Beni, Bolivia. Botanical Journal of the Linnean Society 122:9–34.
Hall, J. B. 1981. Ecological islands in south-eastern Nigeria. African Journal of Ecology 19:55–72.
Hallé, F., R. A. A. Oldemann, and P. B. Tomlinson. 1978. Tropical trees and forests: an architectural analysis. Springer, Berlin, Germany.
Hart, T. B. 1990. Monospecific dominance in tropical rain forests. Trends in Ecology and Evolution 5:6–11.
Hart, T. B. 1995. Seed, seedling and sub-canopy survival in monodominant and mixed forests of the Ituri Forest, Africa. Journal of Tropical Ecology 11:443–459.
Hart, T. B., J. A. Hart, and P. G. Murphy. 1989. Monodominant and species-rich forests of the humid tropics: causes for their co-occurrence. American Naturalist 133:613–633.
Hawthorne, W. D. 1995. Ecological profiles of Ghanaian forest trees. Tropical Forestry Papers. No. 29. Oxford Forestry Institute, Oxford, UK.
Hawthorne, W. D. 1996. Holes and the sum of parts on Ghanaian forest: regeneration, scale and sustainable use. Proceedings of the Royal Society of Edinburgh 104B:75–176.
Henkel, T. W. 2003. Monodominance in the ectomycorrhizal *Dicymbe corymbosa* (Caesalpiniaceae) from Guyana. Journal of Tropical Ecology 19:417–437.
Huston, M. 1979. General hypothesis of species diversity. American Naturalist 113:81–101.
Huston, M., and T. Smith. 1987. Plant succession: life history and competition. American Naturalist 130:168–198.
Illian, J., A. Penttinen, H. Stoyan, and D. Stoyan 2008. Statistical analysis and modelling of spatial point patterns. John Wiley and Sons, Chichester, UK.
Ishii, H., and D. Ford. 2002. Persistence of *Pseudotsuga menziesii* (Douglas-fir) in temperate coniferous forests of the Pacific Northwest Coast, USA. Folia Geobotanica 37:63–69.
Jentsch, A. 1911. Der Urwald Kameruns. Pages 1–199 *in* O. Warburg and F. Wohltmann, editors. Beihefte zum Tropenpflanzer. Kolonial-Wirtschaftliches Komitee, Berlin, Germany.
Jones, E. W. 1945. The structure and reproduction of the virgin forest of the north temperate zone. New Phytologist 44:130–148.
Jones, E. W. 1950. Some aspects of natural regeneration in the Benin rain forest. Empire Forestry Review 29:108–124.
Jones, E. W. 1956. Ecological studies on the rain forest of southern Nigeria IV (continued). The plateau forest of the Okomu Forest Reserve. Journal of Ecology 44:83–117.
Jongman, R. H. G., C. J. F. ter Braak, and O. F. R. van Tongeren. 1995. Data analysis in community and landscape ecology. Cambridge University Press, Cambridge, UK.
Kohyama, T., and T. Takada. 1998. Recruitment rates in forest plots: Gf estimates using growth rates and size distributions. Journal of Ecology 86:633–639.
Letouzey, R. 1968. Etude Phytogéographique du Cameroun. P. LeChevalier, Paris, France.
Letouzey, R. 1985. Notice de la Carte Phytogéographique du Cameroun Au 1:500 000. Institut de la Carte Internationale de la Végétation, Toulouse, France.
Lusk, C. H. 1999. Long-lived light-demanding emergents in southern temperate forests: the case of *Weinmannia trichosperma* (Cunoniaceae) in Chile. Plant Ecology 140:111–115.
Makana, J. R., C. N. Ewango, S. M. McMahon, S. C. Thomas, T. B. Hart, and R. Condit. 2011. Demography and biomass change in monodominant and mixed old-growth forest of the Congo. Journal of Tropical Ecology 27:447–461.
McCune, B., and J. B. Grace. 2002. Analysis of ecological communities. MjM Software Design, Glenedon Beach, Oregon, USA.
Newbery, D. M., I. J. Alexander, and J. A. Rother. 1997. Phosphorus dynamics in a lowland African rain forest: the influence of ectomycorrhizal trees. Ecological Monographs 67:367–409.
Newbery, D. M., I. J. Alexander, and J. A. Rother. 2000. Does proximity to conspecific adults influence the establishment of

ectmycorrhizal trees in rain forest? New Phytologist 147:401–409.

Newbery, D. M., I. J. Alexander, D. W. Thomas, and J. S. Gartlan. 1988. Ectomycorrhizal rain-forest legumes and soil phosphorus in Korup National Park, Cameroon. New Phytologist 109:433–450.

Newbery, D. M., G. B. Chuyong, J. J. Green, N. C. Songwe, F. Tchuenteu, and L. Zimmerman. 2002. Does low phosphorus supply limit seedling establishment and tree growth in groves of ectomycorrhizal trees in a central African rainforest? New Phytologist 156:297–311.

Newbery, D. M., G. B. Chuyong, and L. Zimmerman. 2006*a*. Mast fruiting of large ectomycorrhizal African rain forest trees: importance of dry season intensity, and the resource-limitation hypothesis. New Phytologist 170:561–579.

Newbery, D. M., G. B. Chuyong, L. Zimmermann, and C. Praz. 2006*b*. Seedling survival and growth of three ectomycorrhizal caesalpiniaceous tree species in a Central African rain forest. Journal of Tropical Ecology 22:499–511.

Newbery, D. M., and J. S. Gartlan. 1996. A structural analysis of rain forest at Korup and Douala-Edea, Cameroon. Proceedings of the Royal Society of Edinburgh 104B:177–224.

Newbery, D. M., C. J. Praz, X. M. van der Burgt, J. M. Norghauer, and G. B. Chuyong. 2010. Recruitment dynamics of the grove-dominant tree *Microberlinia bisulcata* in African rain forest: extending the light response versus adult longevity trade-off concept. Plant Ecology 206:151–177.

Newbery, D. M., S. Schwan, G. B. Chuyong, and X. M. van der Burgt. 2009. Buttress form of the central African rain forest tree *Microberlinia bisulcata*, and its possible role in nutrient acquisition. Trees Structure and Function 23:219–234.

Newbery, D. M., N. S. Songwe, and G. B. Chuyong. 1998. Phenology and dynamics of an African rainforest at Korup, Cameroon. Pages 267–308 *in* D. M. Newbery, H. H. T. Prins, and N. D. Brown, editors. Dynamics of tropical communities. Blackwell Science, Oxford, UK.

Newbery, D. M., X. M. van der Burgt, and M.-A. Moravie. 2004. Structure and inferred dynamics of a large grove of *Microberlinia bisulcata* trees in central African rain forest: the possible role of periods of multiple disturbance events. Journal of Tropical Ecology 20:131–143.

Newman, M. E. J. 2005. Power laws, Pareto distributions and Zipf's law. Contemporary Physics 46:323–351.

Nicholson, S. E., D. Klotter, and A. K. Dezfuli. 2012. Spatial reconstruction of semi-quantitative precipitation fields over Africa during the nineteenth century from documentary evidence and gauge data. Quaternary Research 78:13–23.

Norghauer, J. M., and D. M. Newbery. 2010. Recruitment limitation after mast-seeding in two African rain forest trees. Ecology 91:2303–2312.

Norghauer, J. M., and D. M. Newbery. 2011. Seed fate and seedling dynamics after masting in two African rain forest trees. Ecological Monographs 81:443–469.

Payne, R. W., et al. 2009. GenStat release 12 reference manual. VSN International, Hemel Hempstead, UK.

Peh, K. S. H., S. L. Lewis, and J. Lloyd. 2011. Mechanisms of monodominance in diverse tropical tree-dominated systems. Journal of Ecology 99:891–898.

Pickett, S. T. A., J. Kolasa, and C. G. Jones. 2007. Ecological understanding: the nature of theory and the theory of nature. Second edition. Elsevier, Amsterdam, The Netherlands.

Platt, W. J., G. W. Evans, and S. L. Rathbun. 1988. The population dynamics of a long-lived conifer (*Pinus palustris*). American Naturalist 131:491–525.

Pollmann, W. 2004. Regeneration dynamics and life-history differences in southern Chilean *Nothofagus* forest: a synthesis. Plant Ecology 174:353–369.

Pollmann, W., and T. T. Veblen. 2004. *Nothofagus* regeneration dynamics in south-central Chile: a test of a general model. Ecological Monographs 74:615–634.

Poorter, L., F. Bongers, R. S. A. R. van Rompaey, and M. de Klerk. 1996. Regeneration of canopy tree species at five sites in West African moist forest. Forest Ecology and Management 84:61–69.

R Development Core Team. 2010. R: a language and environment for statistical computing. R Foundation for Statistical Computing, Vienna, Austria.

Read, J., and M. J. Brown. 1996. Ecology of Australian *Nothofagus* forests. Pages 131–181 *in* T. T. Veblen, R. S. Hill, and J. Read, editors. The ecology and biogeography of *Nothofagus* forests. Yale University Press, New Haven, Connecticut, USA.

Read, J., G. Hope, and R. Hill. 1990. The dynamics of some *Nothofagus*-dominated rain forests in Papua New Guinea. Journal of Biogeography 17:185–204.

Read, J., T. Jaffre, E. Godrie, G. S. Hope, and J. M. Veillon. 2000. Structural and floristic characteristics of some monodominant and adjacent mixed rainforests in New Caledonia. Journal of Biogeography 27:233–25.

Richards, P. W. 1952. The tropical rain forest: an ecological study. First edition. Cambridge University Press, Cambridge, UK.

Richards, P. W. 1963. Ecological notes on West African vegetation. II. Lowland forest of the Southern Bakundu Forest Reserve. Journal of Ecology 51:123–149.

Richards, P. W. 1996. The tropical rain forest: an ecological study. Second edition. Cambridge University Press, Cambridge, UK.

Schulz, J.-P. 1960. Ecological studies on rain forest in northern Suriname. Verhandelingen der Koningklijke Nederlandse Akademie van Wetenschappen, afd. Natururkunde 53:1–267.

Sheil, D. 2001. Long-term observations of rain forest succession, tree diversity and responses to disturbance. Plant Ecology 155:183–199.

Sheil, D., A. Salim, J. R. Chave, J. Vanclay, and W. D. Hawthorne. 2006. Illumination-size relationships of 109 coexisting tropical forest tree species. Journal of Ecology 94:494–507.

Stephenson, N. L. 1994. Long-term dynamics of giant sequoia populations: implications for managing a pioneer species. Pages 56–63 *in* P. S. Aune, editor. Proceedings of the symposium on giant sequoias: their place in the ecosystem and society. PSW-151. USDA Forest Service, Visalia, California, USA.

Swaine, M. D., and J. B. Hall. 1988. The mosaic theory of forest regeneration and the determination of forest composition in Ghana. Journal of Tropical Ecology 4:253–269.

Swaine, M. D., D. Lieberman, and F. E. Putz. 1987. The dynamics of tree populations in tropical forest: a review. Journal of Tropical Ecology 3:359–366.

Swaine, M. D., and T. C. Whitmore. 1988. On the definition of ecological species groups in tropical rain forests. Vegetatio 75:81–86.

Tansley, A. G. 1935. The use and abuse of vegetation concepts and terms. Ecology 16:284–307.

Torti, S. D., and P. D. Coley. 1999. Tropical monodominance: a preliminary test of the ectomycorrhizal hypothesis. Biotropica 31:220–228.

Torti, S. D., P. D. Coley, and T. A. Kursar. 2001. Causes and consequences of monodominance in tropical lowland forests. American Naturalist 157:141–153.

Turner, I. M. 2000. The ecology of trees in the tropical rain forest. Cambridge University Press, Cambridge, UK.

van der Burgt, X. M., M. Eyakwe, and J. Motoh. 2012. *Gilbertiodendron newberyi* (Leguminosae: Caesalpinioideae), a new tree species from Korup National Park, Cameroon. Kew Bulletin 67:51–57.

van Gemerden, B. S., H. Olff, M. P. E. Parren, and F. Bongers. 2003. The pristine rain forest? Remnants of historical human impacts on current tree species composition and diversity. Journal of Biogeography 30:1381–1390.

van Steenis, C. G. G. J. 1958. Rejuvenation as a factor for judging the status of vegetation types: the biological nomad theory. Pages 212–215 *in* Study of tropical vegetation. Proceedings of the Kandy Symposium. UNESCO, Paris, France.

Veblen, T. T., R. S. Hill, and J. Read, editors. 1996. The ecology and biogeography of *Nothofagus* forests. Yale University Press, New Haven, Connecticut, USA.

Watt, A. S. 1947. Pattern and process in the plant community. Journal of Ecology 35:1–22.

Whitmore, T. C. 1982. On pattern and process in forests. Pages 45–59 *in* E. I. Newman, editor. The plant community as a working mechanism. Blackwell Scientific Publications, Oxford, UK.

Whittaker, R. H. 1975. Communities and ecosystems. Second edition. MacMillan, New York, New York, USA.

Worbes, M., and J. Junk. 1989. Dating tropical trees by means of ^{14}C from bomb tests. Ecology 70:503–507.

Worbes, M., R. Staschel, A. Roloff, and W. J. Junk. 2003. Tree ring analysis reveals age structure, dynamics and wood production of a natural forest stand in Cameroon. Forest Ecology and Management 173:105–123.

Wright, S. J., H. C. Muller-Landau, R. Condit, and S. P. Hubbell. 2003. Gap-dependent recruitment, realized vital rates, and size distributions of tropical trees. Ecology 84:3174–3185.

Supplemental Material

Appendix A

Further methodological details concerning P- and NW-plot measurements (*Ecological Archives* M083-012-A1).

Appendix B

Complete taxonomic tree species list for P and NW plots at Korup (*Ecological Archives* M083-012-A2).

Appendix C

Contour plots of soil (with PCA results) and vegetation components in the P plot (*Ecological Archives* M083-012-A3).

Appendix D

Ordination of medium-sized trees in subplots of the P plot (*Ecological Archives* M083-012-A4).

Appendix E

Spatial statistics of large–medium tree patterns for the three dominant species (*Ecological Archives* M083-012-A5).

Appendix F

Tables of densities and basal areas of all tree species in the P and NW plots (*Ecological Archives* M083-012-A6).

Appendix G

Less-abundant tree species in the 140-ha composite sample at Korup (*Ecological Archives* M083-012-A7).

Appendix H

Fits of the Zipf-Mandelbrot model, with and without dominant tree species (*Ecological Archives* M083-012-A8).

Appendix I

Calculations for the population projection matrices of the three dominant species (*Ecological Archives* M083-012-A9).

Data Availability

Data associated with this paper have been deposited in Dryad: http://dx.doi.org/10.5061/dryad.t85n3